

**Theoretical studies of the
magnetic and superconducting
properties of super-oxygenated
 $\text{La}_{2-x}\text{Sr}_x\text{CuO}_{4+y}$**

Marcella Cabrera Berg

Copenhagen 2014

NBI-M.Sc.-2014

Supervisor: Brian Møller Andersen

Co-supervisor: Linda Udby

University of Copenhagen
Faculty of Science
Niels Bohr Institute
NBI-M.sc.-2014

Summary (English)

Theoretical study and brief review of $\text{La}_2\text{CuO}_{4+y}$ (LCO+O), $\text{La}_{2-x}\text{Sr}_x\text{CuO}_4$ (LSCO) and $\text{La}_{2-x}\text{Sr}_x\text{CuO}_{4+y}$ (LSCO+O). In these types of cuprates there have experimentally been observed stripe order.

The occurrence of high temperature superconductivity in cuprates is due to the CuO_2 planes. In LCO the Cu atoms form strongly hybridized bonds with oxygen, this can approximately be explained by assuming there is one hole in the d-bond per Cu atom. The Cu sites can interact via the oxygen atoms through the super exchange mechanism and thereby forming a AFM-insulator (Mott insulator) best described by the one band Hubbard model. The excess oxygen will be described by a Thomas Fermi screening added to the one-band Hubbard Hamiltonian. By self consistent calculations, we have stabilized stripe order in a 2D and 3D model. The calculations show that the spin settles in periodicity of 8 in the layers and anti-parallel between the layers.

This type of calculation does not seem to work for compound with intermediate oxygen with modulations in the c-axis since the system stabilize homogeneously.

Summary (Danish)

Teoretisk studie og kort gennemgang af $\text{La}_2\text{CuO}_{4+y}$ (LCO + O), $\text{La}_{2-x}\text{Sr}_x\text{CuO}_4$ (LSCO) og $\text{La}_{2-x}\text{Sr}_x\text{CuO}_{4+y}$ (LSCO + O). I disse typer af cuprater er der experimentielt blevet observeret stribe orden.

Forekomsten af høj temperatur superledning i cuprater skyldes CuO_2 planerne. Cu atomer vil forme stærke hybridiserede bindinger med ilt, som tilnærmelsesvis kan forklares ved at antage, at der er et hul i d-binding pr Cu atom. Cu atomet kan interagere via oxygenatomer gennem "super mekanismen" for udveksling og derved danne en AFM-isolator (Mott isolator) bedst beskrevet ved en et-bånds Hubbard model. Den overskydende ilt vil blive beskrevet ved en Thomas Fermi screening der tilføjes til et-bånds Hubbard Hamiltonen. Ved selv konsistente beregninger, vi har stabiliseret stribe orden i en 2D-og 3D-model. Beregningerne viser, at spin har en perode på 8 i lagene og de ligger sig anti-parallel mellem lagene.

Denne type beregning ser ikke ud til at virke for systemer med mellemliggende ilt der har modulationer i c-aksen, da systemet stabilisere sig homogent

.

Preface

This thesis was prepared at the Niels Bohr Institute, University of Copenhagen in fulfilment of the requirements for acquiring an M.Sc.

Copenhagen, 01-November

Marcella Cabrera Berg

Acknowledgements

I would first like to thank Brian M. Andersen and Linda Udby for providing me the project and good guidance throughout the process. I would also like to thank Henrik Jacobsen and Pia Jensen for constructive feedback on my thesis and Johan Jacobsen for providing me with this LaTeX template.

Contents

Summary (English)	i
Summary (Danish)	iii
Preface	v
Acknowledgements	vii
1 Introduction	1
2 Superconductivity	3
2.1 Introduction to Superconductivity	3
2.1.1 Meissner-Oschenfeld effect	3
2.1.2 Two types of superconductors	6
2.1.3 BCS Theory	7
2.2 Hamiltonian and mathematical methods	17
2.2.1 Screening of the Coulomb interactions	17
2.2.2 The Hamiltonian	19
2.2.3 The mean-field Hamiltonian	19
2.2.4 The Bogoliubov transformation	21
2.2.5 The Bogoliubov-de Gennes Equations	23
3 Cuprates	27
3.1 Cuprates, properties and structure	27
3.1.1 Introduction to Cuprates	27
3.1.2 Doping in Cuprates	29
3.1.3 The superconducting order parameter	31
3.1.4 Electronic structure in the normal state	31
3.1.5 Interlayer hopping	35
3.2 Experimental results on LSCO, LCO+O and LSCO+O	35
3.2.1 LSCO	35
3.2.2 Superoxygenated LCO+O	37
3.2.3 Superoxygenated LSCO+O	40

4	Mathematical Model	49
4.1	Mathematical Methods for a 2D model	49
4.1.1	Guessing parameters	54
4.1.2	2D Model matrix	54
4.2	Mathematical Methods for 3D Model	56
4.2.1	The 3D matrix	61
4.3	The excess oxygen	63
5	Numerical Results	65
5.1	2D model	65
5.1.1	Homogeneous system	65
5.1.2	Striped system	67
5.1.3	Striped superconducting system	68
5.1.4	Striped system with excess oxygen	71
5.2	Two layers	79
5.2.1	Mirroring	82
5.2.2	Modulation of stripes in the z -direction	84
5.2.3	Stripes with intermediate oxygen	84
5.3	3D model	89
5.3.1	Different μ	89
5.3.2	Stripes	89
5.3.3	The excess oxygen	90
6	Conclusion	93
	Bibliography	97

List of Figures

2.1	<i>Periodic table with all known superconducting elements. The blue marked elements are for ambient pressure, the green are for high pressure. [41]</i>	4
2.2	<i>Diagram of the Meissner-Ochsenfeld effect. Magnetic field lines, represented as arrows, in the normal state (left) and the superconducting state, are expelled from the sample when it is below its critical temperature T_c (right).</i>	5
2.3	<i>Illustration of the phases of temperature as a function of applied field for type-I(left) and type-II (right) superconductor. From [22]</i>	7
2.4	<i>Schematic illustration of the temperature dependence of the flux lines of a type-II superconductor.</i>	8
2.5	<i>Feynman diagram for an electron-phonon interaction. The electron is scattered from K to $K + q$ resulting in an annihilation of a phonon of wave vector $-q$.</i>	10
2.6	<i>Feynman diagram for an electron-electron interaction. The electron with spins σ_1 and σ_2 are scattered from K_1 to $K_1 + q$ and K_2 to $K_2 + q$ via the phonon with wave vector $-q$. The vertex is for an electron-phonon interaction.</i>	11
2.7	<i>Schematic illustration of the Fermi surface. There is an attraction between electrons near the Fermi surface. The electrons are scattered to $\pm q$ if they lie within $\epsilon_f \pm \hbar\omega_D$.</i>	12
2.8	<i>Schematic illustration of the Fermi spherical surface at zero temperature. All the states are within $k < k_F$ are occupied. Two electrons are placed outside the Fermi surface and interact via electron-phonon interaction.</i>	13
3.1	<i>Crystal structure of LSCO. The Copper is yellow, oxygen is pink and Lanthanum/strontium is red.</i>	28
3.2	<i>Crystal structure of YBCO. The Copper is orange, oxygen is red and Barium is dark blue and the Yttrium is blue.</i>	28

3.3	<i>Schematic phase diagram of hole-doped cuprates. The different phases of hole-doped cuprates are plotted as a function of temperature and hole-doping [37].</i>	30
3.4	<i>Scematic illustration of the electron structure of Cu-O planes.</i>	32
3.5	<i>Angular distribution of the orbitals s, d and p. [7]. The orbitals show the angular part of a wave function.</i>	33
3.6	<i>phase diagram of the cuprate LSCO. The different phases of hole-doping are plotted as a function of temperature and hole-doping x.</i>	37
3.7	<i>Proposed phase diagram of LCO + O. [5]. The oxygen places itself in different layers called staging.</i>	38
3.8	<i>Illustration of the staging in LCO+O. Left we see the tilt in the CuO_6 octahedron for undoped LCO. Right we see scematic illustration of stage 6 tilt structure in the CuO_6 octahedron in LCO+O. The different shadings represent different antiphase tilt domains. [5]</i>	39
3.9	<i>Scematic phase diagram of superoxygenated LSO+O. The light area represent the superconducting phase, and dark arc regions are magnetic line phases. The cross-hatched regions indicate miscibility gaps. A large area of the phase diagram remains blank as it is an unexplored area. The figure is taken from Mohottala et al.[23]</i>	43
3.10	<i>Crystal structure of superoxygenated LSCO+O. Pink represent copper, white represent lanthenum and strontium, and blue is the added oxygen. The design of the structure is based on [26]</i>	44
3.11	<i>Hypothesized stripe model for the CuO_2-planes in LSCO for $x = 0.125$. The arrows indicate spin on a copper site. The filled circles represent holes. The figure is based on [29]</i>	46
4.1	<i>Schematic illustration of the Cu-O-Cu bond. Yellow represents copper and pink represents oxygen. Right: Crystal structure of LSCO. The colored represent the important CuO_2 layer in the tight-binding model. Left: Simplified diagram of the CuO_2 planes in the tight-binding model. The copper $3d_{x^2-y^2}$ orbital hybridize with the oxygen $2p_{x,y}$ orbital allowing the electrons to hop from one copper site to the neighboring copper site trough interstitial Cu-O-Cu bond.</i>	50

4.2	<i>Schematic illustration of the Cu-O-Cu bond in 3D. Yellow represents copper and pink represents oxygen. Right: Crystal structure of LSCO. The colored represent the important CuO₂ layer in the tight-binding model. Left: Simplified diagram of the CuO₂ planes in the tight-binding model. The copper 3d_{x²-y²} orbital hybridize with the oxygen 2p_{x,y} orbital allowing the electrons to hop from one copper site to the neighboring copper site trough interstitial Cu-O-Cu bond.</i>	60
5.1	<i>DOS for a homogeneous system with no doping $x = 0.0$, the Coulomb term is $U = 0$ and different hopping terms t'. Blue represent $t' = 0.0t$, black represent $t' = 0.1t$, yellow represent $t' = 0.2t$ and red represent $t' = 0.3t$. The Computed for a 16×16 system.</i>	66
5.2	<i>DOS for a homogeneous system with a doping at $x = 0.125$, the Coulomb term at $U = 0$ and the hopping term $t' = 0.2t$. Computed for a 16×16 system.</i>	67
5.3	<i>Density and magnetization for a striped system with a doping at $x = 0.125$ and the Coulomb term at $U = 4t$. Left corresponds to the density and right corresponds to the magnetization. Computed for a 16×16 system.</i>	69
5.4	<i>DOS for a striped system with a doping at $x = 0.125$ and the Coulomb term at $U = 4t$. The energy scale corresponds to the Fermi level. Computed for a 16×16 system.</i>	70
5.5	<i>The stripe order for a system with doping $x = 0.125$ and the Coulomb term at $U = 4t$. The figure shows the stripe order for the first 16 sites Computed for a 16×16 system.</i>	70
5.6	<i>DOS for a system with doping $x = 0.125$ and the Coulomb term at $U = 4t$, $\Delta_x = 0.243485t$, $\Delta_y = -0.243485t$ and $V = 1t$. $t' = 0.0$ Computed for a 16×16 system.</i>	71
5.7	<i>DOS for a system with doping $x = 0.125$ and the Coulomb term at $U = 4t$, $\Delta_x = 0.243485t$, $\Delta_y = -0.243485t$ and $V = 1t$. $t' = 0.2t$. Computed for a 16×16 system.</i>	72
5.8	<i>Contour plot of the effect of the mean field potential $W_{R_o}(r)$ in the xy- plane from one oxygen placed between site 1 and 2 in both the x, y, z direction in a lattice of size 8×8. Dark purple/blue corresponds to a value of 0.01 and white correspond to a value of size 0.18</i>	73

5.9	<i>Contour plot of the effect of the mean field potential $W_{R_o}(r)$ in the xy- plane from one oxygen placed between site 1 and 2 in both the x, y, z direction in a lattice of size 16×16. Dark purple/blue corresponds to a value of 0.01 and white correspond to a value of size 0.18</i>	74
5.10	<i>Striped system with a mean field potential from one oxygen placed between site 1 and 2 in both the x, y, z direction. Calculated for a system of size 8×8. The figure shows the first 16 sites in the case of additional oxygen.</i>	75
5.11	<i>Striped system with a mean field potential from one oxygen placed between site 1 and 2 in both the x, y, z direction. Calculated for a system of size 16×16. The figure shows the first 32 sites in the case of additional oxygen.</i>	75
5.12	<i>DOS for a striped system without a superconducting phase with a mean field potential from one oxygen placed between site 1 and 2 in both the x, y, z. Calculated for a system of size 16×16.</i>	76
5.13	<i>Contour plot of the effect of the mean field potential from two oxygen, one placed between site 1 and 2 in both the x, y, z direction and the other placed between site 1 and 2 in the xz direction, and 4 and 5 in the y direction. The lattice is of size 16×16. Dark purple/blue corresponds to a value of 0.0 and white correspond to a value of size 0.2</i>	77
5.14	<i>Density and magnetization for a striped system with a doping at $x = 0.125$, the Coulomb term at $U = 4t$ mean field potential from two oxygen, one placed between site 1 and 2 in both the x, y, z direction and the other placed between site 1 and 2 in the xz direction, and 4 and 5 in the y direction. Left corresponds to the density and right corresponds to the magnetization. Computed for a 16×16 system.</i>	78
5.15	<i>Striped system with mean field potential from two oxygen, one placed between site 1 and 2 in both the x, y, z direction and the other placed between site 1 and 2 in the xz direction, and 4 and 5 in the y direction. The lattice is of size 16×16. The figure shows the first 32 sites in the case of additional oxygen without a superconducting phase.</i>	78
5.16	<i>DOS for a striped system without a superconducting phase mean field potential from two oxygen, one placed between site 1 and 2 in both the x, y, z direction and the other placed between site 1 and 2 in the xz direction, and 4 and 5 in the y direction. The lattice is of size 16×16.</i>	79

- 5.17 *Contour plot of the effect of the mean field potential from two oxygen, one placed between site 1 and 2 in both the x , y , z direction and the other placed between site 1 and 2 in the x z direction, and 4 and 5 in the y direction. The lattice is of size 16×16 . Dark purple/blue corresponds to a value of 0.0 and white correspond to a value of size 1.2* 80
- 5.18 *Density and magnetization for a striped system with a doping at $x = 0.125$, the Coulomb term at $U = 4t$ mean field potential from two oxygen, one placed between site 1 and 2 in both the x , y , z direction and the other placed between site 1 and 2 in the x z direction, and 4 and 5 in the y direction. Left corresponds to the density and right corresponds to the magnetization. Computed for a 16×16 system.* 81
- 5.19 *Striped system with mean field potential from two oxygen, one placed between site 1 and 2 in both the x , y , z direction and the other placed between site 1 and 2 in the x z direction, and 4 and 5 in the y direction. The lattice is of size 16×16 . The figure shows the first and last 16 sites in the case of additional oxygen without a superconducting phase.* 81
- 5.20 *DOS for a two layer system. The first layer (red) is a striped system with Coulomb term $U = 4t$ and doping $x = 0.125$. The second layer (blue) is a homogeneous system with Coulomb term $U = 0$, and doping $x = 0.125$. The calculations are for a system of 16×16 and with the next nearest neighbor term $t' = -0.2t$ and $t_{\perp} = -0.1t$. The two-layer system stabilizes to two homogeneous layers but with the different densities.* 82
- 5.21 *DOS for a two layer system. The first layer (red) is a striped system with Coulomb term $U = 5t$ and doping $x = 0.125$. The second layer (blue) is a homogeneous system with Coulomb term $U = 0$, and doping $x = 0.125$. The calculations are for a system of 16×16 and with the next nearest neighbor term $t' = -0.2t$ and $t_{\perp} = -0.1t$. The two-layer system stabilizes to two homogeneous layers but with the different densities.* 83
- 5.22 *The stripe order for a two layered system with doping at $x = 0.125$ and the Coulomb term at $U = 4t$. The length and size of the stripes should be understood relative to each other. Computed for a 16×16 system.* 85
- 5.23 *The DOS for a striped two layered system with doping at $x = 0.125$ and the Coulomb term at $U = 4t$. The first layer is red the second layer is blue. Computed for a 16×16 system.* 85

5.24	<i>Contour plot of the effect of the mean field potential from intermediate oxygen placed with a periodicity of 4 in the y direction. Left correspond to the first layer and right side corresponds to the second layer. The lattices are of size 16×16. Dark purple/blue corresponds to a value of 0.01 and white correspond to a value of size 0.18</i>	86
5.25	<i>The stripe order for a two layered coupled system with doping at $x = 0.125$, the Coulomb term at $U = 4$ and a mean field potential from intermediate oxygen placed with a periodicity of 4 in the y direction. The first 16 sites from above corresponds to the first layer and the next 16 sites correspond to the second layer. The length and size of the stripes should be understood relative to each other. Computed for a 16×16 system.</i>	87
5.26	<i>The stripe order for a two non-coupled layers with doping at $x = 0.125$, the Coulomb term at $U = 4$ and a mean field potential from intermediate oxygen placed with a periodicity of 4 in the y direction. The first 8 sites from above corresponds to the first layer and the next 8 sites correspond to the second layer. The length and size of the stripes should be understood relative to each other. Computed for a 16×16 system.</i>	87
5.27	<i>The stripe order for a multiple-layered system with doping at $x = 0.125$ and the Coulomb term at $U = 5t$ and hopping between layers are $t_{\perp} = 0.05t$. The length and size of the stripes should be understood relative to each other. Computed for a 8×8 system.</i>	90
5.28	<i>DOS for the first layer of a striped multiple layered system with doping at $x = 0.125$ and the Coulomb term at $U = 5t$. All DOS for the different layers are identical. Computed for a 8×8 system.</i>	92

Introduction

Superconductivity was first discovered in 1911 by the Dutch physicist Heike Kamerlingh Onnes. He showed that by cooling metal's, such as mercury and lead with liquid helium to a finite critical temperature T_c , the metals resistivity drops to zero, thereby creating a new state: superconductivity. Ever since 1911 superconductivity has been studied worldwide leading to the discovery of high-temperature superconductors with a critical temperature as high as 130 K. This new generation of superconductors first seen in the eighties aroused great interest among many physicists. Suddenly the idea of room temperature superconductors seemed obtainable.

Among the high-temperature superconductors were the cuprates a copper-based compound. The cuprates were first discovered in 1986 where they showed many new and exciting properties. They form a new class of d-wave superconductors with high critical temperatures not seen elsewhere. Cuprates are still a mystery and possibly hold the key to understanding and exploiting high-temperature superconductors. Cuprates are very sensitive to disorder due to their d-wave nature (breaking time reversal symmetries when probed) which furthers the interest in studying them.

The case of $\text{La}_2\text{CuO}_{4+y}$ (LCO+O) and $\text{La}_{2-x}\text{Sr}_x\text{CuO}_4$ (LSCO) have been studied since 1986 and many interesting things have been discovered such as stripe order and spin glass phases [27].

The simple lattice structure of cuprates and more particularly LSCO, makes them suitable for studying both from an experimental and theoretical point of view. Newer studies of $\text{La}_{2-x}\text{Sr}_x\text{CuO}_{4+y}$ (LSCO+O), which is the cuprate I will focus on, shows interesting results. It has the same lattice structure as LSCO with the one exception of excess oxygen in between the Cu layers. Interestingly, the critical temperature of LSCO+O is the same of an optimal doped LSCO crystal. Another interesting property of LSCO+O is that the the critical temperature is independent of strontium doping as long as the crystals are super-oxygenated. Furthermore the crystal shows, independent of strontium content, the stripe behavior of an optimal doped LSCO.

The superoxygenated crystal shows almost all of the behavior of an optimal doped LSCO, which poses a lot of questions. Another interesting feature of the cuprate is that we see that the superconducting transition temperature, T_c , coincides with the magnetic ordering temperature, T_N , $T_c = T_N$. Some questions to be answered are: Do we believe that the excess oxygen take over the characteristics of the strontium? Are the stripes generated by the excess oxygen?

From a theoretical point of view there are no calculations (to the best of my knowledge) involving LSCO+O. It is interesting to investigate some of the effects of this excess oxygen in a different doped crystal. Do we see if stripes appear and stabilizes no matter the strontium content? Another interesting calculation could be to see if the $T_c = T_N$ naturally appears from this excess oxygen.

In this Thesis I will give a review of the experimental study of LSCO+O until the present day. I will also try to explain some of the theoretical tools used to make calculations on superconductors in the crystal structure. And finally try to theoretically reproduce some of the experimental data and answer some of the questions raised from newly experiments.

CHAPTER 2

Superconductivity

In 1911 Heike Kamerlingh Onnes won the Nobel Prize [35] for his discovery of superconductivity. He cooled mercury down to less than 4.2 K whereupon he discovered that it lost its electrical resistance: superconductivity. In the following years scientists found that many other materials became superconducting at a low temperature named the critical temperature T_c . This critical temperature was around a few Kelvin. Later on it was discovered that those certain elements also exhibit superconducting properties under high pressure see 2.1. We now know that around half of all elements have a superconducting phase under the right circumstances. In this chapter we will review the theory necessary for the for understanding the calculations in chapter 5.

2.1 Introduction to Superconductivity

In this section there will be a brief description of the basic theoretical principles behind the phenomenon of superconductivity and an introduction to the first microscopic theory of superconductivity called BCS theory.

2.1.1 Meissner-Oschenfeld effect

The Meissner-Ochsenfeld effect is the expulsion of a magnetic field from a superconductor during its phase-transition to the superconducting state. Below the transition temperature, T_c , superconductors expel all interior magnetic fields. This is possible because there is a relation between the magnetic flux and a superconductor allowing the magnetic flux to be conserved by the superconductor see fig. 2.2.

KNOWN SUPERCONDUCTIVE ELEMENTS																	
■ BLUE = AT AMBIENT PRESSURE ■ GREEN = ONLY UNDER HIGH PRESSURE																	
1	2															3	4
1	H	2	He													5	6
3	Li	4	Be	5	B	6	C	7	N	8	O	9	F	10	Ne	11	12
11	Na	12	Mg	13	Al	14	Si	15	P	16	S	17	Cl	18	Ar	19	20
21	Sc	22	Ti	23	V	24	Cr	25	Mn	26	Fe	27	Co	28	Ni	29	30
37	Rb	38	Sr	39	Y	40	Zr	41	Nb	42	Mo	43	Tc	44	Ru	45	Rh
55	Cs	56	Ba	57	*La	72	Hf	73	Ta	74	W	75	Re	76	Os	77	Ir
87	Fr	88	Ra	89	+Ac	104	Rf	105	Ha	106	106	107	107	108	108	109	109
112	112	113	113	114	114	115	115	116	116	117	117	118	118	119	119	120	120

SUPERCONDUCTORS.ORG

* Lanthanide Series	58	59	60	61	62	63	64	65	66	67	68	69	70	71
	Ce	Pr	Nd	Pm	Sm	Eu	Gd	Tb	Dy	Ho	Er	Tm	Yb	Lu
+ Actinide Series	90	91	92	93	94	95	96	97	98	99	100	101	102	103
	Th	Pa	U	Np	Pu	Am	Cm	Bk	Cf	Es	Fm	Md	No	Lr

Figure 2.1: Periodic table with all known superconducting elements. The blue marked elements are for ambient pressure, the green are for high pressure. [41]

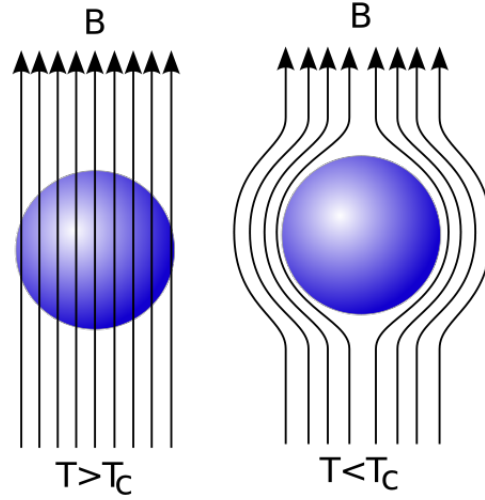


Figure 2.2: *Diagram of the Meissner-Ochsenfeld effect. Magnetic field lines, represented as arrows, in the normal state (left) and the superconducting state, are expelled from the sample when it is below its critical temperature T_c (right).*

One of the many properties that follows from having zero resistance and therefore being in a perfect conductor, the current can only be finite when the electric field in the conductor is zero:

$$\mathbf{E} = 0, \quad (2.1)$$

From Maxwell's equations we furthermore have:

$$\nabla \times \mathbf{E} = -\frac{\partial \mathbf{B}}{\partial t}, \quad (2.2)$$

In other words, the internal magnetic field is constant in time. From the equation above, we know that if you had a magnetic field in the superconductor at $T > T_c$ and then cools down the magnetic field will have the same value for $T < T_c$, when $\frac{\partial \mathbf{B}}{\partial t} = 0$.

The magnetic induction inside a superconductor is zero, and therefore the magnetic field cannot penetrate the superconductor. This is also true when the superconductor is placed in a weak external magnetic field.

When a superconductor is in the superconducting state, the moving surface charge, surface current, will induce a field that will exactly cancel out the applied field, so that the magnetic field inside the sample can maintain the value of zero. If however the external field becomes too strong, it will destroy the superconducting phase and the sample will return to its normal state. That the magnetic field inside is zero means that the magnetization is equal with opposite sign to the external field $\mathbf{M} = -\mathbf{H}$. We see this easily [7]:

$$\mathbf{B} = \mu_0(\mathbf{H} + \mathbf{M}) = 0. \quad (2.3)$$

Note that In the specific case of $\mathbf{B} = 0$ we have a perfect diamagnet. These properties were first observed in 1933 by W. Meissner and R. Oschenfeld[40] of which the name Meissner-Oschenfeld effect comes.

2.1.2 Two types of superconductors

The transition from a normal phase to a superconducting phase during an applied magnetic field can happen in two ways. We characterize these two ways with two classes of superconductors: type-I and type-II[3].

For the first type of superconductor, type-I, that the transition from superconducting state to normal state depends on the applied fields temperature-dependent critical value $H_c(T)$. Inside the entire sample the field \mathbf{B} is zero until the critical value $H_c(T)$ is reached where the sample transitions to a normal state. In other words, the sample exhibits the Meissner effect below the critical value $H_c(T)$ see fig. 2.3 left.

In a type-II superconductor, the magnetic field is not completely expelled from the sample at one certain critical value $H_c(T)$ [22]. In this type of superconductor there is instead two critical values for the applied field, an upper value $H_{c2}(T)$ and a lower value $H_{c1}(T)$ see fig. 2.3. At the lower critical value the applied magnetic field will gradually penetrate the sample until it is completely penetrated which is achieved at the upper critical value. Thus, the sample exhibits the Meissner effect below the lower critical value $H_{c1}(T)$. When the applied field is between the two critical values for this field, the sample becomes inhomogeneous containing both normal and superconducting states, in what is called a mixed state see fig. 2.4. In this mixed state cylinder shaped flux lines can pass through the sample creating

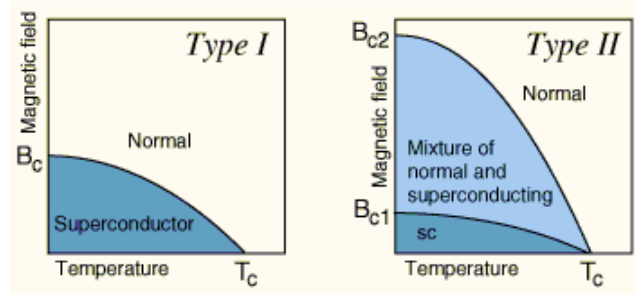


Figure 2.3: *Illustration of the phases of temperature as a function of applied field for type-I(left) and type-II (right) superconductor. From [22]*

regions where the superconductivity is suppressed. The current around the cylinders screens the flux lines so that the regions in between the normal state cylinders is superconducting. These cylinders are called vortices and the mix state is also referred to as the vortex state.

2.1.3 BCS Theory

BCS theory is a microscopic theory for superconductivity, proposed by John Bardeen, Leon Cooper, and John Robert Schrieffer in 1957[24],[25]. In 1972 they received the Nobel prize in physics for this theory.

With a microscopic theory for superconductivity, two important predictions were made: Namely the isotopic effect $T_c M^{-\alpha}$, which tells us that the transition temperature changes with the mass of the crystal lattice ions M . The BCS theory predicts the isotopic exponential to be $\alpha = 1/2$. The second main prediction is the existence of the energy gap 2Δ , due to electron-phonon coupling, at the Fermi level, separating the occupied and unoccupied states. The BCS theory is built upon three major insights:

- 1: The effective forces between electrons can sometimes be attractive in a solid, due to coupling between electrons and phonons in the underlying crystal lattice.
- 2: For a simple system of just two electrons outside an occupied Fermi surface, the electrons form a stable pair bound state also called a “Cooper pair”.

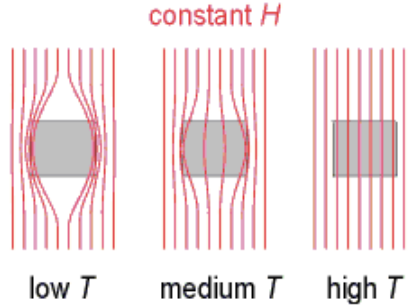


Figure 2.4: *Schematic illustration of the temperature dependence of the flux lines of a type-II superconductor.*

3: There must exist a many-particle wave function for which all the electrons near to the Fermi surface are paired up. This has the form of a coherent state wave function.

We will discuss the three insights in the following.

2.1.3.1 The electron-phonon interaction

It seems counter intuitive that that there must exist an attractive force, since electrons usual repel each other due to the Coulomb repulsion:

$$V(r - r') = \frac{e^2}{4\pi\epsilon_0|r - r'|}. \quad (2.4)$$

The Coulomb repulsion is always true for bare electrons, however for electrons in a metal we should think of the them as quasiparticles. Where quasiparticles should be interpreted as a perturbation, in a solid, that behaves as a electron (with different mass) and that may conveniently be regarded as one. When an electron moves another must move out of the way due to both the Pauli Principle , and because they prefer to minimize the repulsive Coulomb energy $V(r - r')$. It turns out that between quasiparticles the effective Coulomb force is substantially reduced by screening.

The Thomas Fermi model (screening method) predicts an effective electron-

electron interaction of the form [3]:

$$V_{TF}(r - r') = \frac{e^2}{4\pi\epsilon_0 |r - r'|} e^{-|r - r'|/r_{TF}}, \quad (2.5)$$

where r_{TF} is the Thomas Fermi screening length. This will be discussed later in this chapter. The effect of the screening is to reduce the Coulomb repulsion, and the effective repulsion force is then short range in space. i.e. it vanishes for $|r - r'| > r_{TF}$. The electrons interact with each other via their interaction with the phonons of the crystal lattice.

So how does an electron-phonon interaction arise? Consider a phonon of wave vector q in a solid. The effective Hamiltonian for the phonon in the solid will just be a set of quantum harmonic oscillators, one for each wave vector q and phonon mode [3]:

$$\hat{H} = \sum_{q,\lambda} \hbar\omega_{q,\lambda} (a_{q,\lambda}^\dagger a_{q,\lambda} + \frac{1}{2}), \quad (2.6)$$

where $a_{q,\lambda}^\dagger$ and $a_{q,\lambda}$ create or annihilates a phonon mode λ . There are $3N_a$ phonon modes in a crystal with N_a atoms per unit cell, where N_a is a natural number. For simplicity let us assume that there is only one atom per unit cell. In other words there are just three phonon modes.

Remembering the expression for the ladder operator the wave function with n phonons is:

$$\Psi_n(x) = \frac{1}{n!^{1/2}} (\hat{a}^\dagger)^n \Psi_0(x). \quad (2.7)$$

The atoms located at R_i will be displaced by:

$$\delta R_i = \sum_{q,\lambda} e_{q\lambda} \left(\frac{\hbar}{2M\omega_{q\lambda}} \right) (a_{q\lambda}^\dagger + a_{-q\lambda}) e^{iqR}, \quad (2.8)$$

where $e_{q,\lambda}$ is the interaction in the direction of the atomic displacement for the mode $q\lambda$. The displacement δR_i of the crystal lattice will produce a modulation of the electron charge density and the effective potential for the electron in the solid $v_f(r)$. We define the deformation potential by:

$$V_i(r) = \sum_i \frac{\partial v_i(\mathbf{r})}{\partial \mathbf{R}_i} \delta \mathbf{R}_i. \quad (2.9)$$

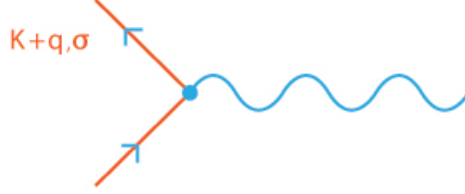


Figure 2.5: *Feynman diagram for an electron-phonon interaction. The electron is scattered from K to $K + q$ resulting in an annihilation of a phonon of wave vector $-q$.*

This is a periodic modulation of the potential with wavelength $2\pi/q$. An electron moving through the crystal lattice will experience this periodic potential and undergo scattering so if it is initially in a Bloch state $\Psi_{n,k}(r) = e^{ikr}u(r)$ it can be diffracted into a new Bloch state $\Psi_{n',k-q}(r')$. The net effect is that the diffraction is that an electron has been scattered from a state with crystal momentum k to one with momentum $q - k$. We see that the "extra momentum" has been provided by the phonon. In this formalism we do not distinguish between creating a phonon of momentum q or annihilating a phonon of momentum $-q$. In other words, the electron-phonon interaction arises because an electron moving through a crystal lattice will experience a periodic potential and undergo diffraction. So if the electron is initially in a periodic and repeating state (Bloch state) k , it can be scattered to another Bloch state k' . The net effect of this is that an electron has been scattered from a state with crystal momentum k to one with momentum $k - q$, where the extra momentum q has been provided by the phonon. The electron emits a phonon which propagates for a while and is then absorbed by another electron. So electrons can transfer momentum to one another implying an effective interaction between them. This is in the literature normally illustrated by a electron-phonon interaction, vertex $g_{q,\lambda}$, in a Feynman diagram fig. 2.5 and 2.6

We wish to simplify the interaction between the electron and phonon, and do so by replacing the vertex $g_{q,\lambda}$ by a constant g_{eff} . We then get the following expression for the interaction

$$V_{\text{eff}}(q, \omega) = |g_{\text{eff}}| \frac{1}{\omega^2 - \omega_D^2} \quad (2.10)$$



Figure 2.6: *Feynman diagram for an electron-electron interaction. The electron with spins σ_1 and σ_2 are scattered from K_1 to $K_1 + q$ and K_2 to $K_2 + q$ via the phonon with wave vector $-q$. The vertex is for an electron-phonon interaction.*

where ω_D is the Debye frequency. We note that for $\omega < \omega_D$ the interaction is attractive, and for $\omega > \omega_D$ the interaction is repulsive. We are only interested in electrons which lie within $\pm k_B T$ of the Fermi energy. The temperature of interest to SC is $\hbar\omega_D \gg k_B T$. With this in consideration we can assume the simple form:

$$V_{\text{eff}} = -|g_{\text{eff}}|^2, \quad (2.11)$$

Where $k_B T \ll \hbar\omega_D$. The corresponding effective Hamiltonian for the effective electron-electron interaction is then given by

$$\hat{\mathcal{H}}_1 = -|g_{\text{eff}}|^2 \sum_{k_1 \sigma_1 k_2 \sigma_2 q} c_{k_1+q \sigma_1}^\dagger c_{k_2-q \sigma_1}^\dagger c_{k_1 \sigma_1} c_{k_2 \sigma_2} \quad (2.12)$$

We have the restriction that the energy of the electron must be in the range of $\pm \hbar\omega_D$ of the Fermi surface, i.e. $|\epsilon_{k_i} - \epsilon_F| < \hbar\omega_D$. So we have interacting electrons near the Fermi surface, but the Bloch state for inside and outside the Fermi surface are unaffected [2.7](#).

2.1.3.2 Cooper pairs

In the previous section we have established that the effective interaction between electrons can be attractive, but only near the Fermi surface. This

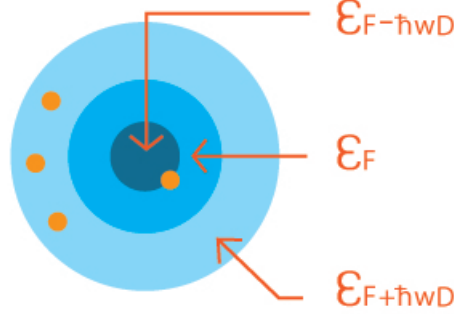


Figure 2.7: *Schematic illustration of the Fermi surface. There is an attraction between electrons near the Fermi surface. The electrons are scattered to $\pm q$ if they lie within $\epsilon_f \pm \hbar\omega_D$.*

naturally raises the question, what is the effect of the attraction for only a single pair of electrons? Surprisingly, they form a bound state.

The independent Bloch electrons are unstable to even the weakest attractive interaction between the particles. Therefore, the full BCS state is a configuration where every electron at the Fermi surface is part of a pair. With this in mind we model the phenomenon as following:

We assume a spherical Fermi surface at zero temperature, where all the states with $k < k_F$ are occupied. Then place two extra electrons outside of the Fermi surface which interact by the electron -phonon interaction see fig. 2.8.

The two particle wave function of the extra electrons is given by [3]:

$$\Psi(r_1, \omega_1, r_2, \omega_2) = e^{ik_{cm}R_{cm}\varphi(r_1-r_2)}\psi_{\omega_1,\omega_2}^{spin}, \quad (2.13)$$

where k_{cm} is the total pair momentum and R_{cm} is the center of mass $(r_1 + r_2/2)$. Note that the minimum energy corresponds to the center of mass where in the ground state $k_{cm} = 0$. We will from now on always assume that the particles are in the ground state i.e $k_{cm} = 0$. The spin wave function $\psi_{\omega_1,\omega_2}^{spin}$ can either be a spin singlet or spin triplet. For a spin singlet we have that the total spin is zero, $S = 0$. For a spin triplet we on the other hand

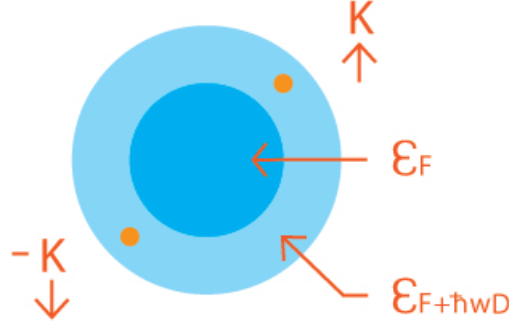


Figure 2.8: *Schematic illustration of the Fermi spherical surface at zero temperature. All the states are within $k < k_F$ are occupied. Two electrons are placed outside the Fermi surface and interact via electron-phonon interaction.*

have that the total spin must be one, $S = 1$. So for a singlet we have:

$$\psi_{\omega_1, \omega_2}^{spin} = \frac{1}{\sqrt{2}}(|\uparrow\downarrow\rangle - |\downarrow\uparrow\rangle), \quad (2.14)$$

and for triplet we have:

$$\psi_{\omega_1, \omega_2}^{spin} = \left\{ \begin{array}{l} |\uparrow\uparrow\rangle \\ \frac{1}{\sqrt{2}}(|\uparrow\downarrow\rangle + |\downarrow\uparrow\rangle) \\ |\downarrow\downarrow\rangle \end{array} \right\}. \quad (2.15)$$

Let us from now on assume that Cooper pairs are singlets [3]. We remember the fermion antisymmetry which indicates:

$$\Psi(r_1, \omega_1, r_2, \omega_2) = -\Psi(r_2, \omega_2, r_1, \omega_1). \quad (2.16)$$

Since $\psi_{\omega_1, \omega_2}^{spin}$ is odd, the wave function φ must be even. We now expand $\psi(r_1 - r_2)$ in terms of the Bloch waves (free electron plane wave). Note first that a single Bloch state is $\Psi_k(r) = e^{ikr}u(r)$, where $u(r) = u(r + R)$. We get the following expression:

$$\psi(r_1 - r_2) = \sum_k \psi_k e^{ik(r_1 - r_2)}, \quad (2.17)$$

were ψ_k are the expansion coefficients. Thus we have (due to Fermion antisymmetry) that $\psi_k = \psi_{-k}$. The full pair wave function is:

$$\Psi(r_1, \omega_1, r_2, \omega_2) = \sum_k \psi_k \begin{pmatrix} \Psi_{k\uparrow}(r_1) & \Psi_{k\downarrow}(r_2) \\ \Psi_{-k\uparrow}(r_1) & \Psi_{-k\downarrow}(r_2) \end{pmatrix}, \quad (2.18)$$

where we only sum over k that satisfy $k > k_F$. The above equation is just a sum of Slater determinants, and each Slater determinant product has a spin up \uparrow and a spin down \downarrow and a positive momentum k and negative momentum $-k$. If we now substitute the Slater determinant wave function $\Psi(r_1, \omega_1, r_2, \omega_2)$ into the Schrödinger equation we can get an expression for the total energy for the two particle system. First we remember the relation $|\Psi\rangle = \sum_k \psi_k |\Psi_k\rangle$ where

$$|\Psi_k\rangle = \begin{pmatrix} \Psi_{k\uparrow}(r_1) & \Psi_{k\downarrow}(r_2) \\ \Psi_{-k\uparrow}(r_1) & \Psi_{-k\downarrow}(r_2) \end{pmatrix}, \quad (2.19)$$

which obey the two body Schrödinger equation $\hat{\mathbf{H}} |\Psi_k\rangle = E |\Psi_k\rangle$.

If we then multiply the equation $|\Psi\rangle$ from the left with $\langle\Psi_k|$ we can take out the terms for a given k .

The Hamiltonian consist of the two energies of Bloch states ϵ_k and the effective interaction $-|g_{\text{eff}}|^2$. The effective interaction takes the momentum $q = k' - k$ from one of the electrons and transfer it to the other electron. In other words, a pair of electrons $k, -k$ becomes $k', -k'$ with a matrix element $-|g_{\text{eff}}|^2$. k is limited to a thin shell between k_F and $k_F + \omega_D/v$, where v is the group velocity at the Fermi surface.

The energy E can be found by a self-consistent argument, where we end up with [3]:

$$-E = 2\hbar\omega_D e^{-1/\lambda}. \quad (2.20)$$

Where λ is the electron-phonon coupling parameter given by:

$$\lambda = |g_{\text{eff}}|^2 g(\epsilon_f). \quad (2.21)$$

We know that $\lambda \ll 1$. So a bound state does exist and furthermore we see that its energy is exponentially small when λ is small. The BCS energy scale for a superconductor is set by the Debye energy, but multiplied by a

very small exponentially factor. This is why the transition temperatures T_c are so small compared with other energy scales in solids. It is worth noting that it is not always that an attractive interaction in three dimensions leads to a bound state.

The presence of the filled Fermi sea is a key aspect of the BCS theory. So, the whole Fermi surface would be unstable to the creation of such pairs. As soon as there is an effective attractive interaction essentially every electron at the Fermi surface will become bound into a Cooper pair.

2.1.3.3 The BCS wave function

In this section we will construct a many particle wave function in which every electron is paired. We will write down a coherent state of Cooper pairs. We do so, by assuming it is possible to construct operators which annihilate and create electron pairs at position R , $\hat{\phi}^\dagger(R)$ and $\hat{\phi}(R)$. Note that these operators do not obey normal Bose commutation laws, and cannot create or annihilate boson particles.

We need to find a uniform translationally invariant solution, and it turns out that it is more convenient to work in k -space.

Let us define a pair-creation operator by [3]:

$$\hat{p}_k^\dagger = c_{k\uparrow}^\dagger c_{-k\downarrow}^\dagger. \quad (2.22)$$

The equation above creates a pair of electrons of zero crystal momentum, and opposite spins. In terms of these operators we have the following coherent state of many-body wave functions:

$$|\psi_{BCS}\rangle = c \exp \left(\sum_k \alpha_k \hat{p}_k^\dagger \right) |0\rangle, \quad (2.23)$$

where c is some constant, α_k is a complex number that can be adjusted to minimize the total energy and $|0\rangle$ is the vacuum state. The new operators do not obey the Bose commutation relation $[\hat{p}_k^\dagger, \hat{p}_k] \neq 1$, but they do commute with each other $[\hat{p}_k^\dagger, \hat{p}_{k'}^\dagger] = 0$ for $k \neq k'$.

Let us examine whether they also commute for $k = k'$. We have that the product of $\hat{p}_k^\dagger \hat{p}_k^\dagger$ contains four electron creations for some k point:

$$\hat{p}_k^\dagger \hat{p}_k^\dagger = (\hat{p}_k^\dagger)^2 = \hat{c}_{k\uparrow}^\dagger \hat{c}_{-k\downarrow}^\dagger \hat{c}_{k\uparrow}^\dagger \hat{c}_{-k\downarrow}^\dagger = \hat{c}_{k\uparrow}^\dagger \hat{c}_{k\uparrow}^\dagger \hat{c}_{-k\downarrow}^\dagger \hat{c}_{-k\downarrow}^\dagger = 0 \cdot 0 = 0. \quad (2.24)$$

Knowing that the operators commute we rewrite the coherent state as a product of exponentials:

$$\begin{aligned} |\psi_{BCS}\rangle &= c \exp \left(\sum_k \alpha_k \hat{p}_k^\dagger \right) |0\rangle \\ &= c \prod_k \exp(\alpha_k \hat{p}_k^\dagger) |0\rangle. \end{aligned} \quad (2.25)$$

Expanding the exponential, all terms of quadratic order or higher are zero as seen in equation (2.24):

$$|\psi_{BCS}\rangle = c \prod_k (1 + \alpha_k \hat{p}_k^\dagger) |0\rangle. \quad (2.26)$$

Let us find the normalization constant c :

$$\begin{aligned} 1 &= \langle 0 | (1 + \alpha_k^* \hat{p}_k^\dagger) (1 + \alpha_k \hat{p}_k^\dagger) | 0 \rangle \\ &= \langle 0 | (1 + \hat{p}_k^\dagger \hat{p}_k^\dagger + \alpha_k' \hat{p}_k^\dagger + \alpha_k \hat{p}_k^\dagger + \alpha_k \hat{p}_k^\dagger \alpha_k^*) | 0 \rangle \\ &= \langle 0 | (1 + \alpha_k^* \hat{p}_k^\dagger + \alpha_k \hat{p}_k^\dagger) | 0 \rangle \\ &= 1 |\alpha_k|^2 = c \end{aligned} \quad (2.27)$$

And we get:

$$|\psi_{BCS}\rangle = \prod_k (u_k^* + v_k^*) \hat{p}_0^\dagger |0\rangle. \quad (2.28)$$

Where $u_k^* = 1/(1 + |\alpha_k|^2)$ and $v_k^* = \alpha_k/(1 + |\alpha_k|^2)$, furthermore we have that $|u_k^*|^2 + |v_k^*|^2 = 1$.

Now we have the parameters u_k and v_k which minimizes the energy. For the electron- electron interaction we then get:

$$\hat{\mathcal{H}}_I = -|g_{\text{eff}}|^2 \sum c_{k_1+q\sigma_1}^\dagger c_{k_2-q\sigma_2}^\dagger c_{k_1\sigma_1} c_{k_2\sigma_2}. \quad (2.29)$$

And we get the relevant Hamiltonian for the many-body wave function:

$$\hat{\mathcal{H}} = \sum_{k\sigma} c_{k\sigma}^\dagger c_{k\sigma} - |g_{\text{eff}}|^2 \sum c_{k_1+q\sigma_1}^\dagger c_{k_2-q\sigma_2}^\dagger c_{k_1\sigma_1} c_{k_2\sigma_2}. \quad (2.30)$$

To get the full microscopic theory we still need a mean-field approach to the Hamiltonian and a unitary transformation that will assure that it is diagonal in the operators $c_{k\sigma}^\dagger$ and $c_{k\sigma}$. We will do so later on for a Hamiltonian which is more appropriate for calculations in Chapter 5.

2.2 Hamiltonian and mathematical methods

In this section I will introduce the Hamiltonian and the mathematical methods and techniques that are required for calculating densities in a cuprate system.

2.2.1 Screening of the Coulomb interactions

A necessary element of the Hamiltonian is the description of the extra oxygen in the super oxygenated cuprate $\text{La}_x\text{Sr}_{2-x}\text{CuO}_{4+y}$. We do this by introducing a mean-field potential given by some Coulomb interaction with screening. By not including any type of screening of the long range Coulomb interaction, the spectrum of excitations near the Fermi surface gets an unphysical logarithmic singularity. However, by including screening in the approximation we achieve a more realistic description of the particle interactions.

We are particularly interested in the electrostatic potential $W(r)$ around a small probe charge Q , where we assume no time dependence. The potential without screening is given by:

$$W(r) = \frac{Q}{r}. \quad (2.31)$$

Screening is a consequence of a redistribution of the electronic density due to the potential. The potential will also undergo a change due to the electronic density, and they will affect each other back and forth. Therefore the potential and the density distribution must be calculated self-consistently. The screening itself will be a static linear-response.

The response of the density due to the potential is given in momentum

space by:

$$\delta n(q) = \xi(q)eW(r) - \nu_0, \quad (2.32)$$

where $\xi(q)$ is change due to electronic density and e is the elementary charge. ν_0 is treated like constant(it comes from the change in electron density due to the potential). The reaction of the density modulation due to the potential is given by the Gauss equation [6]:

$$-\frac{1}{4\pi}\nabla^2 W(x) = Q\delta(x) + e\delta n(x). \quad (2.33)$$

In the momentum representation the above takes the form:

$$\frac{q^2}{4\pi}W(q) = Q + e\delta n(q) \quad (2.34)$$

Now, putting equation (2.32) and equation (2.34) together we get:

$$W(q) = \frac{Q}{\frac{q^2}{4\pi}e^2\xi(q)}. \quad (2.35)$$

The Fourier transform of the above gives the screened interaction potential $W(r)$ in real space. The simplest approximation, known as the Thomas-Fermi screening, is under the assumption that all coordinate dependences are slow and that the response due to the potential is in a static approximation. We then get the density of states at the Fermi level:

$$\delta n(q) = \xi(q)eW(r) - \nu_0 = \xi(q = 0), \quad (2.36)$$

We now rewrite the potential $W(q)$:

$$W(q) = \frac{Q}{\frac{q^2}{4\pi} + e^2\nu_0} = \frac{4\pi Q}{q^2 + 4\pi e^2\nu_0} = \frac{4\pi Q}{q^2 + \kappa^2}, \quad (2.37)$$

where $\kappa^2 = 4\pi e^2\nu_0$.

The Fourier transform of this potential gives:

$$W(r) = \frac{Q}{r} \exp(-\kappa r), \quad (2.38)$$

where κ^{-1} should be interpreted as the screening length.

In the case of multiple charges Q_n located at R_n the screening potential becomes:

$$W(r)_n = \frac{Q}{r - R_n} \exp(-\kappa(r - R_n)). \quad (2.39)$$

The above equation is the screening of the Coulomb interactions which we will use to describe the intermediate oxygen y in $\text{La}_x\text{Sr}_{2-x}\text{CuO}_{4+y}$. In the specific case, where the charge comes from intermediate oxygen we will refer to the potential as $W_{R_o}(r_i)$.

2.2.2 The Hamiltonian

The Hamiltonian we use in calculations in this thesis is given by[20]:

$$\begin{aligned} \hat{H} = & - \sum_{ij\sigma} t_{ij} \hat{c}_{i\sigma}^\dagger \hat{c}_{j\sigma} + \sum_{i\sigma} (W_{R_o}(r_i) - \mu) \hat{n}_{i\sigma} \\ & + U \sum_i \hat{n}_{i\uparrow} \hat{n}_{i\downarrow} - V \sum_{\langle ij \rangle} \hat{n}_{i\uparrow} \hat{n}_{j\downarrow}. \end{aligned} \quad (2.40)$$

Here, $\langle ij \rangle$ means summation of nearest neighbors. The first term in the Hamiltonian includes the tight-binding approximation. In the tight-binding approximation, the electrons are assumed to occupy the standard orbitals of their principal atoms. They can then 'hop' between atoms through orbitals which result in conduction. The second term is the potential impurity field, where μ is the chemical potential, and $W_{R_o}(r_i)$ is the mean field potential of oxygen which is situated between the sites, see section 2.2.1. The third term includes the onsite repulsion, which comes from the Coulomb repulsion between electrons at the same atomic orbitals. We assume that $U > 0$. The last term represents the attraction between electrons in the superconducting state. We assume that $V > 0$. There is a nearest neighbor attraction in order to represent the superconducting pairing in cuprates, a d -wave pairing.

2.2.3 The mean-field Hamiltonian

It is too complicated to look at all the interacting particles, so instead we look at the correlation on the average which means that the effect of

the other particles is included as a mean density. Thus we have an effective single particle problem. This is the idea behind mean-field approximation[6]. First note $\hat{a}_{i\uparrow} = \langle \hat{a}_{i\uparrow} \rangle + (\hat{a}_{i\uparrow} - \langle \hat{a}_{i\uparrow} \rangle)$. Secondly we have:

$$\begin{aligned}
 \hat{a}_{i\sigma}\hat{a}_{j\sigma'} &= (\langle \hat{a}_{i\sigma} \rangle + (\hat{a}_{i\sigma} - \langle \hat{a}_{i\sigma} \rangle))(\langle \hat{a}_{j\sigma'} \rangle + (\hat{a}_{j\sigma'} - \langle \hat{a}_{j\sigma'} \rangle)) \\
 &= \langle \hat{a}_{i\sigma} \rangle \langle \hat{a}_{j\sigma'} \rangle + (\hat{a}_{i\sigma} - \langle \hat{a}_{i\sigma} \rangle) \langle \hat{a}_{j\sigma'} \rangle + \langle \hat{a}_{i\sigma} \rangle (\hat{a}_{j\sigma'} - \langle \hat{a}_{j\sigma'} \rangle) \\
 &\quad + (\hat{a}_{i\sigma} - \langle \hat{a}_{i\sigma} \rangle) (\hat{a}_{j\sigma'} - \langle \hat{a}_{j\sigma'} \rangle) \\
 &\approx \langle \hat{a}_{i\sigma} \rangle \langle \hat{a}_{j\sigma'} \rangle - 2 \langle \hat{a}_{i\sigma} \rangle \langle \hat{a}_{j\sigma'} \rangle + \langle \hat{a}_{i\sigma} \rangle \hat{a}_{j\sigma'} + \hat{a}_{i\sigma} \langle \hat{a}_{j\sigma'} \rangle \\
 &= \langle \hat{a}_{i\sigma} \rangle \hat{a}_{j\sigma'} + \hat{a}_{i\sigma} \langle \hat{a}_{j\sigma'} \rangle - c,
 \end{aligned} \tag{2.41}$$

where $c = \langle \hat{a}_{i\sigma} \rangle \langle \hat{a}_{j\sigma'} \rangle$ is a constant. This is also true for $i = j$ and $\sigma = \sigma'$. In the third and fourth term of the Hamiltonian we get:

$$U \sum_i \hat{n}_{i\uparrow} \hat{n}_{i\downarrow} \approx U \sum_i (\langle \hat{n}_{i\uparrow} \rangle \hat{n}_{i\downarrow} + \hat{n}_{i\uparrow} \langle \hat{n}_{i\uparrow} \rangle - c). \tag{2.42}$$

We define the electron density as

$$n_i = \langle \hat{n}_{i\uparrow} + \hat{n}_{i\downarrow} \rangle \tag{2.43}$$

and the magnetization as

$$m_i = \langle \hat{n}_{i\uparrow} - \hat{n}_{i\downarrow} \rangle \tag{2.44}$$

We then get:

$$\begin{aligned}
 U \sum_i \hat{n}_{i\uparrow} \hat{n}_{i\downarrow} &\approx U \sum_i \left(\left(\frac{n_i + m_i}{2} \right) \langle \hat{n}_{i\downarrow} \rangle + \left(\frac{n_i - m_i}{2} \right) \langle \hat{n}_{i\uparrow} \rangle \right) - c_1 \\
 &= U \sum_i \left((n_i + m_i) \langle \hat{n}_{i\downarrow} \rangle + (n_i - m_i) \langle \hat{n}_{i\uparrow} \rangle \right) - 2c_1.
 \end{aligned} \tag{2.45}$$

For the fourth term of the Hamiltonian we get:

$$\begin{aligned}
 -V \sum_{\langle ij \rangle} \hat{n}_{i\uparrow} \hat{n}_{j\downarrow} &= -V \sum_{\langle ij \rangle} \hat{c}_{i\uparrow}^\dagger \hat{c}_{i\uparrow} \hat{c}_{j\downarrow}^\dagger \hat{c}_{j\downarrow} \\
 &= -V \sum_{\langle ij \rangle} \hat{c}_{i\uparrow} \hat{c}_{j\downarrow} \hat{c}_{j\downarrow}^\dagger \hat{c}_{i\uparrow}^\dagger \\
 &\approx -V \sum_{\langle ij \rangle} (\langle \hat{c}_{i\uparrow} \hat{c}_{j\downarrow} \rangle \hat{c}_{j\downarrow}^\dagger \hat{c}_{i\uparrow}^\dagger + \hat{c}_{i\uparrow} \hat{c}_{j\downarrow} \langle \hat{c}_{j\downarrow}^\dagger \hat{c}_{i\uparrow}^\dagger \rangle) - c.
 \end{aligned} \tag{2.46}$$

We define the following potential $\Delta_{ij} = -V\langle\hat{c}_{i\uparrow}\hat{c}_{j\downarrow}\rangle = -V\langle\hat{c}_{i\uparrow}\hat{c}_{j\downarrow}\rangle^*$ and get:

$$-V \sum_{\langle ij \rangle} \hat{n}_{i\uparrow} \hat{n}_{j\downarrow} = \sum_{\langle ij \rangle} (\Delta_{ij} \hat{c}_{j\downarrow}^\dagger \hat{c}_{i\uparrow}^\dagger + \hat{c}_{i\uparrow} \hat{c}_{j\downarrow} \Delta_{ij}^*) - c_2. \quad (2.47)$$

We will in the following calculations absorb the constants in μ . The mean-field Hamiltonian is then:

$$\begin{aligned} \hat{\mathcal{H}} = & - \sum_{ij\sigma} t_{ij} \hat{c}_{i\sigma}^\dagger \hat{c}_{j\sigma} + \sum_{i\sigma} (W_{R_o}(r_i) - \mu) \hat{n}_{i\sigma} \\ & + U \sum_{i\sigma} (n_i - \sigma m_i) \hat{n}_{i\sigma} \\ & + \sum_{\langle ij \rangle} (\Delta_{ij} \hat{c}_{i\uparrow}^\dagger \hat{c}_{j\delta\downarrow}^\dagger + H.c), \end{aligned} \quad (2.48)$$

where H.c means hermitian conjugate.

2.2.4 The Bogoliubov transformation

The Bogoliubov transformation is a unitary transformation i.e. a unitary representation into another unitary representation. Furthermore the transformation is restricted to obey the canonical commutation and anti-commutation relations. We will focus on the anti-commutation since we are interested in the fermionic creation and annihilation operators:

$$\{\hat{\gamma}_n^\dagger, \hat{\gamma}_n\} = 1 \quad (2.49)$$

and

$$\{\hat{\gamma}_n, \hat{\gamma}_n\} = 0. \quad (2.50)$$

This of course applies regardless of the spin orientation of $\hat{\gamma}_n$ and $\hat{\gamma}_n^\dagger$. We define a new set of operators to include both spin and the gammas[3]:

$$\hat{a}_{i,\sigma} = u_{i\sigma} \hat{\gamma}_\sigma + v_{i\sigma}^* \hat{\gamma}_{\sigma'}^\dagger \quad (2.51)$$

and

$$\hat{a}_{i,\sigma}^\dagger = u_{i\sigma}^* \hat{\gamma}_\sigma^\dagger + v_{i\sigma} \hat{\gamma}_{\sigma'}. \quad (2.52)$$

The fermionic anticommutation relations should still apply, let us verify that it is so. Note however the spin dependence of the new operators:

$$\begin{aligned}
 \{\hat{a}_{i,\sigma}, \hat{a}_{j,\sigma'}\} &= (u_{i\sigma}v_{j\sigma'}^* \{\hat{\gamma}_\sigma, \hat{\gamma}_\sigma^\dagger\} + v_{i\sigma}^*u_{j\sigma'} \{\hat{\gamma}_\sigma^\dagger, \hat{\gamma}_\sigma\}) \\
 &= u_{i\sigma}v_{j\sigma'}^* \cdot 1 + v_{i\sigma}^*u_{j\sigma'} \cdot 1 \\
 &= u_{i\sigma}v_{j\sigma'}^* + v_{i\sigma}^*u_{j\sigma'} \\
 &= 0.
 \end{aligned} \tag{2.53}$$

For the case of $\sigma = \sigma'$ we have:

$$\begin{aligned}
 \{\hat{a}_{i,\sigma}^\dagger, \hat{a}_{j,\sigma}\} &= (u_{i\sigma}^*v_{j\sigma} \{\hat{\gamma}_\sigma^\dagger, \hat{\gamma}_\sigma\} + v_{i\sigma}u_{j\sigma}^* \{\hat{\gamma}_\sigma, \hat{\gamma}_\sigma^\dagger\}) \\
 &= u_{i\sigma}^*v_{j\sigma} \cdot 1 + v_{i\sigma}u_{j\sigma}^* \cdot 1 \\
 &= u_{i\sigma}^*v_{j\sigma} + v_{i\sigma}u_{j\sigma}^* \\
 &= \delta_{ij},
 \end{aligned} \tag{2.54}$$

and for different spins:

$$\begin{aligned}
 \{\hat{a}_{i,\sigma}^\dagger, \hat{a}_{j,\sigma'}\} &= (u_{i\sigma}^*v_{j\sigma'} \{\hat{\gamma}_\sigma^\dagger, \hat{\gamma}_{\sigma'}^\dagger\} + v_{i\sigma}u_{j\sigma'}^* (\hat{\gamma}_\sigma, \hat{\gamma}_{\sigma'})) \\
 &= u_{i\sigma}^*v_{j\sigma'} \cdot 0 + v_{i\sigma}u_{j\sigma'}^* \cdot 0 \\
 &= 0
 \end{aligned} \tag{2.55}$$

so finally we see that canonical anticommutation holds:

$$\{\hat{a}_{i,\sigma}^\dagger, \hat{a}_{j,\sigma'}\} = \delta_{ij}\delta_{\sigma\sigma'}, \tag{2.56}$$

$$\{\hat{a}_{i,\sigma}, \hat{a}_{j,\sigma'}\} = 0, \tag{2.57}$$

$$\{\hat{a}_{i,\sigma}^\dagger, \hat{a}_{j,\sigma'}^\dagger\} = 0. \tag{2.58}$$

If we expand the transformations to include more states n we finally arrive at the Bogoliubov transformation:

$$\hat{c}_{i\uparrow} = \sum_n (u_{n,i\uparrow} \hat{\gamma}_{n\uparrow} + v_{n,i\uparrow} \hat{\gamma}_{n\downarrow}^\dagger), \tag{2.59}$$

$$\hat{c}_{i\uparrow}^\dagger = \sum_n (u_{n,i\uparrow}^* \hat{\gamma}_{n\uparrow}^\dagger + v_{n,i\uparrow}^* \hat{\gamma}_{n\downarrow}), \tag{2.60}$$

$$\hat{c}_{i\downarrow} = \sum_n (u_{n,i\downarrow} \hat{\gamma}_{n\downarrow} + v_{n,i\downarrow} \hat{\gamma}_{n\uparrow}^\dagger), \tag{2.61}$$

$$\hat{c}_{i\downarrow}^\dagger = \sum_n (u_{n,i\downarrow}^* \hat{\gamma}_{n\downarrow}^\dagger + v_{n,i\downarrow}^* \hat{\gamma}_{n\uparrow}). \tag{2.62}$$

The sums are over all positive energies. $\hat{\gamma}_{n\sigma}$ and $\hat{\gamma}_{n\sigma}^\dagger$ is the annihilation and creation operator for non-interacting fermionic quasiparticles.

2.2.5 The Bogoliubov-de Gennes Equations

We will derive the Bogoliubov-de Gennes equations by the standard method [14].

We will first examine the commutator of the Hamiltonian and the operators $\hat{c}_{i\downarrow}$ and $\hat{c}_{i\uparrow}$. The mean-field Hamiltonian is given by:

$$\begin{aligned}\hat{\mathcal{H}} = & - \sum_{ij\sigma} t_{ij} \hat{c}_{i\sigma}^\dagger \hat{c}_{j\sigma} + \sum_{i\sigma} (\epsilon_{i\sigma} - \mu) \hat{n}_{i\sigma} \\ & + \sum_{i\sigma} W(r_i) \hat{n}_{i\sigma} + U \sum_{i\sigma} (n_i - \sigma m_i) \hat{n}_{i\sigma} \\ & + \sum_{\langle ij \rangle} (\Delta_{ij} \hat{c}_{i\uparrow}^\dagger \hat{c}_{j\downarrow}^\dagger + h.c.).\end{aligned}\tag{2.63}$$

For any constant A we have the following relation:

$$\begin{aligned}A[\hat{c}_{i\sigma}^\dagger \hat{c}_{j\sigma}, \hat{c}_{i\sigma}] &= A[\hat{c}_{i\sigma}^\dagger \hat{c}_{j\sigma}, \hat{c}_{i\sigma}] \\ &= A(\hat{c}_{i\sigma}^\dagger \hat{c}_{j\sigma}, \hat{c}_{i\sigma} - \hat{c}_{i\sigma}^\dagger \hat{c}_{i\sigma}, \hat{c}_{j\sigma}) \\ &= A(-\{\hat{c}_{i\sigma}^\dagger \hat{c}_{i\sigma}\}, \hat{c}_{j\sigma}) \\ &= -A\hat{c}_{j\sigma},\end{aligned}\tag{2.64}$$

and

$$\begin{aligned}A[\hat{c}_{i\sigma}^\dagger \hat{c}_{j\sigma}^\dagger, \hat{c}_{i\sigma}] &= A[\hat{c}_{i\sigma}^\dagger \hat{c}_{j\sigma}^\dagger, \hat{c}_{i\sigma}] \\ &= A(\hat{c}_{i\sigma}^\dagger \hat{c}_{j\sigma}^\dagger, \hat{c}_{i\sigma} - \hat{c}_{i\sigma}^\dagger \hat{c}_{i\sigma}, \hat{c}_{j\sigma}) \\ &= A(-\{\hat{c}_{i\sigma}^\dagger \hat{c}_{i\sigma}\}, \hat{c}_{j\sigma}) \\ &= -A\hat{c}_{j\sigma}\end{aligned}\tag{2.65}$$

and finally

$$\begin{aligned}
[A\hat{c}_{i\sigma}^\dagger\hat{c}_{i\sigma}, \hat{c}_{i\sigma}] &= A[\hat{c}_{i\sigma}^\dagger\hat{c}_{j\sigma}, \hat{c}_{i\sigma}] \\
&= A(\hat{c}_{i\sigma}^\dagger\hat{c}_{i\sigma}, \hat{c}_{i\sigma} - \hat{c}_{i\sigma}\hat{c}_{i\sigma}^\dagger\hat{c}_{i\sigma}) \\
&= A(-\hat{c}_{i\sigma}\hat{c}_{i\sigma}^\dagger\hat{c}_{i\sigma}) \\
&= -A\hat{c}_{i\sigma}.
\end{aligned} \tag{2.66}$$

So, for the Hamiltonian we get:

$$\begin{aligned}
[\mathcal{H}, \hat{c}_{i\sigma}] &= \sum_{j\sigma} t_{ij}\hat{c}_{j\sigma} - (\epsilon_{i\sigma} - \mu)\hat{c}_{i\sigma} \\
&\quad + W(r_i)\hat{c}_{i\sigma} - U(n_i - \sigma m_i)\hat{c}_{i\sigma} \\
&\quad - \sum_{\langle ij \rangle} \Delta_{ij}\hat{c}_{j\sigma}^\dagger,
\end{aligned} \tag{2.67}$$

where σ is 1 for $\hat{c}_{i\uparrow}$ and -1 for $\hat{c}_{i\downarrow}$.

Furthermore we have that:

$$[\hat{H}, \hat{c}_{i\sigma}] = \sum_n (-\epsilon_n u_{n\sigma} \hat{\gamma}_{n\sigma} + \epsilon_{n\sigma'} v_{n\sigma}^* \hat{\gamma}_{n\sigma'}^\dagger), \tag{2.68}$$

where $-\epsilon_n$ is the negative energy corresponding to the commutation with the annihilation operator $\hat{\gamma}_{n\sigma}$ and ϵ_n is the positive energy corresponding to the creation operator $\hat{\gamma}_{n\sigma}^\dagger$. For $u_{n,i\sigma}$ and $v_{n,i\sigma}^*$ we have the following equations:

$$\begin{aligned}
-\epsilon_{n\uparrow} u_{n,i\uparrow} &= \sum_j t_{ij} u_{n,j\uparrow} \\
&\quad - (-\mu + W(r_i) - U(n_i - m_i)) u_{n,i\uparrow} \\
&\quad - \sum_{ij} \Delta_{ij} v_{n,j\downarrow},
\end{aligned} \tag{2.69}$$

and for $u_{n\downarrow}$ we find

$$\begin{aligned}
-\epsilon_{n\downarrow} u_{n,i\downarrow} &= \sum_j t_{ij} u_{n,j\downarrow} \\
&\quad - (-\mu + W(r_i) - U(n_i - m_i)) u_{n,i\downarrow} \\
&\quad - \sum_{ij} \Delta_{ij} v_{n,j\uparrow},
\end{aligned} \tag{2.70}$$

for $v_{n\uparrow}$ we have

$$\begin{aligned}
-\epsilon_{n\uparrow} v_{n,i\uparrow}^* &= \sum_j t_{ij} v_{n,j\uparrow}^* \\
&\quad - (-\mu + W(r_i) - U(n_i - m_i)) v_{n,i\uparrow}^* \\
&\quad - \sum_{ij} \Delta_{ij} v_{n,j\downarrow}
\end{aligned} \tag{2.71}$$

and finally for $v_{n\downarrow}$

$$\begin{aligned}
-\epsilon_{n\downarrow} v_{n,i\downarrow}^* &= \sum_j t_{ij} v_{n,j\downarrow}^* \\
&\quad - (-\mu + W(r_i) - U(n_i - m_i)) v_{n,i\downarrow}^* \\
&\quad - \sum_{ij} \Delta_{ij} v_{n,j\uparrow}.
\end{aligned} \tag{2.72}$$

It is easy to see that we can write the four equations in matrix form as follows:

$$\begin{pmatrix} \hat{\xi}_{\uparrow} & \hat{\Delta} \\ \hat{\Delta}^* & \hat{\xi}_{\downarrow} \end{pmatrix} \begin{pmatrix} u_{n\uparrow} \\ v_{n\downarrow} \end{pmatrix} = \epsilon_n \begin{pmatrix} u_{n\uparrow} \\ v_{n\downarrow} \end{pmatrix} \tag{2.73}$$

for eigenvalue $\epsilon_{n\uparrow}$ and

$$\begin{pmatrix} \hat{\xi}_{\downarrow} & -\hat{\Delta} \\ -\hat{\Delta}^* & -\hat{\xi}_{\uparrow} \end{pmatrix} \begin{pmatrix} u_{n\downarrow}^* \\ v_{n\uparrow}^* \end{pmatrix} = \epsilon_n \begin{pmatrix} u_{n\downarrow}^* \\ v_{n\uparrow}^* \end{pmatrix} \tag{2.74}$$

for eigenvalues $\epsilon_{n\downarrow}$. The matrix operators are defined as:

$$\hat{\xi}_{\sigma} u_i = - \sum_j t_{ij} u_j + (\epsilon_{i\sigma} - \mu + W_{i\sigma} U(n_i - m_i)) u_i \tag{2.75}$$

$$\hat{\Delta} u_i = \sum_{\langle ij \rangle} \Delta_{ij} u_j \tag{2.76}$$

and likewise for $v_{i\sigma}^*$. The Hamiltonian is now in a diagonal form which is necessary for self-consistent calculations.

CHAPTER 3

Cuprates

In this chapter we review the class of superconducting compounds called cuprates. First a general introduction and then an introduction to the specific cuprates LSCO, LCO+O and LSCO+O that are the subject of this thesis..

3.1 Cuprates, properties and structure

Among high temperature superconductors is a large class called cuprates. Common to these superconductors is that they contain copper oxide layers. Copper oxide lie in planes between other planes of rare elements (such as La, Mg and Y etc.). It is in these copper oxide planes the superconducting properties lies. The planes of other elements provide the charge carriers to the copper oxide planes. Many experimental investigations (such as NMR, μ R and neutron scattering) also suggest the existence of precise complementary relationships between superconductivity and antiferromagnetic ordering , which is commonly observed in LSCO, LBCO and YBCO.

3.1.1 Introduction to Cuprates

The breakthrough to a new era in higher superconductivity transition temperature came in 1986 [28] by the discovery of superconductivity in the $\text{La}_{2-x}(\text{Ba},\text{Sr})_x\text{CuO}_4$ compounds with an onset of superconductivity at about 30 K. This was well above previous records. Shortly after a new important development occurred when the Houston group showed that external pressure could increase T_c noticeably (above 40 k) under 13 kbar pressure. An equivalent effect can be achieved by replacing some of the ions with ones

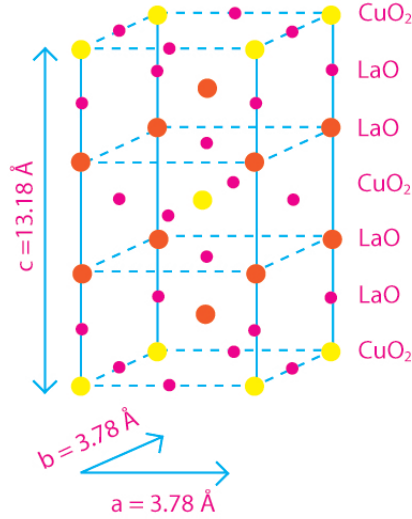


Figure 3.1: *Crystal structure of LSCO. The Copper is yellow, oxygen is pink and Lanthanum/strontium is red.*

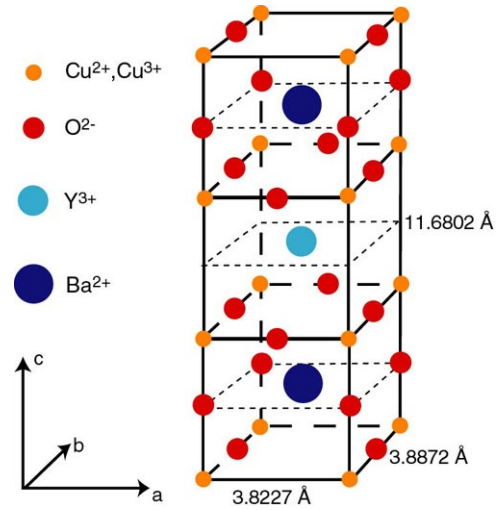


Figure 3.2: *Crystal structure of YBCO. The Copper is orange, oxygen is red and Barium is dark blue and the Yttrium is blue.*

that have different valence but the same chemical properties. In other words by replacing Ba with the smaller ion with lower valence Sr you could achieve a higher T_c . This has attracted the interest of many researchers and this mechanism has to this day not been fully understood.

A significant property in high Temperature superconductor cuprates is their quasi two-dimensional character. Similar among Cuprates is the layered structure, where some structures are more complex than others. Some examples are seen in fig. 3.1 and 3.2.

What we see is that the CuO_2 layers alternate with LaO and BaO, Y in LSCO and YBCO respectively. A similar structure is seen in all cuprates. Interestingly, the critical temperature increases with increasing number of CuO_2 -layers per unit cell. This, among many other things, has contributed to the understanding that the most important structural element of all cuprates are the CuO_2 layers.

There is a very strong covalence between Cu^{2+} ions and O^- ions in the layers, which allows an electron on the copper to easily interact through the neighboring oxygen. It is believed that this structure is what drives su-

perconductivity. The layers (strontium, barium etc.) in between the CuO_2 layers are assumed to contribute as a charge reservoir. In this scheme, it is sufficient to model cuprates as a two-dimensional system.

3.1.2 Doping in Cuprates

We know from experiments that the electronic properties of cuprates depend strongly on the doping concentration. Doping is a technique used to change the chemical properties of a given crystal by substituting atoms in crystals with other atoms which have lower electron number like we do in $\text{La}_{2-x}\text{Sr}_x\text{CuO}_4$. In this technique, we substitute some of the intermediate atoms (like La) that lie in between the CuO layer. Another way to dope a crystal is to add extra oxygen which has higher valence than the intermediate atom like we do in like we do in $\text{LCO}+\text{O}$. Both methods can be used simultaneously for the same crystal as e.g. in $\text{La}_{2-x}\text{Sr}_x\text{CuO}_{4+y}$ ($\text{LSCO}+\text{O}$).

¹

When the number of oxygen ions is changed, the number of holes in CuO_2 layers is also changed. These changes can also occur when the nature of some of the other atoms are changed. The number of additional holes is what we call doping. Whatever type of cuprates we are dealing with, the properties we observe when we change the doping are almost identical and seem to be rather universal. Without the doping in the cuprates they are just quasi two-dimensional antiferromagnetic Mott insulators with Néel temperature T_N of order 300 K. One can dope with a compound of lower valence than the original compound to create a hole. An example being La_2CuO_4 , if you dope by Ba^{2+} or Sr^{2+} instead of La^{3+} an additional hole will go directly into the CuO layer. The doping/temperature phase diagram for cuprates is given in fig. 3.3.

¹Even in a normal metal, electrons are exposed to numerous interactions; this can be interactions with the other electrons or the atoms of the system. A theoretical treatment shows that when an electron is exposed to these interactions, it behaves just like a virtual electron subjected to no interaction. The mass of the electron has changed. The interactions can in some cases, be so dominant that the electric charge of this virtual electron can switch (from negative to positive). We call the result of such a switch a hole. This concept of hole and electron with a variable mass is a powerful theoretical tool because it permits us to describe the electric properties of matter considering only interactions in matter.

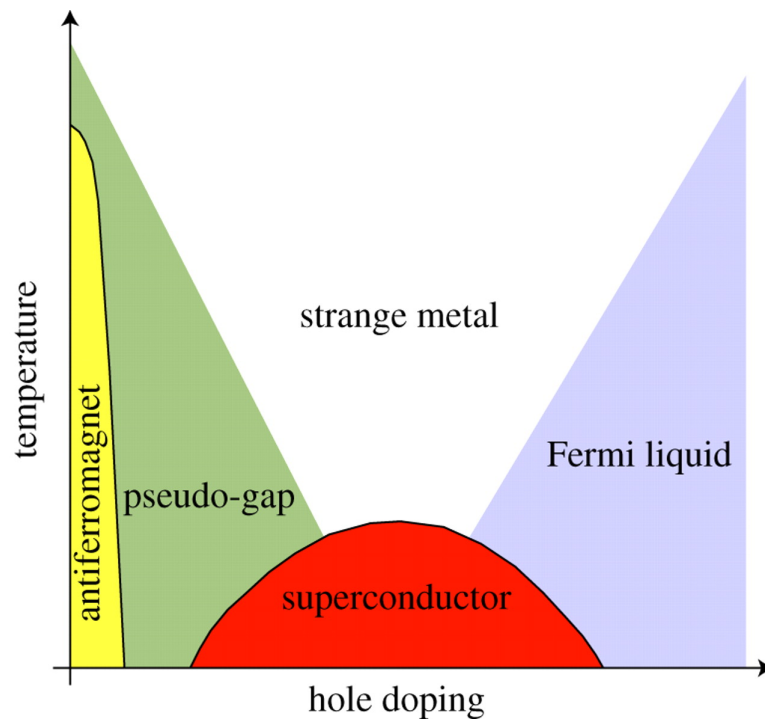


Figure 3.3: *Schematic phase diagram of hole-doped cuprates. The different phases of hole-doped cuprates are plotted as a function of temperature and hole-doping [37].*

The parent compound is an antiferromagnet, and for small dopings the material remains an antiferromagnet with a rapidly decreasing Néel temperature. For the hole concentration around $x = 0.05$ we see the so called pseudo gap, this phase is not fully understood. Subsequently we see the superconducting phase, symmetrically located around a hole concentration of $x = 0.16$, where the maximum critical temperature T_c lies. The superconducting phase goes on until $x = 0.27$ where a phase transition take place and the compound becomes metallic. In literature and in this thesis, p means the total doping in a given crystal.

3.1.3 The superconducting order parameter

What separates cuprates from other superconductors is the superconducting order parameter is a d-wave, given by $d_{x^2-y^2}$. This parameter is supported by a variety of experiments such as NMR[44], phase-sensitive measurements [11, 30, 9, 8], ARPES[19] and polarization dependent scattering [33, 12, 42, 13]. The symmetry of the superconducting order parameter is unconventional, since usually superconductors have s-wave symmetry. For an order parameter of $d_{x^2-y^2}$ we have a gap function given by

$$\Delta_k = \frac{\Delta_0}{2}(\cos k_x - \sin k_y), \quad (3.1)$$

where Δ_0 is the maximum value of the superconducting gap, k_x and k_y are the wave vectors. It is worth noting that in the point separated by the vector $Q = (\pi, \pi)$ the gap has the same values but with different signs. Furthermore at $k_x = k_y$ the gap function Δ_k is zero, which gives us node lines.

3.1.4 Electronic structure in the normal state

It is essential to understand the electronic structure of the cuprates since it is the foundation we use to study the electron density. We assume that it is sufficient to use a one band model for understanding the electronic structure that drives the cuprates. We also believe that the electronic interaction in the layers (in the plane, or x and y direction) is the dominating interaction while the interaction between layers is weak, and so we simplify to a 2D interaction. The electronic structure for CuO_2 -plane is shown in fig. 3.4.

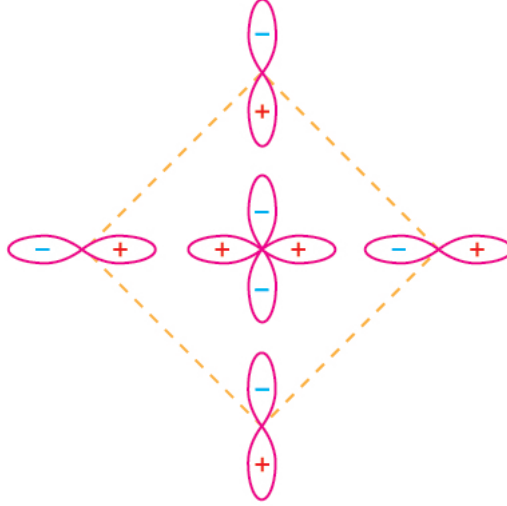


Figure 3.4: *Schematic illustration of the electron structure of Cu-O planes.*

To understand how the electrons interact in the crystal field it is necessary to understand the shapes of the orbitals. The orbitals show the angular dependence of the electron density n i.e. the angular part of a wave function see fig. 3.5.

In this simplification for cuprates we have two orbitals that contribute to the interaction, the p_x or p_y that originates from the oxygen atom and the $d_{x^2-y^2}$ orbital located at the copper site. The highest occupied orbital of the Cu^{2+} -ions are the 3d-orbitals and the highest occupied orbitals of the O^{2+} -ions are the 2p-orbitals (see fig. 3.5).

If we start by looking at 3d-orbitals we see that there are nine electrons per one hole, where the 2d-orbitals are fully occupied, leaving us (for an underdoped cuprate) with one hole per copper site ($3d^9$). We see that the field induced by the crystal removes the degeneracy of the copper 3d-orbitals, giving us a configuration where the $3d_{x^2-y^2}$ -orbital is the highest possible energy and only occupies a single hole. It appears that the remaining 3d-orbitals have a lower energy and are completely occupied and we therefore neglect them in the model and in the calculations. We remember that there is a strong Coulomb repulsion between holes in the cuprates (see section 2.2.1) which shows its importance in 3d-transition metal oxide. The Coulomb repulsion splits the $3d_{x^2-y^2}$ -bands into two, a so called upper

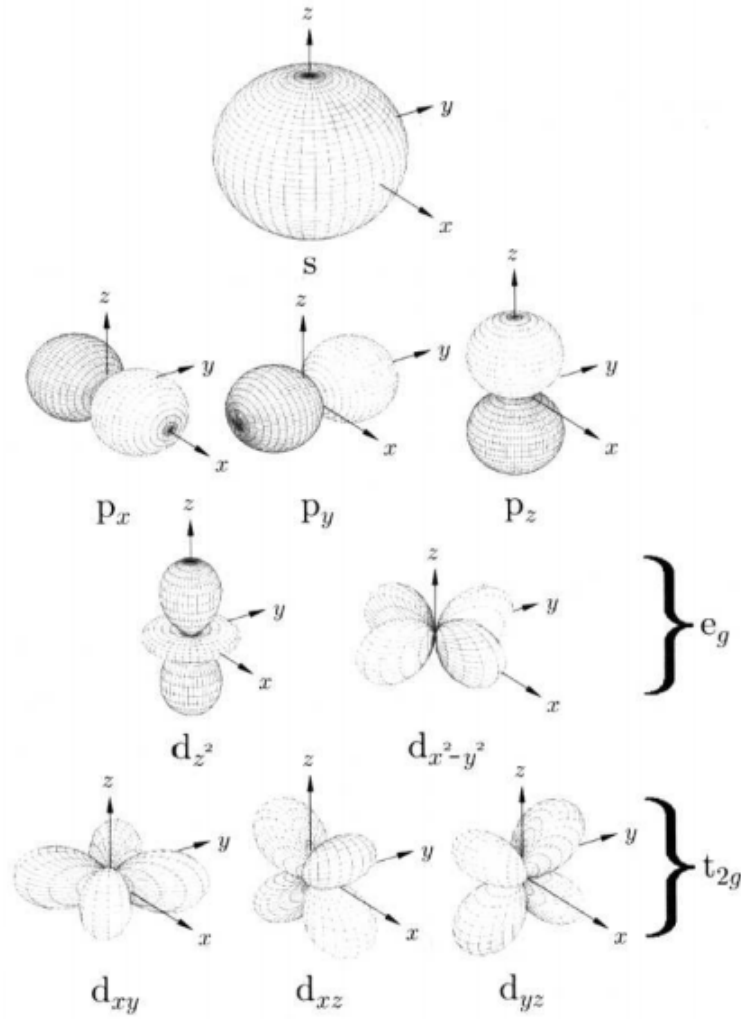


Figure 3.5: Angular distribution of the orbitals s , d and p . [7]. The orbitals show the angular part of a wave function.

Hubbard band and the occupied lower Hubbard band. The lower band lies in lower energies than the 2p-states of oxygen, forcing the chemical potential (in the under-doped cuprate) to lie between the 2p-oxygen state and the upper Hubbard band. When we start hole-doping the crystal the 2p-oxygen states will start to be filled, with means that the holes are mainly doped into the four 2p-oxygen states surrounding the copper sites symmetrically. We have that the holes on the copper site and the surrounding neighbor oxygen sites form a so-called Zhang-Rice singlet [46].

We can therefore map the original three band Hamiltonian into the low energy one-band Hamiltonian. The existing model that best describes the physics of the cuprates is the one band Hubbard Hamiltonian(described in the previous chapter):

$$\hat{\mathcal{H}} = - \sum_{ij\sigma} t_{ij} \hat{c}_{i\sigma}^\dagger \hat{c}_{j\sigma} + \sum_{i\sigma} (\epsilon_{i\sigma} - \mu) \hat{n}_{i\sigma} + U \sum_{\langle ij \rangle} \hat{n}_{i\uparrow} \hat{n}_{i\downarrow} + \dots, \quad (3.2)$$

where $\hat{c}_{i\sigma}^\dagger$ and $\hat{c}_{j\sigma}$ are the creation and annihilation operators, respectively. $\langle ij \rangle$ indicate the summation over nearest-neighbor pairs, we denote the nearest-neighbor hopping term with t , which deterines the amplitude for the hopping in between sites. The next nearest-neighbor hopping term we denote t' . U is the Coulomb interaction between the quasi-particles at the same site, and finally $n_{i\sigma} = c_{i\sigma}^\dagger c_{i\sigma}$ is the density. The above equation is essential for understanding the insulating, undoped, antiferromagnetic phases which almost all cuprates show.

Let us now write the metallic part of the Hamiltonian in k-space where we sum over k_x and k_y in the first Brillouin zone $-\pi \leq k_x \leq \pi$ and $-\pi \leq k_y \leq \pi$:

$$H_{\text{metal}} = \sum_k \epsilon_k c_{k\sigma}^\dagger c_{k\sigma}, \quad (3.3)$$

where $\epsilon_k = \sum_n t_n e^{ikr_n}$. Here t_n include hopping to nearest neighbor and next nearest neighbor, and get the following:

$$\epsilon_k = -2t(\cos(k_x a) + \cos(k_y a)) - 4t' \cos(k_x a) \cos(k_y a) - \mu, \quad (3.4)$$

where μ is the chemical potential as usual and a is the lattice constant normally set to unity. Note that we assume a cubic 2D lattice.

3.1.5 Interlayer hopping

We have already shown that the essential physics is contained in the two dimensional one-band Hubbard model for CuO_2 planes. And we will now look at the effect the three dimensional model brings. Anderson argues that the energy scale that determines the parameters of the 2D Hubbard is not the same energy scale that determines the parameters for T_c and the spin gap [2]. This might seem very obvious, what is not so obvious however is that what is supposed to set the scale for these parameters is the hopping interaction between the planes (layers) which is then an important term we have left out of the 2D Hubbard model.

3.2 Experimental results on LSCO, LCO+O and LSCO+O

I will in this section provide a summary of experimental results on LSCO, LCO+O and LSCO+O so far and point out the areas that have relevance to the calculations in chapter 5.

Because of the conflicting results of LSCO+O it is necessary to study both the sister compounds LSCO and LCO+O. Besides superconductivity the hole-doped crystals show many other interesting properties such as magnetism and a metal-insulator transition. The holes in the crystals occurs when an element is replaced by another of lower valence and thereby providing a "hole" where the missing electron should be. For example in LSCO the holes come from replacing Lanthanum La by Strontium Sr. The amount you replace gives rise to different hole-concentration. For a doping concentration $x = 0.15$ the critical temperature is found to be $T_c = 37.5 \text{ K}$ [34].

3.2.1 LSCO

There has been much confusion concerning the space group of LSCO and $\text{LSCO} + \text{O}$, this is partly because there is no universal consensus regarding the lattice parameters a , b and c . You are so to speak, free to choose the axes

as you wish. We will from now on assume the following lattice parameters $a < b < c$.

At room temperature $\text{La}_{2-x}\text{Sr}_x\text{CuO}_{4-y}$ belongs to a space group of tetragonal form, whereas we have to be above 500 K for $\text{La}_2\text{CuO}_{4-y}$ to belong to the tetragonal space group. For temperatures lower than 500 K $\text{La}_2\text{CuO}_{4-y}$ will be orthorhombic. Under cooling $\text{La}_{2-x}\text{Sr}_x\text{CuO}_{4-y}$ will become orthorhombic at temperature around 250 K for a doping around $x = 15$. The space group for the LSCO compound is Bmab.

Twinning will always occur in LSCO, LCO+O and LSCO+O because of the phase transformation from tetragonal to orthorhombic that occurs around 500 K for $\text{La}_2\text{CuO}_{4+y}$, $\text{La}_{2-x}\text{Sr}_x\text{CuO}_4$ and $\text{La}_{2-x}\text{Sr}_x\text{CuO}_{4+y}$. The CuO_2 layers are built from corner sharing square planar CuO_4 units that can be bonded to another O-atom. This creates a square pyramidal environment or two additional O-atom resulting in an axially elongated octahedral surrounding[39]. The reason that a and b are different is that the octahedra tilt differently. The presence of twins will cause the exchange of a and b axes across twin boundaries[38].

The copper ions in the undoped LCO has spin 1/2 which schematically result in it being a conductor with one hole in the d-band per Cu site. However the cost in energy required to add another electron is too high due to the Coulomb repulsion between the added electron and the electrons in the d-shell which result in that there is a weakly bound electron in almost every Cu site. So under these conditions the LCO is actually a poor conductor.

An important matter needed to build a model is the orientation of the spins in the crystal. As pointed out earlier the physics lie in the CuO_2 planes, where the spins are orientated in the (a, b) -plane in an antiferromagnetic order below $T_N \approx 300$, over distance greater than 200 \AA^2 . Hence LCO is both an antiferromagnetic and a Mott insulator [37].

Recall the generic phase diagram for high-temperature cuprates in fig 3.3. In the specific case of LSCO, we see that when LCO is doped with strontium

²For an antiferromagnetic measured Bragg peak, with a given resolution, we have the correlation length is about $2\pi/\Gamma$, where Γ is the width of the top. The width of their solution is equal to 200 \AA , where the peaks have not been broader than the solution, therefore, one can say that the correlations larger than 200 \AA .

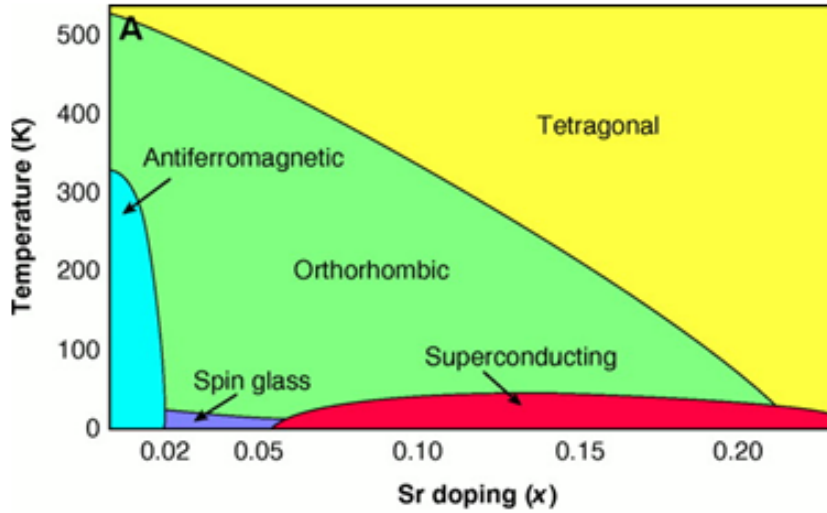


Figure 3.6: *phase diagram of the cuprate LSCO. The different phases of hole-doping are plotted as a function of temperature and hole-doping x .*

(Sr) more holes are created since we replace La^{+3} ions with Sr^{+2} ions resulting in creation of Cu^{+3} ions. The holes in the compound will be placed at the strontium (Sr) sites since Sr has a fewer electrons than La. The holes will then attract the loosely bound electron from the copper site, so the copper sites are in a state where they are able to lead electrons, and hence the compound becomes a conductor. For a specific range of doping $0.2 < x < 0.5$ and temperature $T_c < 40$ K the compound becomes superconducting. See fig. 3.6

3.2.2 Superoxygenated LCO+O

The superoxygenation of LCO+O is done by electrochemical oxidation [21], [36]. In this procedure the oxygen is highly electron-negative and will then oxidize the electron-positive copper. The electrons are transferred from the copper ion to the oxygen, resulting in reduced oxygen ions, and hence creating the Cu^{+3} -ions. The excess oxygen atoms will occupy interstitial

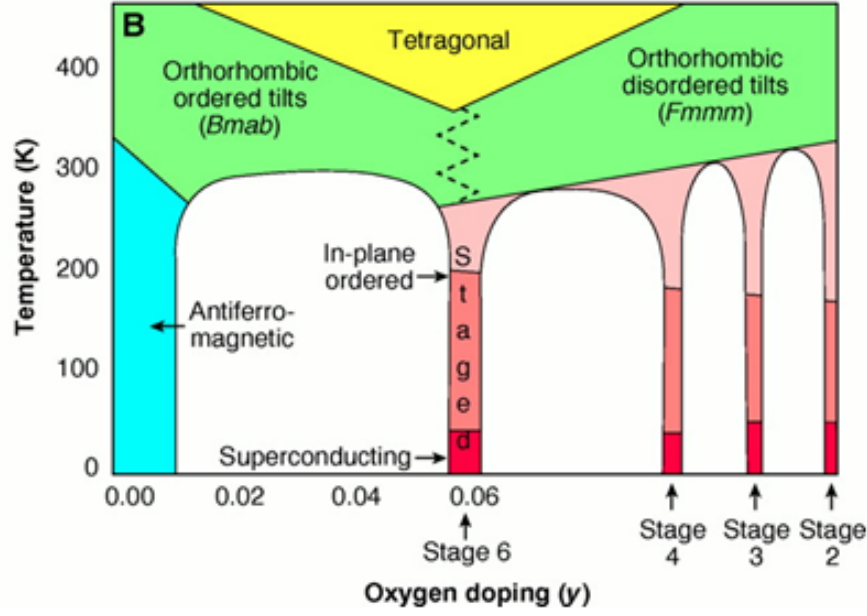


Figure 3.7: *Proposed phase diagram of LCO + O. [5]. The oxygen places itself in different layers called staging.*

sites in the crystal see fig. 3.10.

Although the superconducting properties of LSCO and LCO+O are both generated by hole doping, their phase diagrams are very different see fig. 3.7.

What differs is, among other things, that in LCO+O the oxygen is free to move around in between the layers down to a temperature of 200 K. This temperature is much lower than the temperature needed for the antiferromagnetic exchange coupling between nearest neighbor spins in the Cu site which is 1500 K. Furthermore it is also lower than what is needed for electronic bandwidth ($\omega = 2$ J)[5]. The oxygen is then allowed to rearrange in such a way as to minimize the free energy. As one can see in the phase diagram fig. 3.7 the mobility of the oxygen creates a different phase in which the most conspicuous is the different layers of excess oxygen, staging see fig.

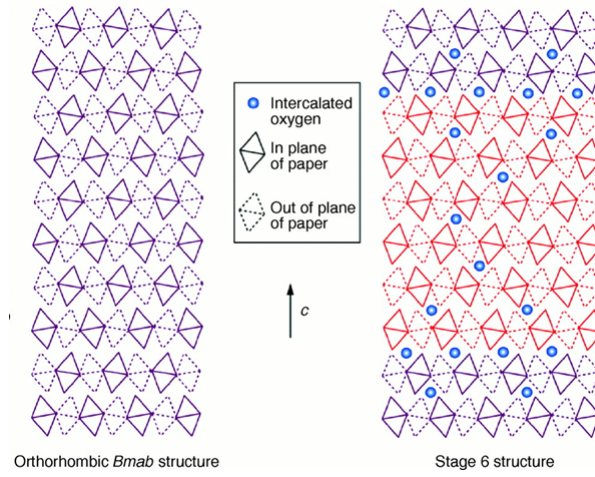


Figure 3.8: *Illustration of the staging in LCO+O. Left we see the tilt in the CuO_6 octahedron for undoped LCO. Right we see schematic illustration of stage 6 tilt structure in the CuO_6 octahedron in LCO+O. The different shadings represent different antiphase tilt domains. [5]*

3.8

For a doping level up to $y < 0.1$ we get an antiferromagnetic region with a Néel temperature T_N at ca 300 K at $y = 0$ and 250 K for $y = 0.01$. We see at the phase diagram fig. 3.7 that the space group depends on temperature and doping. For temperatures below 300 K the crystal is orthorhombic. We also see that the added oxygen only place themselves in certain areas of the phase diagram, this is what we call staging. In the phase diagram there are certain dopants which are not possible in the LCO+O, this is called miscibility gap.

Synchrotron X-ray and neutron powder diffraction on crystals prepared by high oxygen pressure method[10], shows that the orthorhombic Bmab $\text{La}_2\text{CuO}_{4+y}$ undergoes a phase separation at low temperature (around 300 K) into two phases with different oxygen content: The oxygen-poor phase is stoichiometric non-superconducting La_2CuO_4 with orthorhombic Bmab symmetry[10]. Some experiments show that the oxygen-rich is a superconducting phase assigned to the orthorhombic Fmmm space group. Experiments using neutrons indicated that perhaps the phase separation occurs at 290 K and that the superconducting phase is indeed a Bmab space group just like the oxygen-poor non-superconducting phase.

There is evidence of a miscibility gap for $0.010 < y < 0.055$ [10]. Within this gap the samples decompose into an oxygen-rich Fmmm phase and a stoichiometric La_2CuO_4 Bmab phase. Besides, $\text{La}_2\text{CuO}_{4-y}$ with $0.055 < y < 0.100$ are single phases with Fmmm symmetry and show no phase separation down to 10 K. Similar for all y the materials transform into single-phase samples with tetragonal symmetry (f4/mmm) above their transition temperatures. In the case of LCO+O we see the formation of superstructure, this could very well be the case for LSCO+O as well. This theory where the oxygen is over stoichiometry and well defined is supported/or could be related to the special arrangement of interstitial oxygen [10].

3.2.3 Superoxygenated LSCO+O

The relationship between superconducting and magnetic phases are still unclear to scientists, however some new experiments on $\text{La}_{2-x}\text{Sr}_x\text{CuO}_{4+y}$ show a superconducting onset critical temperature at 40 K with a coex-

isting magnetic spin-density wave that also orders near 40 K for various strontium doping and excess oxygen[23]. This raises the question, is this new compound the key to understanding the interplay between magnetism and superconductivity?

A new view is that magnetism and superconductivity are coupled with a continuous transition between the phases. This would allow coexistence in the domains of the short range ordered magnetism and superconductivity. There is still not enough experimental or theoretical evidence to fully support it, however the data from Mohottala et al [23] suggest new evidence for the segregation of a cuprate material into separate magnetic and superconducting phases, where the magnetic state is not the undoped Néel phase, but a spin-density wave connected to the behavior of an optimally doped cuprate.

LSCO (and other optimally hole doped cuprates) show a surprising suppression of the superconducting state with a concomitant appearance of a static spin-density wave. In LCO+O we see a different behavior, where the system has a robust superconducting state with a transition temperature $T_c > 40$ K. This transition temperature is higher than for optimally doped LSCO with a maximum transition value of $T_c = 38$ K. LCO+O also have static magnetism with an ordering temperature T_N very close to T_c [18],[1]

The super oxygenated $\text{La}_{2-x}\text{Sr}_x\text{CuO}_{4+y}$ seems to have a higher T_c than only strontium doped $\text{La}_{2-x}\text{Sr}_x\text{CuO}_4$, namely a T_c around 40 K. The T_c seems to be independent of the strontium content.

Just like in LCO+O, LSCO+O also seems to have a miscibility gap, however for LSCO+O this gap occurs in more hole-rich regions of the phase diagram. Experiments show that the superconducting phases for different strontium content are identical after oxidation. This was verified by measuring the Meissner fraction near 40 K ³ [23].

A series of experiments have been performed on LSCO for different strontium content, where none of them showed magnetic ordering for temperatures higher than 10 K [17] where the mother compound La_2CuO_4 is antiferromagnetic up to 325 K. Structural characterization by X-ray and neutron scattering shows that the superoxygenated $\text{La}_{2-x}\text{Sr}_x\text{CuO}_{4+y}$ is orthorhombic at low temperatures, just like LSCO and LCO+O.

³Meissner fraction is the superconducting volume fraction.

A relationship between the excess oxygen content and the staging number has been observed. The compounds with most oxygen will also have the lowest staging (meaning less distance between oxygen layers) number. So lower oxygen levels lead to higher staging number, and for sufficient low excess oxygen there will be no staging at all. The amount of interstitial excess oxygen seems to vary with the strontium content, in such a way that they always have roughly the same hole-concentration.

The characteristic parameters of the superconducting and magnetic phases are virtually the same for all the superoxygenated samples. Only the relative volume fraction seems to change [32], [23]. In conclusion a suggestion for a phase diagram is shown in the fig. 3.9

The light and dark arc regions are the superconducting and magnetic line phases, respectively. The cross-hatched regions indicate miscibility gaps. A large area of the phase diagram remains blank as it is still unexplored. There are experiments that suggest that it is the electronic interaction of the doped holes that is the primary driver of the phase separation rather than, the specific chemistry of the excess oxygen and the strontium in the compound. Furthermore it is also suggested that the mobility of the excess intercalated oxygen dopant is the key element that allows phase separation over length and timescales long enough to measure easily. For other compounds with the same phase separation it may also be the case, but only over smaller times and length scale. It may be that the presence of highly mobile oxygen dopant can provide the information needed to understand the inherent physics of holes in a copper oxide plane.

Hamed et al. [45] also argue that at room temperature the electronic system of holes induced by excess oxygen is similar to that induced by doping with strontium over a considerable range of doping levels. The transport ability, at very low doping levels is quite similar for oxygen induced holes and strontium induced holes.

There exists a critical hole concentration ($p_c = 0.06$) and this is not seen in the excess oxygen vs charge transfer process. This indicates that the change in doping efficiency is of an electronic origin. It should be emphasized that the critical concentration p_c is at the hole concentration where the conductivity versus temperature behavior of all high T_c layered cuprates becomes metallic around room temperature and superconducting at low temperature. It is believed that the doping efficiency is controlled by the

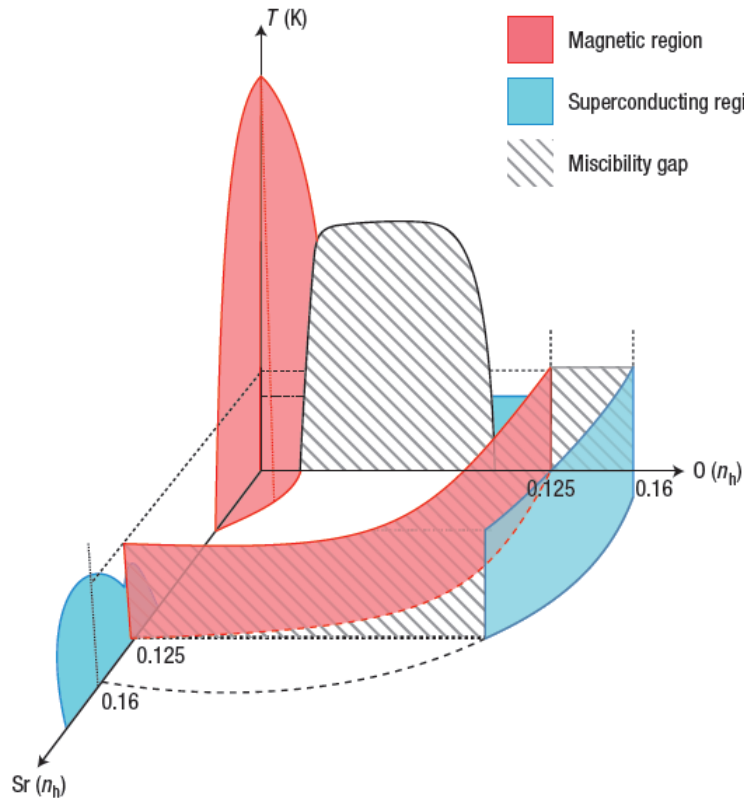


Figure 3.9: *Scematic phase diagram of superoxygenated LSCO+O. The light area represent the superconducting phase, and dark arc regions are magnetic line phases. The cross-hatched regions indicate miscibility gaps. A large area of the phase diagram remains blank as it is an unexplored area. The figure is taken from Mohottala et al.[23]*

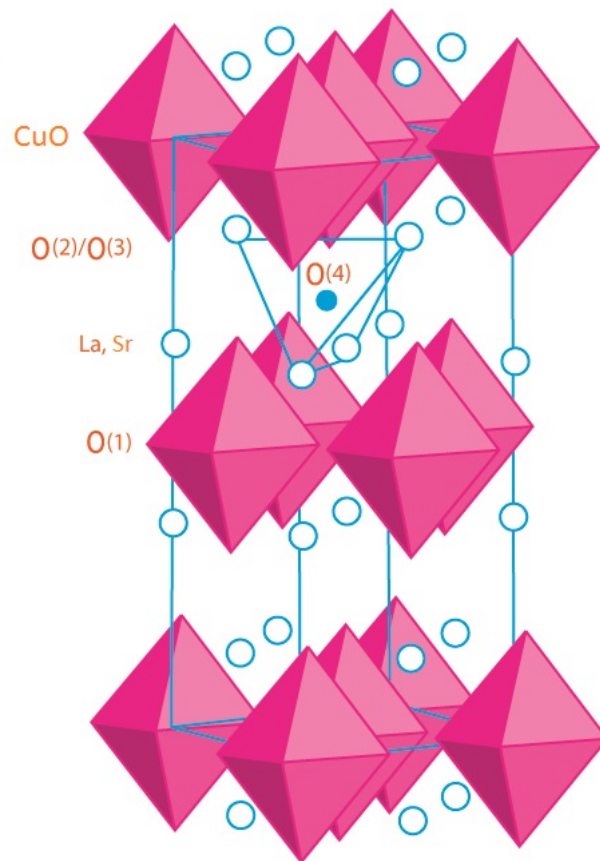


Figure 3.10: *Crystal structure of superoxygenated LSCO+O. Pink represent copper, white represent lanthanum and strontium, and blue is the added oxygen. The design of the structure is based on [26]*

intrinsic characteristics of the electronic system of LCO+O (perhaps also LSCO+O). Two holes are created in the Cu-O plane for each excess oxygen atom (O2) in the insulating region and 1.3 holes per additional excess oxygen atom (O1.3) in the metallic region. The Gas effusion spectra experiments indicate that both O1.3 and O2 co-exist in the compound.

3.2.3.1 Stripes in superoxygenated LSCO+O

Stripes are the word we use to describe a certain systematic electron spin configuration in a solid. The electrons organize themselves into an inhomogeneous nano-scale structure which give rise to a new state of matter. For example an antiferromagnetic order where spin switches between up and down is a scheme called stripes. There are many different ways for the spins to systemize also including the holes, the lattice point not occupied by an electron and therefore no spin see fig. 3.11. The stripes in LSCO have periodicity 8 with an anti-ferromagnetic order, except in the empty sites. The evidence of stripes is strongly supported by neutron and X-ray scattering among many other techniques [4],[31]. .

It is still not clear from a theoretical point of view why exactly the stripes formation occur. It is believed that they originate from a competition between the magnetic and kinetic energy. Theoretically, the idea of stripes has been around since 1989. They were first found by studying a 2D mean-field two band Hubbard model. Not long after, there was also evidence of stripes in a one band model, which is what I will use in my dissertation. The studies of these stripes in one band models narrate to the fact that when excess carriers are introduced to the system the spatially modulated spins are more energetically beneficial than uniform phases. These discoveries give rise to some changes in the phase diagram of the mean field Hubbard model.

Tranquada et al.[29] has, based an experiment on La_2NiO_4 , $\text{La}_{1.6-x}\text{Nd}_{0.4}\text{Sr}_x\text{CuO}_4$ and $\text{La}_{2-x}\text{Sr}_x\text{CuO}_4$, suggested a stripe pattern of period eight with some antiferromagnetic order like behavior (see fig.3.11). This is strongly supported by Udby et al[32]. The experimental work done suggests that all the $\text{La}_{2-x}\text{Sr}_x\text{CuO}_{4+y}$ samples have the same stripe order. Namely the one for optimal doped $\text{La}_{2-x}\text{Sr}_x\text{CuO}_4$ given in fig. 3.11.

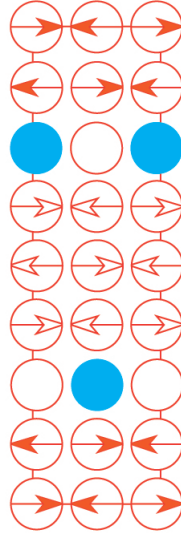


Figure 3.11: *Hypothesized stripe model for the CuO_2 -planes in LSCO for $x = 0.125$. The arrows indicate spin on a copper site. The filled circles represent holes. The figure is based on [29]*

3.2.3.2 Determination of excess oxygen concentration and the placement

For the type of calculations that is presented in chapter 5, it is essential that we know where the added oxygen is, and how much oxygen there is in the system. It is easy to measure the oxygen content with relatively high precision, but quite difficult to determine where the excess oxygen is located.

There are three ways to determine the amount of interstitial oxygen. One way is by thermogravimetric analysis and the other is by iodometric titration [16]. When doing thermogravimetric analysis one first has to pulverize the crystal and then slowly heat it up in a hydrogen reducing atmosphere. This way the interstitial oxygen will evaporate from the sample leaving only La_2O_3 , Sr and Cu. The loss in mass is then measured as a function of time and the concentration of the oxygen can be deduced.

The second method, iodometric titration, one takes a sample and dissolved in a liquid (preferable an acid) and titrate. a sample is dissolved in a liquid

and then titrated. The concentration of oxygen can then be determined by measuring the oxidation state of copper.[16].

Rial et al[10] argue an exact value of y . For a given sample y is determined by taking a disc of the sample with diameter and thickness 0.6 cm and 0.6 mm, respectively, and mass of around 80 mg. Then the disc is wrapped in Au foil (of mass 20 mg) and heated up to a 110° C for one hour to check if the sample has been thoroughly dried in vacuum. This showed no weight loss within the resolution of $\Delta W = \pm 2\mu g$. After ensuring that the sample is carefully dried the sample with Au foil is heated up to 550° C in flowing nitrogen gas for 6 hours and then furnace quenched. The final weight loss was then measured and the corresponding value of y was calculated and found to be less than 0.0005.

However another value for y was found. Based on the experiments of heating the different samples to measure weight loss the results indicate that a single uniform overall electrochemical oxidation is operational up to $y = 0.11$ and that no electrochemical side reaction was involved even when samples were oxidized at 70°C. Furthermore Hamed et al. [45] argue that the maximum oxidation state of LCO+O by doping is limited by optimal hole doping concentration $p = 0.16$. This is also consistent with the previous reports that maximum effective hole doping $p = 0.16$ is always observed independent of the material (LSCO+O and LCO+O), oxidation time and techniques used for oxidation. This is also in agreement with what Mohottala et al.[23]. The exact value of y will prove important in the calculations in chapter 5

The location of the interstitial oxygen is determined by neutron diffraction. Neutron diffraction experiments can determine the atomic and magnetic structure of various kinds of compound such as crystalline solids, glasses, liquids or amorphous materials. Neutron diffraction is elastic neutron scattering. The neutrons leaving the experiment sample have around the same energy as the incoming neutrons. The technique is similar to X-ray diffraction but the different type of radiation gives complementary information. The sample is placed in a beam of thermal or cold neutrons, and the intensity of scattered neutrons as function of scattering angle is measured. This gives information about the structure of the material.

By analyzing the scattering pattern the space group of the crystal can be determined. The intensity of the scattering depends on which atoms are scattered. Oxygen does not scatter very much, and is therefore difficult to see in experiments. This is the primary reason why it is difficult to locate

the position of the oxygen in crystals.

Rial et al. [10] believes that the extra oxygen sits on site 8e in the Cmce space-group 64, with is an orthorhombic space-group with $b > c > a$. In this case "8" means, that there are eight symmetry equivalent positions where the oxygen can be. Note they are not necessarily all occupied. We use the standard notation Bmab instead of Cmce used in [10]. In the standard notation we have that $c > b > a$. In this notation, the symmetry equivalent positions of the site 8e, according to international tables of crystallography, are given in table 3.1

x	$(1/4, -1/4, z) = (1/4, 3/4, z)$
x	$(3/4, -3/4, -z+1/2) = (3/4, 1/4, -z+1/2)$
x	$(3/4, -3/4, -z) = (3/4, 1/4, 1-z)$
x	$(1/4, -1/4, z+1/2) = (1/4, 3/4, z+1/2)$
x	$(3/4, -1/4, z+1/2) = (3/4, 3/4, z+1/2)$
x	$(1/4, -3/4, -z) = (1/4, 1/4, 1-z)$
x	$(1/4, -3/4, -z+1/2) = (1/4, 1/4, -z+1/2)$
x	$(3/4, -1/4, z) = (3/4, 3/4, z)$

Table 3.1: Allowable symmetry positions in Bmab notation for site 8e.

It is always allowed to add by one or subtract by one in any coordinates. This simply correspond to translating into the next unit cell. I have done this in the right column of table 3.1 to have positive coordinate values. In this notation z is a free parameter, z can be whatsoever from a symmetry point of view, but for a specific system, like the one we are looking at, z has a specific value. In our case $z = 0.21$ [10] or 0.25 [45].

Regarding the occupation on each site, i.e., how many percent of the eight authorized positions there on average are for oxygen. This will be counted based on the table entry labeled 'Occ' divided by 2 (as occupation would be if all 8e sites were fully occupied). It also directly links to the amount of oxygen one managed to put in the sample. in our case somewhere between 0.08 and 0.12 for a fully oxygenated sample is probably a good estimate, so let's say for example/for simplicity Occ = 0.1. Thereby we get something along the line of $\frac{0.1}{2} = 0.05$ i.e. 5 "% of the allowed symmetry positions are occupied[10].

CHAPTER 4

Mathematical Model

In this chapter we will elaborate on the mathematics and computing techniques needed to do the self-consistent calculations of electron densities. We will start with the 2D system, then the 3D system. Afterwards we will put in the excess oxygen as a mean field potential.

4.1 Mathematical Methods for a 2D model

As mentioned earlier in the section on cuprates a lot of essential physics can be explained by a one band Hubbard model for one plane in the cuprate crystal. We use the tight-binding approximation to describe the electron interaction via a Cu-O-Cu bond. In this approximation the free electrons are restricted to move via oxygen to discrete positions corresponding to copper sites on a crystal lattice. We simplify our crystal to have a quadratic structure with $a = b$.

The Hamiltonian (see section 2.2.2) is written in second quantization, and in this setup it is given by:

$$\begin{aligned}\hat{\mathcal{H}} = & - \sum_{ij\sigma} t_{ij} \hat{c}_{i\sigma}^\dagger \hat{c}_{j\sigma} + \sum_{i\sigma} (\epsilon_{i\sigma} - \mu) \hat{n}_{i\sigma} \\ & + U \sum_{\langle ij \rangle} \hat{n}_{i\uparrow} \hat{n}_{i\downarrow} - V \sum_{\langle ij \rangle} \hat{n}_{i\uparrow} \hat{n}_{j\downarrow},\end{aligned}\tag{4.1}$$

where $\hat{c}_{i\sigma}^\dagger$ and $\hat{c}_{j\sigma}$ are the creation and annihilation operators, respectively. $\langle ij \rangle$ indicates the summation over nearest-neighbor pairs; we denote the nearest-neighbor hopping term with t , and the next nearest-neighbor hopping term with t' . $\epsilon_{i\sigma}$ is the impurity potential at site i , and μ is the chemical potential.

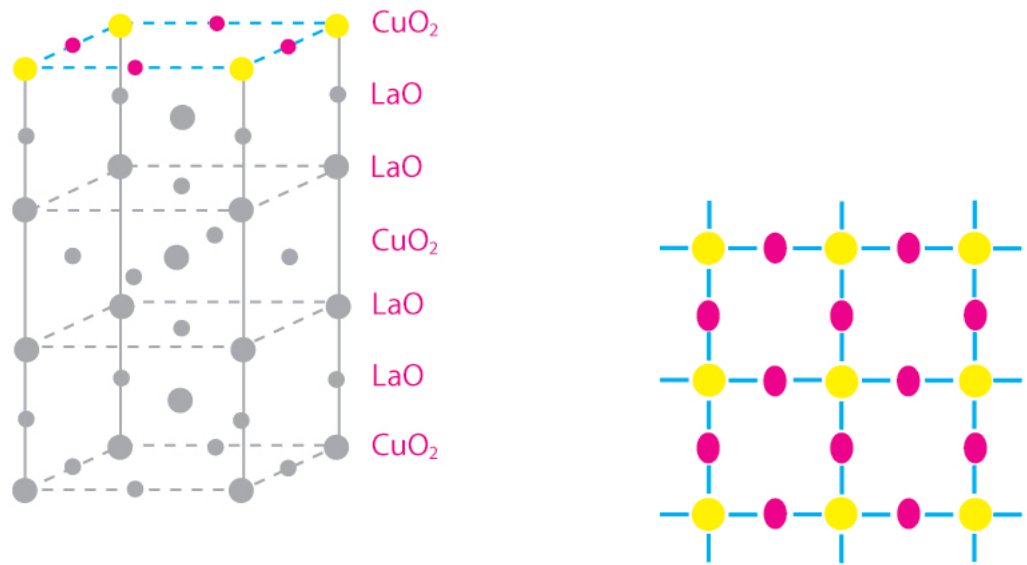


Figure 4.1: *Schematic illustration of the Cu-O-Cu bond. Yellow represents copper and pink represents oxygen. Right: Crystal structure of LSCO. The colored represent the important CuO₂ layer in the tight-binding model. Left: Simplified diagram of the CuO₂ planes in the tight-binding model. The copper $3d_{x^2-y^2}$ orbital hybridize with the oxygen $2p_{x,y}$ orbital allowing the electrons to hop from one copper site to the neighboring copper site trough interstitial Cu-O-Cu bond.*

We make a mean-field approximation of the Hamiltonian get the following expression:

$$\begin{aligned} \hat{\mathcal{H}} = & - \sum_{ij\sigma} t_{ij} \hat{c}_{i\sigma}^\dagger \hat{c}_{j\sigma} + \sum_{i\sigma} (\epsilon_{i\sigma} - \mu) \hat{n}_{i\sigma} \\ & + U \sum_{i\sigma} (n_i - \sigma m_i) \hat{n}_{i\sigma} + \sum_{\langle ij \rangle} (\Delta_{ij} \hat{c}_{i\uparrow}^\dagger \hat{c}_{j\downarrow}^\dagger + H.c). \end{aligned} \quad (4.2)$$

Here σ is +1 for spin up and -1 for spin down and H.c represents the Hermitian conjugate. The chemical potential is a free parameter we use to adjust the electron filling. The parameter is adjusted by self-consistency until the desired density is achieved. The nearest neighbor hopping interaction is set as a unit of the energy of the system, so that all the other parameters are given in terms of t . The mean field quantities, which we in this method guess as the initial value, and then self-consistently solve, are the following:

$$n_i = \langle \hat{n}_{i\uparrow} + \hat{n}_{i\downarrow} \rangle, \quad (4.3)$$

$$m_i = \langle \hat{n}_{i\uparrow} - \hat{n}_{i\downarrow} \rangle, \quad (4.4)$$

$$\Delta_{\delta i} = V \langle \hat{c}_{i\uparrow} \hat{c}_{i+\delta\downarrow} \rangle. \quad (4.5)$$

It is crucial that we can diagonalize the Hamiltonian in order to continue with computer calculations, the term needs to be quadratic in the creation and annihilation operators. To diagonalize this Hamiltonian we use the standard diagonalization method called Bogoliubov transformation. The spin-generalized Bogoliubov equation are given by [3]:

$$\hat{c}_{i\uparrow} = \sum_n (u_{n,i\uparrow} \hat{\gamma}_{n\uparrow} + v_{n,i\uparrow}^* \hat{\gamma}_{n\downarrow}^\dagger), \quad (4.6)$$

$$\hat{c}_{i\uparrow}^\dagger = \sum_n (u_{n,i\uparrow}^* \hat{\gamma}_{n\uparrow}^\dagger + v_{n,i\uparrow} \hat{\gamma}_{n\downarrow}), \quad (4.7)$$

$$\hat{c}_{i\downarrow} = \sum_n (u_{n,i\downarrow} \hat{\gamma}_{n\downarrow} + v_{n,i\downarrow}^* \hat{\gamma}_{n\uparrow}^\dagger), \quad (4.8)$$

$$\hat{c}_{i\downarrow}^\dagger = \sum_n (u_{n,i\downarrow}^* \hat{\gamma}_{n\downarrow}^\dagger + v_{n,i\downarrow} \hat{\gamma}_{n\uparrow}). \quad (4.9)$$

where u and v are eigenvectors. The sum is over all positive energies. The transformation express the electron creation and annihilation as a linear

combination of the creation operators $\hat{\gamma}_{i\sigma}^\dagger$ and the annihilation operators $\hat{\gamma}_{i\sigma}$ for non-interacting Fermionic quasiparticles with positive eigenvalues. After more mathematical manipulations (see section 2.2.4) we arrive at the Bogoliubov-de Gennes equations:

$$\begin{pmatrix} \hat{\xi}_\uparrow & \hat{\Delta} \\ \hat{\Delta}^* & \hat{\xi}_\downarrow \end{pmatrix} \begin{pmatrix} u_{n\uparrow} \\ v_{n\downarrow} \end{pmatrix} = \epsilon_\uparrow \begin{pmatrix} u_{n\uparrow} \\ v_{n\downarrow} \end{pmatrix} \quad (4.10)$$

for positive eigenvalue ϵ_\uparrow and

$$\begin{pmatrix} \hat{\xi}_\downarrow & -\hat{\Delta} \\ -\hat{\Delta}^* & -\hat{\xi}_\uparrow \end{pmatrix} \begin{pmatrix} u_{n\downarrow}^* \\ v_{n\uparrow}^* \end{pmatrix} = \epsilon_\downarrow \begin{pmatrix} u_{n\downarrow}^* \\ v_{n\uparrow}^* \end{pmatrix} \quad (4.11)$$

for eigenvalues ϵ_\downarrow . The operators are defined as follow:

$$\hat{\xi}_\sigma u_i = \sum_j t_{ij} u_j + (\epsilon_{i\sigma} - \mu + U(n_i - \sigma m_i)) u_i \quad (4.12)$$

and

$$\hat{\Delta} u_i = \sum_\delta \Delta_{\delta i} u_{i+\delta} u_i. \quad (4.13)$$

There are some symmetries between the equations that can be exploited. First we have that $\langle \hat{c}_{i\uparrow} \hat{c}_{i+\delta\downarrow} \rangle = \langle \hat{c}_{i+\delta\uparrow} \hat{c}_{i\downarrow} \rangle$. In addition, we have that if $\begin{pmatrix} u \\ v \end{pmatrix}$ is the eigenvector to the negative eigenvalues $-\epsilon$ then $\begin{pmatrix} u^* \\ v^* \end{pmatrix}$ must be the eigenvector for the positive eigenvalues ϵ . As a consequence, we can simply look at the matrix with positive eigenvalues:

$$\begin{pmatrix} \hat{\xi}_\uparrow & \hat{\Delta} \\ \hat{\Delta}^* & -\hat{\xi}_\downarrow^* \end{pmatrix} \begin{pmatrix} u_n \\ v_n \end{pmatrix} = \epsilon_n \begin{pmatrix} u_n \\ v_n \end{pmatrix} \quad (4.14)$$

The mean field terms n, m , and Δ , depend upon their own eigenvalues and eigenvectors. They are self-consistent quantities and must be found interactively by guessing an initial value for the parameters, and then diagonalizing the matrix. The parameter is then computed from the new eigenvalues and eigenvectors. The process is repeated until the change in the parameter in each iteration is less than an acceptable tolerance. It would therefore at this

point be wise to express the quantities n, m, δ in terms of the eigenvalues and eigenvectors u and v . We begin with the densities n :

$$\begin{aligned} n_i &= \langle \hat{n}_{i\uparrow} + \hat{n}_{i\downarrow} \rangle \\ &= \langle \hat{c}_{i\uparrow}^\dagger \hat{c}_{i\uparrow} + \hat{c}_{i\downarrow}^\dagger \hat{c}_{i\downarrow} \rangle \\ &= \langle \hat{c}_{i\uparrow}^\dagger \hat{c}_{i\uparrow} \rangle + \langle \hat{c}_{i\downarrow}^\dagger \hat{c}_{i\downarrow} \rangle \end{aligned} \quad (4.15)$$

and magnetization m :

$$\begin{aligned} m_i &= \langle \hat{n}_{i\uparrow} - \hat{n}_{i\downarrow} \rangle \\ &= \langle \hat{c}_{i\uparrow}^\dagger \hat{c}_{i\uparrow} - \hat{c}_{i\downarrow}^\dagger \hat{c}_{i\downarrow} \rangle \\ &= \langle \hat{c}_{i\uparrow}^\dagger \hat{c}_{i\uparrow} \rangle - \langle \hat{c}_{i\downarrow}^\dagger \hat{c}_{i\downarrow} \rangle. \end{aligned} \quad (4.16)$$

so to get an expression for both the density n and the magnetization m , we need to evaluate the term:

$$\begin{aligned} \langle \hat{c}_{i\sigma}^\dagger \hat{c}_{i\sigma} \rangle &= \sum_n ((u_{n,i\sigma} \hat{\gamma}_{n\sigma} + v_{n,i\sigma}^* \hat{\gamma}_{n\sigma'}^\dagger)(u_{n,i\sigma}^* \hat{\gamma}_{n\sigma} + v_{n,i\sigma'} \hat{\gamma}_{n\sigma'})) \\ &= \sum_n (|u_{n\sigma}|^2 \langle \hat{\gamma}_{n\sigma}^\dagger \hat{\gamma}_{n\sigma} \rangle + |v_{n\sigma}|^2 \langle \hat{\gamma}_{n\bar{\sigma}}^\dagger \hat{\gamma}_{n\bar{\sigma}} \rangle) \\ &= \sum_n (|u_{n\sigma}|^2 f_{n\sigma} + |v_{n\sigma}|^2 (1 - f_{n\bar{\sigma}})), \end{aligned} \quad (4.17)$$

where σ represent the spin \uparrow or \downarrow and σ' represent the same spin, but of different orientation than σ . And

$$f_{n\sigma} = \frac{1}{e^{(\epsilon - \mu)/kT} + 1} \quad (4.18)$$

is the Fermi-Dirac distribution for particles with eigenvalues given by $\epsilon_{n\sigma}$.

The superconducting term it:

$$\begin{aligned} \Delta_{\delta i} &= \langle \hat{c}_{i\sigma} \hat{c}_{i+\delta\sigma'} \rangle \\ &= V \sum_n (u_{n,i\sigma} v_{n,i+\delta\sigma'} \langle \hat{\gamma}_{n\sigma} \hat{\gamma}_{n\sigma'}^\dagger \rangle + v_{n,i\sigma}^* u_{n,i+\delta\sigma'} \langle \hat{\gamma}_{n\sigma'} \hat{\gamma}_{n\sigma}^\dagger \rangle) \\ &= V \sum_n (u_{n,i\sigma} v_{n,i+\delta\sigma'} (1 - f_{n\sigma}) + v_{n,i\sigma}^* u_{n,i+\delta\sigma'} f_{n\sigma'}). \end{aligned} \quad (4.19)$$

The expressions can be further reduced, but I find it to be easier to just work with them as they are. The reduced terms are given by [43]:

$$n_i = 1 - \frac{1}{2} \sum_n (|u_{n,i}|^2 - |v_{n,i}|^2) \tanh \left(\frac{\epsilon_n}{2k_b T} \right), \quad (4.20)$$

$$m_i = \frac{1}{2} \sum_n (|u_{n,i}|^2 - |v_{n,i}|^2) \tanh \left(\frac{\epsilon_n}{2k_b T} \right), \quad (4.21)$$

$$\Delta_{ij} = \frac{v}{4} \sum_n (u_{n,i} v_{n,j} + u_{n,i+j} v_{n,i}^*) \tanh \left(\frac{\epsilon_n}{2k_b T} \right), \quad (4.22)$$

where the sums are over all energies.

4.1.1 Guessing parameters

In many cuprates we see different stripe orders, and this can not necessarily be stabilized self-consistent in the calculations. The tricks one should use to stabilise stripes is to guess on something with same periodicity. In LSCO we have stripe with periodicity 8, so a good initial guess would be:

$$n_{\text{guess}} \pm m_{\text{guess}} = 0.5 \pm 0.05 (\cos(0.750\pi x + 0.375\pi)) (-1)^y. \quad (4.23)$$

If one wants to stabilize for example, an antiferromagnet one should have an initial guess that supports this. We do this because a self-consistent solution usually takes a minimum close to the value one have given as input. If one gives a bad initial guess, a minimum value can take a very long time to achieve and in some cases a minimum is not found at all.

4.1.2 2D Model matrix

The size of the system we calculate is severely limited by computing power. This means that the lattice size also depends on the type of calculation one wants calculated. Density calculation in 2D a lattice size of 20×20 takes a reasonable amount of time and is large enough to reflect reality. In order to make a more real life model we use periodic boundary conditions, since in real life you will not find so small systems. This means that the last lattice

point in the row will interact with the first lattice point in the row. The same goes for the columns. In the matrix below the nearest neighbor with periodic boundary conditions to $a_{1,1}$ (in blue) are marked with red.

$$\begin{pmatrix} a_{1,1} & a_{1,2} & a_{1,3} & \cdots & a_{1,n} \\ a_{2,1} & a_{2,2} & a_{2,3} & \cdots & a_{2,n} \\ a_{3,1} & a_{3,2} & a_{3,3} & \cdots & a_{2,n} \\ \vdots & \vdots & \vdots & \ddots & \vdots \\ a_{m,1} & a_{m,2} & a_{m,3} & \cdots & a_{m,n} \end{pmatrix} \quad (4.24)$$

The periodic boundary conditions for next-nearest neighbor are:

$$\begin{pmatrix} a_{1,1} & a_{1,2} & a_{1,3} & \cdots & a_{1,n} \\ a_{2,1} & a_{2,2} & a_{2,3} & \cdots & a_{2,n} \\ a_{3,1} & a_{3,2} & a_{3,3} & \cdots & a_{1,n} \\ \vdots & \vdots & \vdots & \ddots & \vdots \\ a_{m,1} & a_{m,2} & a_{m,3} & \cdots & a_{m,n} \end{pmatrix} \quad (4.25)$$

We compute the mean field values self consistently by representing the Hamiltonian in a matrix and then diagonalizing it. m , n and Δ are calculated, and the new Hamiltonian with these values is diagonalized. This process is repeated until it converges. To do so, we need to construct our matrix according to the BdG equation $\begin{pmatrix} \hat{\xi}_\uparrow & \hat{\Delta} \\ \hat{\Delta} & \hat{\xi}_\downarrow \end{pmatrix}$. Let us first look at the diagonal $\hat{\xi}$, for a lattice of size $N_x \times N_y$ we will have $N_x N_y$ lattice points. This will be represented by a matrix of size $N_x^2 \times N_y^2$ for both spin up and spin down. For this matrix the diagonal represents the lattice points (in this case the Cu atoms) from 1 to $N_x N_y$. If one wishes to have a square matrix one must make sure that $N_x = N_y$. A square matrix will be symmetrical about the diagonal, this is because, in this model, if a lattice point (n, m) can interact with another lattice point (n', m') then (n', m') can also interact with (n, m) . Note however, the spins are named from 1 to $N_x \times N_y$, and the entry number (n, m) denotes the interaction between the spin number n and m . The matrix then becomes:

$$\hat{\xi}_\sigma = \begin{pmatrix} \text{Cu}_{1\sigma} & t_{\text{Cu}_1, \text{Cu}_2} & t_{\text{Cu}_1, \text{Cu}_3} & \cdots & t_{\text{Cu}_1, \text{Cu}_{N_x N_y}} \\ t_{\text{Cu}_2, \text{Cu}_1} & \text{Cu}_{2\sigma} & t_{\text{Cu}_2, \text{Cu}_3} & \cdots & t_{\text{Cu}_2, \text{Cu}_{N_x N_y}} \\ t_{\text{Cu}_3, \text{Cu}_1} & t_{\text{Cu}_3, \text{Cu}_2} & \text{Cu}_{3\sigma} & \cdots & t_{\text{Cu}_3, \text{Cu}_{N_x N_y}} \\ \vdots & \vdots & \vdots & \ddots & \vdots \\ t_{\text{Cu}_{N_y}, \text{Cu}_1} & t_{\text{Cu}_{N_y}, \text{Cu}_2} & \cdots & \cdots & \text{Cu}_{N_x N_y \sigma} \end{pmatrix} \quad (4.26)$$

Again σ represent the spins \uparrow, \downarrow . All interactions will be zero except the nearest and next-nearest neighbor. The location of the nearest neighbor interaction t_{ij} in the matrix $\hat{\xi}$ for the lattice cite Cu_{N_x+n} where $n \in 0, \dots, N_x^2 N_y^2$ is given in the matrix by eq. 4.27

Where $t_{\text{Cu}_{N_x+n}, \text{Cu}_{N_x+n-1}}$ represent the interaction from Cu_{N_x+n} to Cu_{N_x+n-1} and so on. The location the next-nearest neighbor interaction in the matrix $\hat{\xi}$ is given by eq. 4.28.

Where $t_{\text{Cu}_{N_x+n}, \text{Cu}_{N_x+n-N_x-1}}$ represent the interaction from Cu_{N_x+n} to $\text{Cu}_{N_x+n-N_x-1}$. You can in principle make any of the lattice point interact, and not necessarily in a symmetrical manner, if you felt the need to. The superconducting order parameter has a $d_{x^2-y^2}$ symmetry which means that the sign of the interaction will be different between the x and the y directions. When we include the superconductivity parameter in the matrix describing \mathcal{H} , which also has the nearest neighbor interaction (as shown in the matrix above) the full matrix becomes the following eq. 4.29

Where all interactions will be zero except for the t corresponding to nearest and next nearest neighbor and the Δ corresponding to nearest neighbor. Because of the symmetry between the eigenvalues we do not need to construct the matrix corresponding to the negative eigenvalues.

4.2 Mathematical Methods for 3D Model

The treatment of the 3D model follows the same outline as the 2D model. The interaction is still between the Cu-O-Cu bonds but now they can also interact in the c direction. In reality LSCO, LCO+O and LSCO+O get a more complicated structure because the layers are not symmetric but have at orthorhombic/tetragonal space group. We compensate for this by regulating the hopping term between the layers. In our case this means that it is smaller than the hopping in the layers. We simplify our crystal to have this structure fig. 4.2

$$\left(\begin{array}{ccccccc} \dots & \cdot & \dots & \cdot & \dots & \cdot & \dots \\ \dots & \cdot & \dots & \cdot & \dots & \cdot & \dots \\ \dots & \cdot & \dots & \cdot & \dots & \cdot & \dots \\ \dots & t_{\text{Cu}_{N_x+n}, \text{Cu}_{N_x+n-N_x}} & \dots & t_{\text{Cu}_{N_x+n}, \text{Cu}_{N_x+n-1}} & \text{Cu}_{N_x+n} & t_{\text{Cu}_{N_x+n}, \text{Cu}_{N_x+n+1}} & \dots \\ \dots & \cdot & \dots & \cdot & \cdot & \cdot & \dots \\ \dots & \cdot & \dots & \cdot & \cdot & \cdot & \dots \\ \dots & \cdot & \dots & \cdot & \cdot & \cdot & \dots \end{array} \right) t_{\text{Cu}_{N_x+n}, \text{Cu}_{N_x+n+N_x}} \quad (4.27)$$

(4.28)

$$\mathcal{H} = \begin{pmatrix} \text{Cu}_1\uparrow & t_{\text{Cu}_1,\text{Cu}_2} & t_{\text{Cu}_1,\text{Cu}_3} & \dots & t_{\text{Cu}_1,\text{Cu}_{N_x}} & \Delta_{\text{Cu}_1,\text{Cu}_2} & \Delta_{\text{Cu}_1,\text{Cu}_3} & \dots & \Delta_{\text{Cu}_1,\text{Cu}_{N_x}} \\ t_{\text{Cu}_2,\text{Cu}_1} & \text{Cu}_2\uparrow & t_{\text{Cu}_2,\text{Cu}_3} & \dots & t_{\text{Cu}_2,\text{Cu}_{N_x}} & \Delta_{\text{Cu}_2,\text{Cu}_1} & \Delta_{\text{Cu}_2,\text{Cu}_3} & \dots & \Delta_{\text{Cu}_2,\text{Cu}_{N_x}} \\ t_{\text{Cu}_3,\text{Cu}_1} & t_{\text{Cu}_3,\text{Cu}_2} & \text{Cu}_3\uparrow & \dots & t_{\text{Cu}_3,\text{Cu}_{N_x}} & \Delta_{\text{Cu}_3,\text{Cu}_1} & \Delta_{\text{Cu}_3,\text{Cu}_2} & \dots & \Delta_{\text{Cu}_3,\text{Cu}_{N_x}} \\ \vdots & \vdots & \vdots & \ddots & \vdots & \vdots & \vdots & \vdots & \vdots \\ t_{\text{Cu}_{N_y},\text{Cu}_1} & t_{\text{Cu}_{N_y},\text{Cu}_2} & \dots & \dots & \text{Cu}_{N_xN_y}\uparrow & \Delta_{\text{Cu}_{N_y},\text{Cu}_1} & \Delta_{\text{Cu}_{N_y},\text{Cu}_2} & \dots & \Delta_{\text{Cu}_{N_y},\text{Cu}_{N_x}} \\ \Delta_{\text{Cu}_1,\text{Cu}_2} & \Delta_{\text{Cu}_1,\text{Cu}_3} & \dots & \dots & \Delta_{\text{Cu}_1,\text{Cu}_{N_x}} & \text{Cu}_1\downarrow & t_{\text{Cu}_1,\text{Cu}_2} & \dots & t_{\text{Cu}_1,\text{Cu}_{N_x}} \\ \Delta_{\text{Cu}_2,\text{Cu}_1} & \Delta_{\text{Cu}_2,\text{Cu}_3} & \dots & \dots & \Delta_{\text{Cu}_2,\text{Cu}_{N_x}} & t_{\text{Cu}_2,\text{Cu}_1} & \text{Cu}_2\downarrow & t_{\text{Cu}_2,\text{Cu}_3} & t_{\text{Cu}_2,\text{Cu}_{N_x}} \\ \Delta_{\text{Cu}_3,\text{Cu}_1} & \Delta_{\text{Cu}_3,\text{Cu}_2} & \dots & \dots & \Delta_{\text{Cu}_3,\text{Cu}_{N_x}} & t_{\text{Cu}_3,\text{Cu}_1} & t_{\text{Cu}_3,\text{Cu}_2} & \text{Cu}_3\downarrow & t_{\text{Cu}_3,\text{Cu}_{N_x}} \\ \vdots & \vdots & \vdots & \ddots & \vdots & \vdots & \vdots & \ddots & \vdots \\ \Delta_{\text{Cu}_{N_y},\text{Cu}_1} & \Delta_{\text{Cu}_{N_y},\text{Cu}_2} & \dots & \dots & \dots & t_{\text{Cu}_{N_y},\text{Cu}_1} & t_{\text{Cu}_{N_y},\text{Cu}_2} & \dots & \text{Cu}_{N_xN_y}\downarrow \end{pmatrix} \quad (4.29)$$

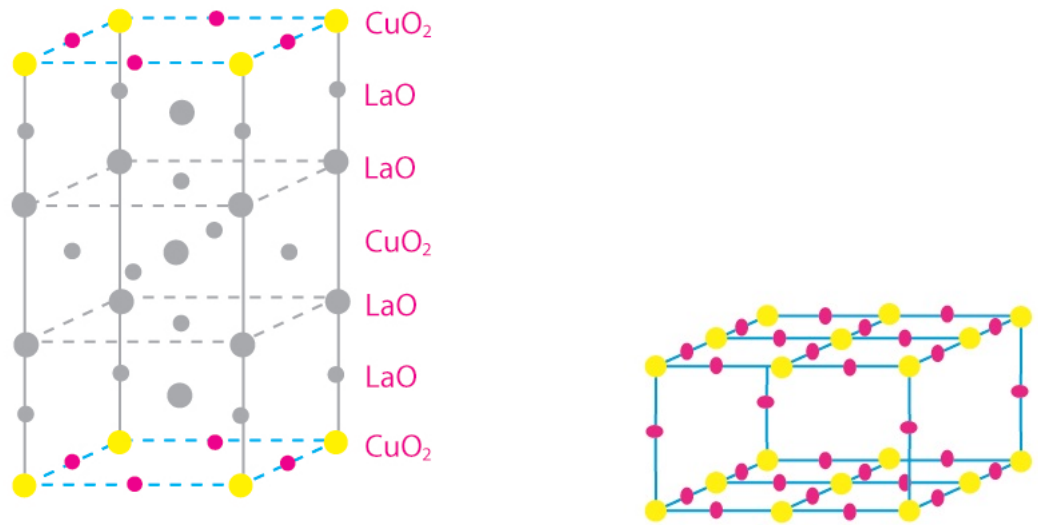


Figure 4.2: *Schematic illustration of the Cu-O-Cu bond in 3D. Yellow represents copper and pink represents oxygen. Right: Crystal structure of LSCO. The colored represent the important CuO_2 layer in the tight-binding model. Left: Simplified diagram of the CuO_2 planes in the tight-binding model. The copper $3d_{x^2-y^2}$ orbital hybridize with the oxygen $2p_{x,y}$ orbital allowing the electrons to hop from one copper site to the neighboring copper site through interstitial Cu-O-Cu bond.*

The Hamiltonian for this model is given by:

$$\begin{aligned}\hat{\mathcal{H}} = & - \sum_{ij\sigma} t_{ij} \hat{c}_{ik\sigma}^\dagger \hat{c}_{j\sigma} + \sum_{i\sigma} (\epsilon_{i\sigma} - \mu) \hat{n}_{i\sigma} \\ & + U \sum_i \hat{n}_{i\uparrow} \hat{n}_{i\downarrow} - V \sum_{\langle ij \rangle} \hat{n}_{i\uparrow} \hat{n}_{i\downarrow}\end{aligned}\quad (4.30)$$

Where t_{ij} stand for nearest neighbor t next-nearest neighbor t' and nearest interlayer neighbor t_\perp . Exactly as in the case of a single layer, the three-dimensional Hamilton must be quadratic in creation and annihilation operators. By using the mean field theory, we get the following:

$$\begin{aligned}\hat{\mathcal{H}} = & - \sum_{ij\sigma} t_{ij} \hat{c}_{i\sigma}^\dagger \hat{c}_{j\sigma} + \sum_{i\sigma} (\epsilon_{i\sigma} - \mu) \hat{n}_{i\sigma} \\ & + U \sum_{i\sigma} (n_i - \sigma m_i) \hat{n}_{i\sigma} + \sum_{ij} (\Delta_{ij} \hat{c}_{i\uparrow}^\dagger \hat{c}_{j\downarrow}^\dagger + H.c)\end{aligned}\quad (4.31)$$

The Hamiltonian can be diagonalized as in the section for the 2D case.

4.2.1 The 3D matrix

The model is built up of several layers to represent a 3 dimensional crystal, wher all the layers of the model are built in the same way.

There are periodic boundary interaction between the layers, so that the first layer interacts with the last layer. The rest of the interactions are as in the 2D case. The full 3D matrix becomes:

$$\mathbf{H}_k^{3D} = \begin{pmatrix} \mathbf{H}_1 & \mathbf{C}_1 & \mathbf{0} & \cdots & \mathbf{0} & \mathbf{0} \\ \mathbf{C}_1 & \mathbf{H}_2 & \mathbf{C}_2 & \ddots & \mathbf{0} & \mathbf{0} \\ \mathbf{0} & \mathbf{C}_2 & \mathbf{H}_3 & \ddots & \mathbf{0} & \mathbf{0} \\ \vdots & \ddots & \ddots & \ddots & \ddots & \vdots \\ \mathbf{0} & \mathbf{0} & \mathbf{0} & \ddots & \ddots & \mathbf{C}_k \\ \mathbf{0} & \mathbf{0} & \mathbf{0} & \cdots & \mathbf{C}_k & \mathbf{H}_k \end{pmatrix}\quad (4.32)$$

The elements in the matrix are given by the matrices:

$$\mathbf{H}_l = \begin{pmatrix} \hat{\xi}_{\uparrow}^l & \hat{\Delta}^l \\ \hat{\Delta}^{l*} & \hat{\xi}_{\downarrow}^l \end{pmatrix}, \quad (4.33)$$

where $l \in 1, \dots, k$, and k is the number of layers in the 3D Hamiltonian-Matrix \mathbf{H}_k^{3D} . \mathbf{H}_l is equal to the matrix \mathbf{H} from the 2D case.

$$\mathbf{C}_l = \begin{pmatrix} \hat{c}_{\uparrow}^l & \mathbf{0} \\ \mathbf{0} & \hat{c}_{\downarrow}^l \end{pmatrix} \quad (4.34)$$

\mathbf{C}_l is the coupling matrix, that couples the layers in the 3D model. Again $l \in 1, \dots, k$, and k is the number of layers in the 3D Hamiltonian-Matrix \mathbf{H}_k^{3D} . The element \hat{c}_{σ}^l is also a matrix given by:

$$\hat{c}_{\uparrow}^l = \begin{pmatrix} t_{\perp 1,1} & 0 & \dots & 0 \\ 0 & t_{\perp 2,2} & \dots & 0 \\ \vdots & \vdots & \ddots & \vdots \\ 0 & 0 & \dots & t_{\perp n} \end{pmatrix} \quad (4.35)$$

and

$$\hat{c}_{\downarrow}^l = \begin{pmatrix} -t_{\perp 1,1} & 0 & \dots & 0 \\ 0 & -t_{\perp 2,2} & \dots & 0 \\ \vdots & \vdots & \ddots & \vdots \\ 0 & 0 & \dots & -t_{\perp n} \end{pmatrix} \quad (4.36)$$

Where $n = N_x N_y$ and \hat{c}_{\uparrow}^l and \hat{c}_{\downarrow}^l describes the coupling between the layers of spin up and down, respectively. \mathbf{C}_l describes the coupling between layers in the B-dG formalism. The last element $\mathbf{0}$ is the null-matrix, where all elements are zero.

$$\mathbf{0} = \begin{pmatrix} \hat{0} & \hat{0} \\ \hat{0} & \hat{0} \end{pmatrix} \quad (4.37)$$

Note The dimensionality of the matrices: We have that $\text{Dim}[\mathbf{0}] = \text{Dim}[\mathbf{H}_l] = \text{Dim}[\mathbf{C}_l]$ and $\text{Dim}[\hat{0}] = \text{Dim}[\hat{c}_{\sigma}^l] = \text{Dim}[\hat{\xi}_{\sigma}^l] = \text{Dim}[\hat{\Delta}^l]$. Furthermore, we have that the matrix must satisfy $\mathbf{U}^* \mathbf{H} \mathbf{U} = \mathbf{D}$, where \mathbf{D} is a diagonal matrix.

4.3 The excess oxygen

We cannot put the oxygen in directly, since it exists between the lattice sites, but we can however make up for it by adding a potential, corresponding to the effect of the oxygen, to every site. We do this by imagining a coordinate-system at the bottom of our 3D lattice. In this coordinate system we define the position of the extra oxygen $R_o = X_o, Y_o, Z_o$, where we can freely change the position and occupancy of the oxygen. The potential as a function of the position of the lattice is then given by (see section 2.2.1) :

$$\hat{W}(r) = \alpha \frac{\exp(\kappa(r - R_o))}{|r - R_o|}. \quad (4.38)$$

This is the Coulomb interaction with screening. The position R_o and the occupancy of the oxygen is chosen according to experiments and literature. The parameters α (referred to section 2.2.1 in as Q) and κ are adjustable parameters, meaning that you can play around with them. There is to the best of my knowledge still no good estimates of these parameters in the literature. The Hamiltonian is given by (2.75) and (2.76) in section 2.2.5.

In the calculation, the oxygen mean-field potential will be represented by the same site in the matrices as the chemical potential μ . The presence of the oxygen in the staging will induce a potential that will effectively repel all electrons from the sites, and we will see a suppression of the d-wave order. So we should choose the sign so that they are opposite of the hopping-parameter for nearest-neighbor and has the same sign as the hopping- parameter for next nearest neighbor.

We know that there are tight-binding effect between the extra oxygen and the Cu sites in the crystal, but we do not take it into account in this model.

If we now for example look at a lattice, containing 10 unit-cells¹ in one direction, 4 in the second direction and 2 in the third direction, we will have $10 \times 4 \times 2 \times 8 = 640$ symmetry allowed positions. The oxygen can sit in 1 – 5% of 640 allowed positions, so for 5 percent there will be 32 interstitial oxygen atoms in such a unit cell. We may place them as we wish, as long as they sit on one of the allowable coordinates in a unit cell, and provides the correct periodicity of 10 along a ($= 5.38 \text{ \AA}$), 4 along the

¹Note, there is 8 lattice points in one unit cell

b ($= 5.40 \text{ \AA}$) and 2 along the c ($= 13.20 \text{ \AA}$). One can choose the positions one think support the stripes in the system.

CHAPTER 5

Numerical Results

In this chapter we present the results and calculations. The chapter is structured such that we first look at a one layer system then a two layer system and finally a multi-layer system. Within these three sections we will examine the stripe order and further the effect the intermediate oxygen has on this order

5.1 2D model

If we are to have any hope of calculating and understanding the consequences of a multilayer system with superconductivity, intermediate oxygen and stripe order, we must first make ourselves familiar with a one layer system. In this section we will look at numerical calculations for a one CuO_2 layer for both a homogeneous and striped system. We will also include calculations with the oxygen mean-field potential. All parameters in this chapter are normalized to hopping terms t .

5.1.1 Homogeneous system

We will first look at the homogeneous case without superconductivity $\Delta = 0$ and no excess oxygen $y = 0$, with a doping of both $x = 0.125$ and $x = 0.0$. The next nearest neighbor hopping terms we put to $t' = -0.2t$ and the Coulomb term to $U = 0t$. We investigate these cases because they can be indicators and provide guidelines for future guesses of normalized parameters such as U , V , and the parameters from the intermediate oxygen potential α and κ . In both cases of $x = 0.0$ and $x = 0.125$ we get a density which is identical for all sites in spin up and spin down. All the densities

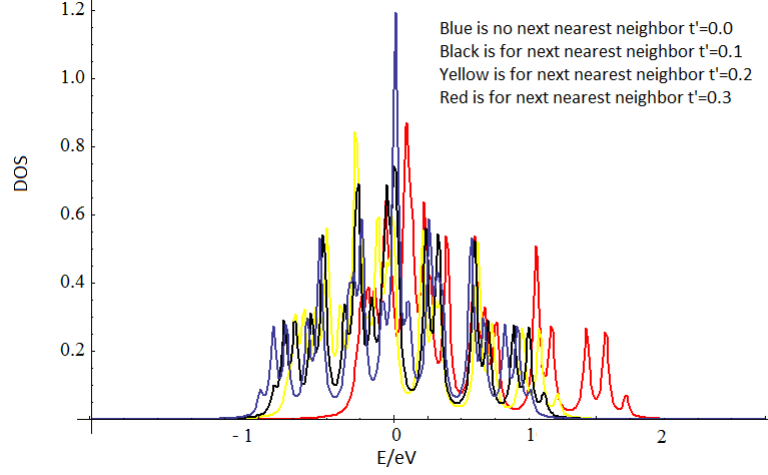


Figure 5.1: *DOS for a homogeneous system with no doping $x = 0.0$, the Coulomb term is $U = 0$ and different hopping terms t' . Blue represent $t' = 0.0t$, black represent $t' = 0.1t$, yellow represent $t' = 0.2t$ and red represent $t' = 0.3t$. The Computed for a 16×16 system.*

from each site satisfies the following $n_{i\uparrow} + n_{i\downarrow} = 1 - x$ and $n_{i\uparrow} = n_{i\downarrow}$. In the case without doping $x = 0.0$, we get an electron density of $n_{i\sigma} = 0.5t$ for both spin up and down, corresponding to a half-filled system. In the case of doping $x = 0.125$, we get $n_{i\sigma} = 0.448t$. In the following calculations we will always (unless otherwise stated) have doping $x = 0.125$ as it is well established that this particular doping supports stripes and for comparison we keep it even in the homogeneous cases. We will also keep the temperature at $Tk_B = 0.01t$ unless otherwise stated. We have plotted the density of state for the two homogeneous cases for future comparison. The density of states (DOS) is defined as:

$$\text{DOS} = \frac{1}{2} \sum_{i\sigma} (|u_{n,i\sigma}|^2 \delta(E - \epsilon_{n\sigma}) + |v_{n,i\sigma}|^2 \delta(E + \epsilon_{n\sigma})), \quad (5.1)$$

where $\delta(x)$ is the Dirac-Delta function.

If we adjust the next nearest neighbor term to $t' = -0.0t, -0.1t, -0.2t, -0.3t$ in a system of size 16×16 (see fig. 5.1), we see a Van Hove peak in $E = 0 \sim \text{eV}$ in the Dos plot fig. 5.1 for $t' = 0.0t$ (blue) corresponding to critical points in the Brillouin zone. The smaller peaks that occur in all the cases

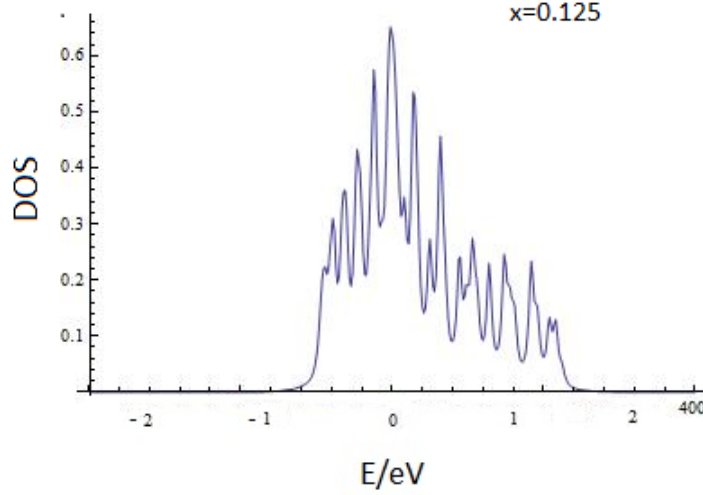


Figure 5.2: *DOS for a homogeneous system with a doping at $x = 0.125$, the Coulomb term at $U = 0$ and the hopping term $t' = 0.2t$. Computed for a 16×16 system.*

of t' are the peak corresponding to the distance $Ut/16 \times 16$. In the following calculations we will stick to $t' = 0.2$ (unless otherwise specified) as it supports stripes and is consistent with previous calculations on the subject.

The homogeneous system will serve as the backbone of the model from where we expand by including superconductivity, intermediate oxygen potential $W_{R_o}(r)$, z -axis and stripe order.

5.1.2 Striped system

We now want to extend our system to include stripes, this is done by guessing on a striped density. The guess used in this thesis is $n_{\text{guess}} = 0.5 \pm 0.05 (\cos(0.750\pi x + 0.375\pi)) (-1)^y$ where the minus sign correspond to spin up and the plus sign correspond to spin down. When the obtained striped densities are calculated self-consistently, we interpret them as follows: The spin lengths are given by the difference of the densities $n_{i\sigma}$, and the orientations are given by the sign of the difference where positive cor-

responds to spin up \uparrow and negative corresponds to spin down \downarrow :

$$m_i^s = n_{i\uparrow} - n_{i\downarrow}. \quad (5.2)$$

The arrow-heads represent the one minus the sum of the densities $1 - (n_{i\uparrow} + n_{i\downarrow})$ for spin up \uparrow and down \downarrow :

$$n_i^s = 1 - (n_{i\uparrow} + n_{i\downarrow}). \quad (5.3)$$

The reason we subtract by 1 is that the overall average of density for the system is 1 and we want to find the holes of the system. The length and size of the strips should be interpreted relative to one another.

In the case of a striped system without the superconducting term Δ and no excess oxygen $y = 0$ with a doping $x = 0.125$ and the Coulomb term at $U = 4t$ we get the following striped system (see fig. 5.5). We see that the stripes have a periodicity of 8 and that they lie antiferromagnetic which is in line with [29]. The system also stabilizes for $U = 3.4t$ to $U = 8t$. Presumably also higher, but this has not been tested in this system. The electron densities are plotted as a square matrix with lengths that correspond to the system size of 16×16 in 5.3. Dos in the case of $U = 4t$ and $t' = 0.2t$ is given in fig. 5.4. The first 16 sites of fig. 5.3 are plotted as a cartoon plot in fig. 5.5.

In the density plots we see an obvious stripe pattern corresponding to relatively high and low densities n_i . In the right plot of the figure we see the magnetization m_i for the striped system. The magnetization has a checkered-like pattern corresponding to the changing sign.

The plots of the striped cases will be used later, for a comparison on a more complex system

5.1.3 Striped superconducting system

We now expand the system to include the superconducting phase Δ as explained in Chapter 4. We will omit the results for the homogeneous case as it has been done many times before and we do not intend to use it for

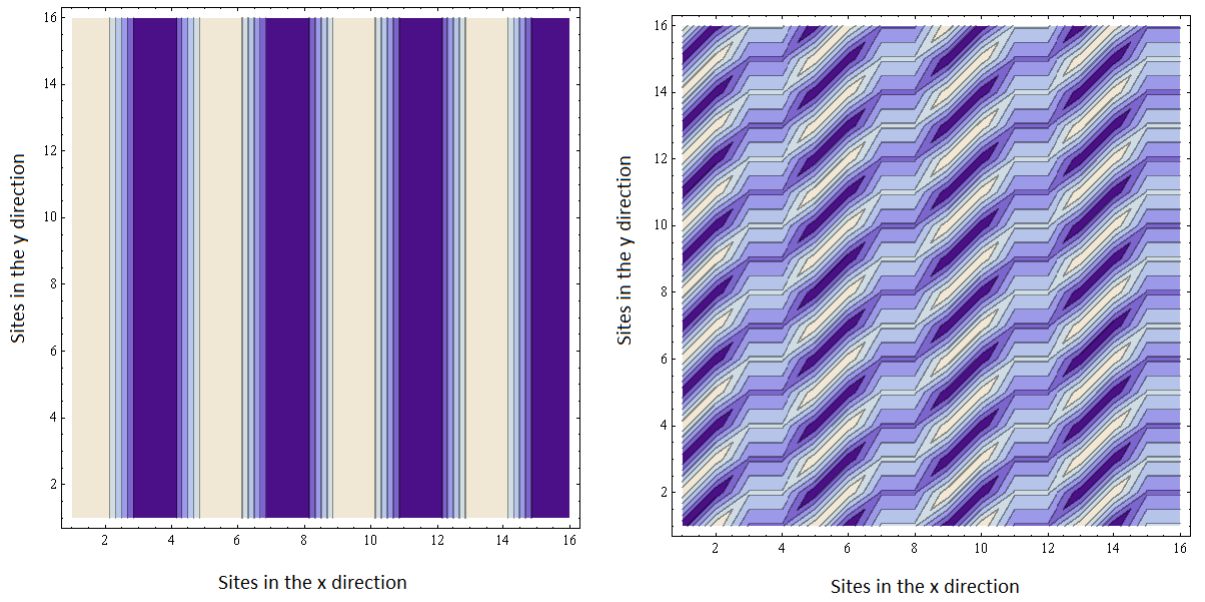


Figure 5.3: *Density and magnetization for a striped system with a doping at $x = 0.125$ and the Coulomb term at $U = 4t$. Left corresponds to the density and right corresponds to the magnetization. Computed for a 16×16 system.*

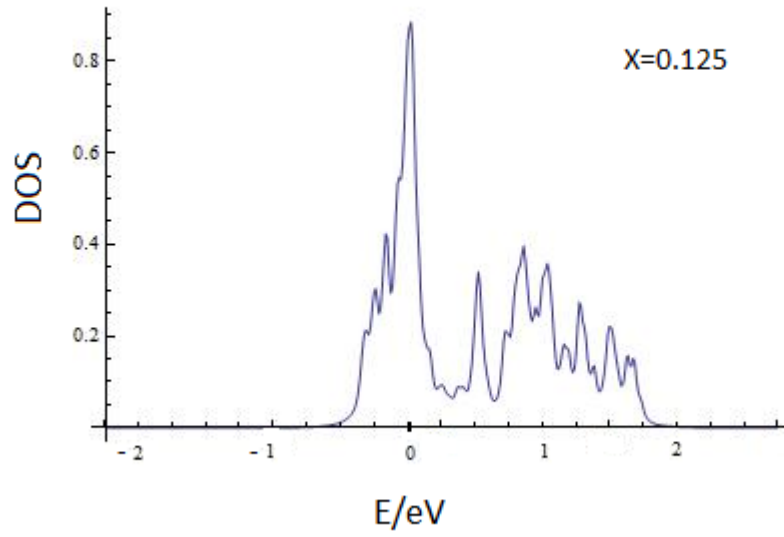


Figure 5.4: *DOS for a striped system with a doping at $x = 0.125$ and the Coulomb term at $U = 4t$. The energy scale corresponds to the Fermi level. Computed for a 16×16 system.*

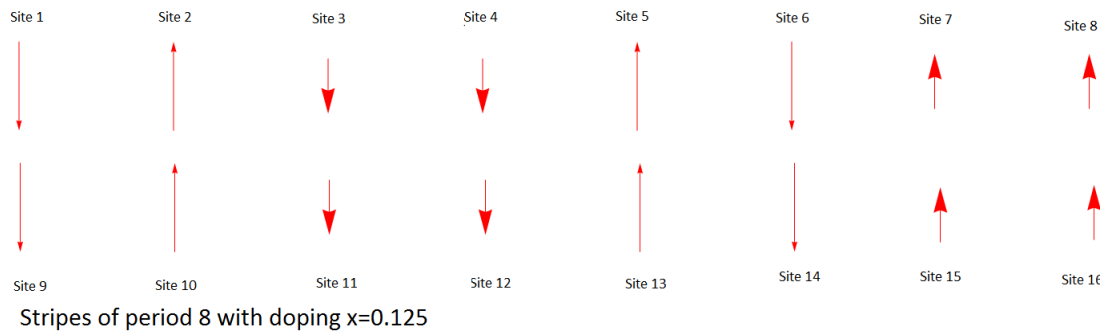


Figure 5.5: *The stripe order for a system with doping $x = 0.125$ and the Coulomb term at $U = 4t$. The figure shows the stripe order for the first 16 sites. Computed for a 16×16 system.*

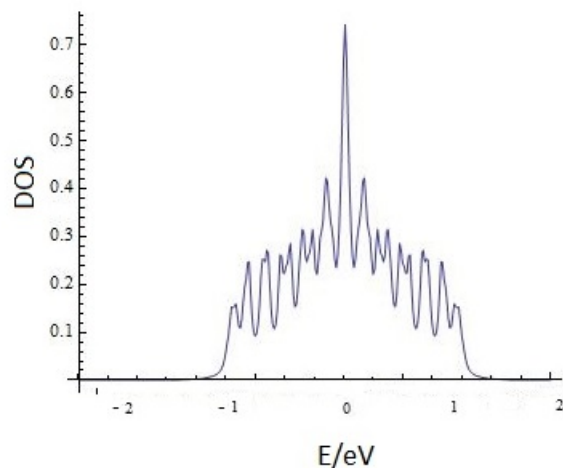


Figure 5.6: *DOS for a system with doping $x = 0.125$ and the Coulomb term at $U = 4t$, $\Delta_x = 0.243485t$, $\Delta_y = -0.243485t$ and $V = 1t$. $t' = 0.0$ Computed for a 16×16 system.*

comparison with the other results in this chapter. However, we will look at the parameters needed to stabilize the stripes order.

To stabilize a stripe order in a superconducting phase it will prove necessary to guess a small value for Δ in the order of $\sim 0.01t$. In self-consistent calculations, the homogeneous order usually wins if it becomes too dominant in magnitude. We will see this in some of the calculations below. If we guess a homogeneous Δ in the order of $\sim 0.2t$ with striped 8 period density n we get a homogeneous system. For comparison with the homogeneous system from above fig. 5.2, fig. 5.1 and the striped system fig. 5.4, DOS for a superconducting system where Δ is homogeneous of the order $\sim 0.2t$. is given in 5.6 and 5.7. We see that the system looks more like the homogeneous case than the striped case because the high value of Δ has destroyed the stripes.

5.1.4 Striped system with excess oxygen

To include the potential from the intermediate oxygen $W_{ro}(r)$, we will further expand the system as explained in Chapter 4. The first step in this calculation is to find the appropriate values for the parameters of the potential.

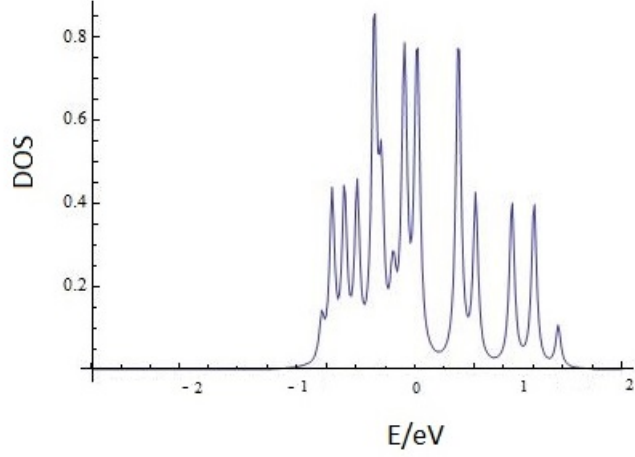


Figure 5.7: *DOS for a system with doping $x = 0.125$ and the Coulomb term at $U = 4t$, $\Delta_x = 0.243485t$, $\Delta_y = -0.243485t$ and $V = 1t$. $t' = 0.2t$. Computed for a 16×16 system.*

To my knowledge there is no documented normalized value for the mean-field potential from the intermediate oxygen, so we will have to make an educated guess. In this subsection, we will calculate two general scenarios, one with a relatively low potential (first case) and one with a relatively high potential (second case).

Let us start with the first case, a relatively low potential. In this model, all parameters are normalized to hopping between nearest neighbor parameter t . Furthermore, we have calculated that a uniform system without doping will stabilize a density of both spin up and spin down to $n_{i\sigma} = 0.5$ equal to half filled system. We have also calculated that in a striped system the densities vary from $\approx 0.2t - 0.7t$. So we do not want our potential values to exceed $W_{R_o}(r) > 0.3t$ since that would result in an over-filled. But at the same time the potential should not be too low since we want to obtain a homogeneous system with appropriate doping and excess oxygen to vary in density as a stripes system. How quickly the potential decreases as a function of the distance to the excess oxygen is still a matter of guessing. We guess $\kappa = 0.4t$ and $\alpha = 0.1t$ for potential given by:

$$W_{R_o}(r) = \alpha \frac{\exp(\kappa(R_o - r))}{|R_o - r|}, \quad (5.4)$$

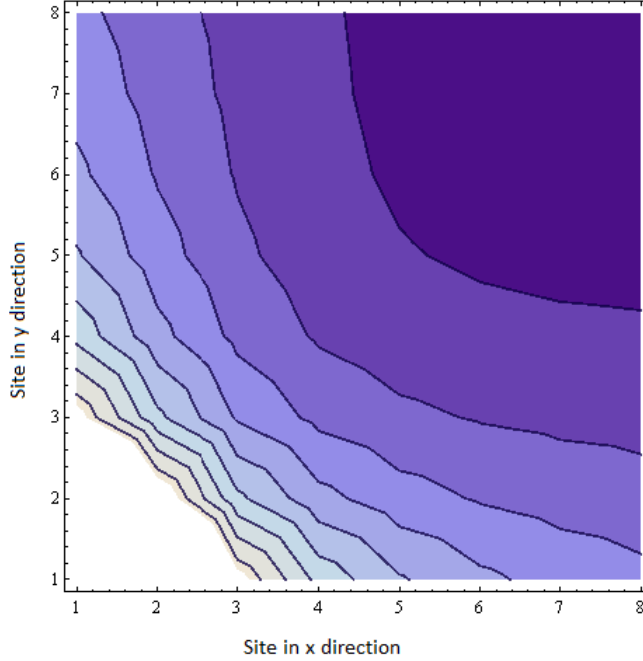


Figure 5.8: *Contour plot of the effect of the mean field potential $W_{R_o}(r)$ in the xy - plane from one oxygen placed between site 1 and 2 in both the x, y, z direction in a lattice of size 8×8 . Dark purple/blue corresponds to a value of 0.01 and white correspond to a value of size 0.18*

where R_o is the position of the oxygen. For these guessed parameters we get the right order of magnitude $\sim 0.2t$. For illustration, a plot of the effect in the xy - plane of the potential $W_{R_o}(r)$ from one oxygen placed between site 1 and 2 in both the x, y, z direction of an 8×8 and a 16×16 lattice are given in fig. 5.8 and fig. 5.9. The figures illustrate, a matrix plot of a square lattice where the first site (1, 1) starts in the left corner.

The first step on the agenda is to examine whether the added potential $W_{R_o}(r)$ can stabilize stripes on its own. If we guess a homogeneous density where the only non-homogeneous element is the mean-field potential from the intermediate oxygen $W_{R_o}(r)$ and try to solve the system self-consistently we neither get a homogeneous densities or striped densities. We have learned after many various attempts that the system has difficulty stabilizing under

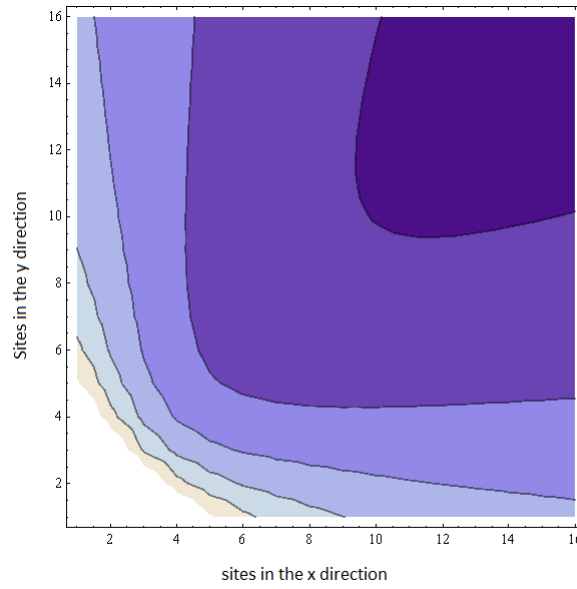


Figure 5.9: *Contour plot of the effect of the mean field potential $W_{R_o}(r)$ in the xy - plane from one oxygen placed between site 1 and 2 in both the x , y , z direction in a lattice of size 16×16 . Dark purple/blue corresponds to a value of 0.01 and white correspond to a value of size 0.18*

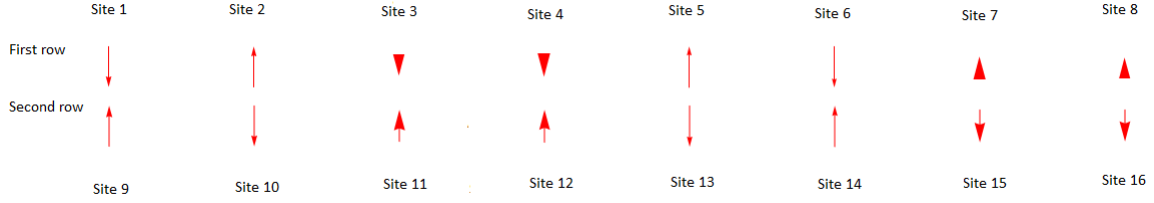


Figure 5.10: *Striped system with a mean field potential from one oxygen placed between site 1 and 2 in both the x , y , z direction. Calculated for a system of size 8×8 . The figure shows the first 16 sites in the case of additional oxygen.*

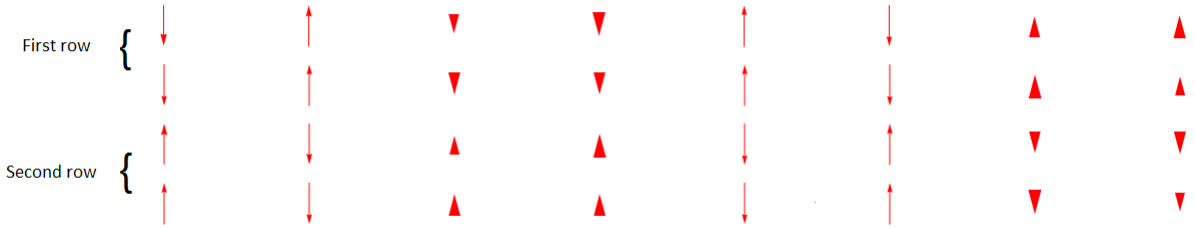


Figure 5.11: *Striped system with a mean field potential from one oxygen placed between site 1 and 2 in both the x , y , z direction. Calculated for a system of size 16×16 . The figure shows the first 32 sites in the case of additional oxygen.*

these conditions. If, on the other hand, we do as we have done before and guess a striped system, we can stabilize neat 8 period stripes 5.10 and 5.11. The figures show how the stripes stabilize in the case of a 8×8 matrix and a 16×16 matrix. In both cases we see that the spins settle antiparallel from row to row and that the oxygen does not destroy the strips. The DOS of the 16×16 system is given in 5.12. If we compare the DOS and with that from the striped system, we see that they are very similar.

In the case of two additional oxygen in a 16×16 system located respectively between $(x, y) = (1, 4)$, $(x, y) = (2, 5)$ and $(x, y) = (10, 4)$, $(x, y) = (11, 5)$ the effect of the potential $W_{R_o}(r)$ projected to the xy plan is given in 5.13. The stabilized 8 period stripes are given in 5.15. They stabilize, with the

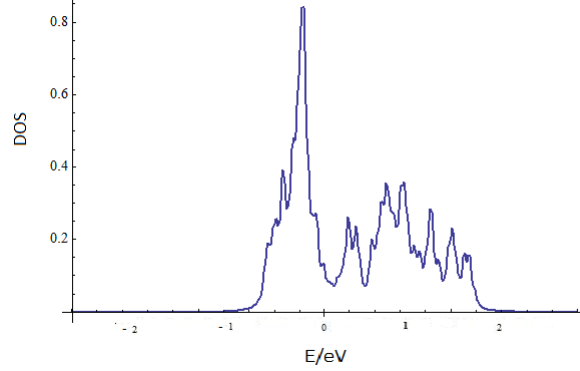


Figure 5.12: *DOS for a striped system without a superconducting phase with a mean field potential from one oxygen placed between site 1 and 2 in both the x , y , z . Calculated for a system of size 16×16 .*

same pattern as in the case of one and no intermediate oxygen. The DOS [5.16](#) is similar to a striped system without a mean field potential from an intermediate oxygen.

We see that in the first case the potential supports the stripes, and we experience that we can easily stabilize a stripe order in the densities. By comparing [fig. 5.14](#) and [fig. 5.3](#) we see nevertheless a breakage in the structure from the case without the potential $W_{R_o}(r) = 0$ to the case of with the potential $W_{R_o}(r)$. In the case with the potential $W_{R_o}(r)$ we see circle areas within the stripes that have higher value than the rest of the strip-band. These areas, however, seem to be homogeneously distributed. We also see a difference in the magnetization pattern however there is still a structure in this pattern.

In the second case, a relatively high potential, we want a maximum potential value corresponding to an overfilled system. In other words, will want the highest value from the potential $W_{R_o}(r)$ exceeding $1t$. In order to compare the two cases, we keep the parameter $\kappa = 0.4t$ identical and guess on an $\alpha = 0.7t$ see [fig. 5.17](#).

In this case the stripes are less visible and the overall pattern of the densities are not systematic as in the previous cases. A density plot is shown in [fig. 5.18](#) and a cartoon plot of the first and last 16 sites are given in [fig. 5.19](#).

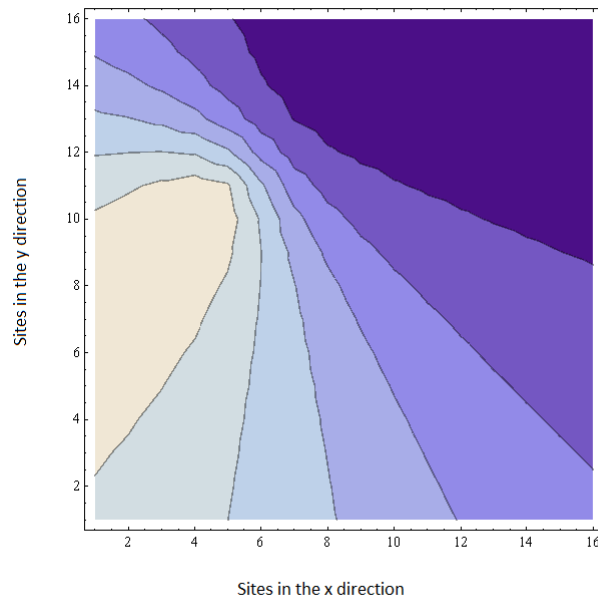


Figure 5.13: *Contour plot of the effect of the mean field potential from two oxygen, one placed between site 1 and 2 in both the x , y , z direction and the other placed between site 1 and 2 in the x z direction, and 4 and 5 in the y direction. The lattice is of size 16×16 . Dark purple/blue corresponds to a value of 0.0 and white correspond to a value of size 0.2*

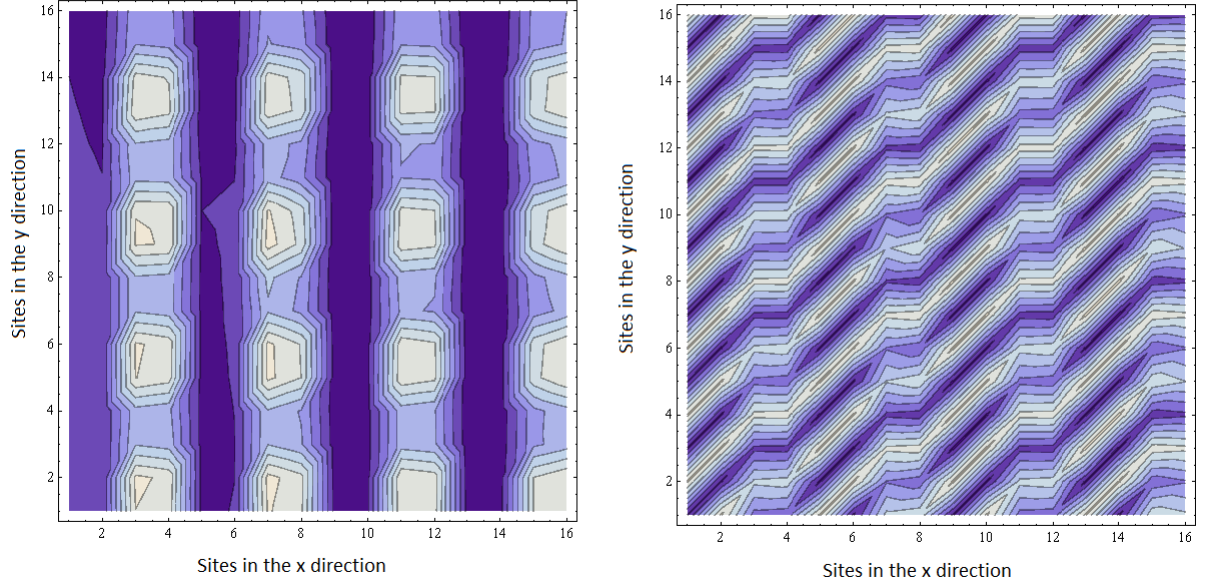


Figure 5.14: *Density and magnetization for a striped system with a doping at $x = 0.125$, the Coulomb term at $U = 4t$ mean field potential from two oxygen, one placed between site 1 and 2 in both the x , y , z direction and the other placed between site 1 and 2 in the xz direction, and 4 and 5 in the y direction. Left corresponds to the density and right corresponds to the magnetization. Computed for a 16×16 system.*

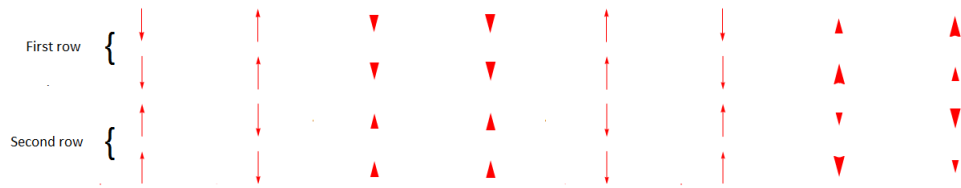


Figure 5.15: *Striped system with mean field potential from two oxygen, one placed between site 1 and 2 in both the x , y , z direction and the other placed between site 1 and 2 in the xz direction, and 4 and 5 in the y direction. The lattice is of size 16×16 . The figure shows the first 32 sites in the case of additional oxygen without a superconducting phase.*

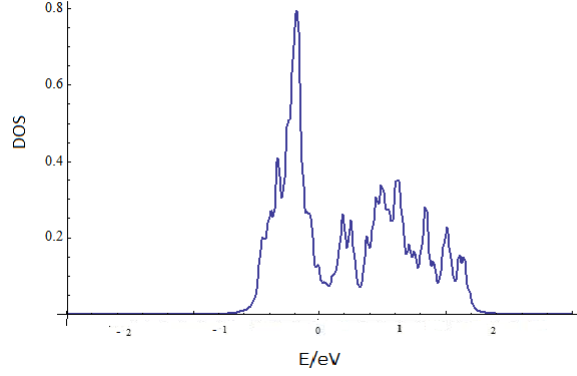


Figure 5.16: *DOS for a striped system without a superconducting phase mean field potential from two oxygen, one placed between site 1 and 2 in both the x , y , z direction and the other placed between site 1 and 2 in the xz direction, and 4 and 5 in the y direction. The lattice is of size 16×16 .*

The system seems to have much more difficulty stabilizing. The attempt to stabilize a stripe and a metallic area within the plane has not been proven possible in this scenario. It cannot be excluded that it is possible under other assumptions. However, we do see the effect of the potential pushing the electrons away. The area in the plot with low densities (left corner) correspond to the location of the potential from the oxygen fig. 5.17.

5.2 Two layers

In this section we will make a non physical system consisting of two layers. The purpose is to examine how the layers can affect each other in the 3D model. This is relevant because in a system of intermediate oxygen in modulated positions, the mean-field potential affects the layers different. We will also examine whether we see stripe modulations in the c -direction with only two layers.

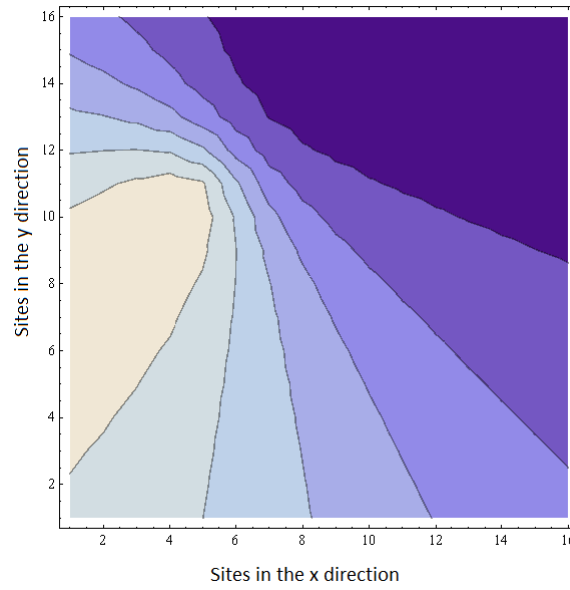


Figure 5.17: *Contour plot of the effect of the mean field potential from two oxygen, one placed between site 1 and 2 in both the x , y , z direction and the other placed between site 1 and 2 in the x z direction, and 4 and 5 in the y direction. The lattice is of size 16×16 . Dark purple/blue corresponds to a value of 0.0 and white correspond to a value of size 1.2*

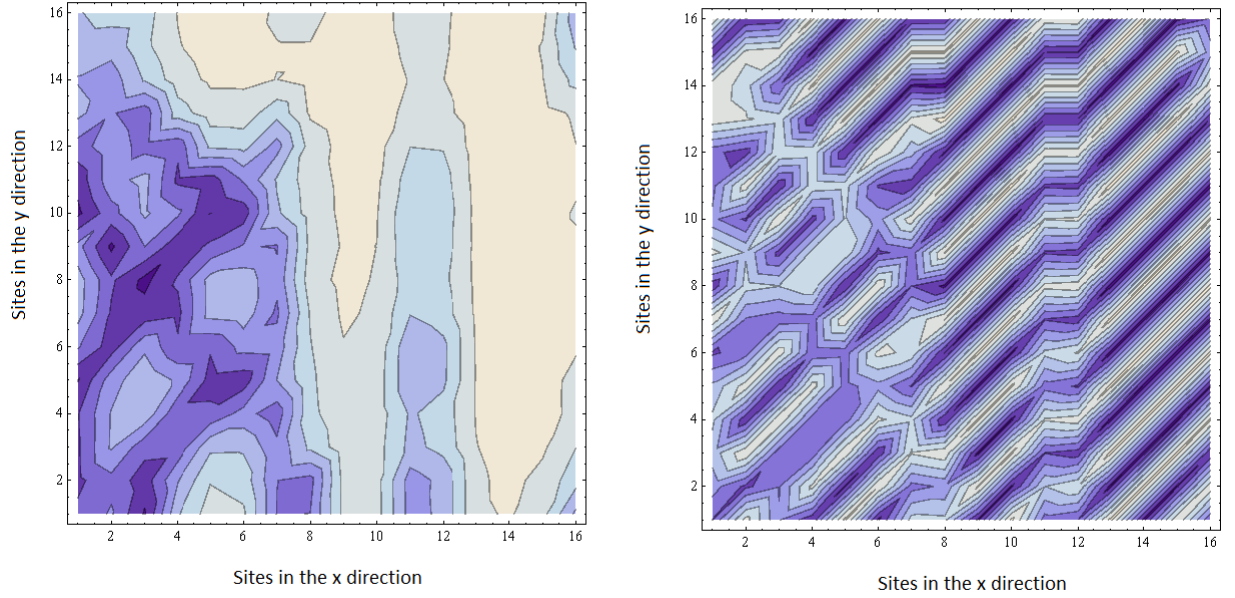


Figure 5.18: *Density and magnetization for a striped system with a doping at $x = 0.125$, the Coulomb term at $U = 4t$ mean field potential from two oxygen, one placed between site 1 and 2 in both the x, y, z direction and the other placed between site 1 and 2 in the xz direction, and 4 and 5 in the y direction. Left corresponds to the density and right corresponds to the magnetization. Computed for a 16×16 system.*

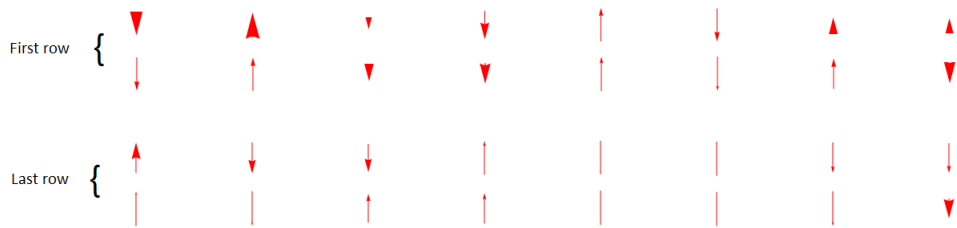


Figure 5.19: *Striped system with mean field potential from two oxygen, one placed between site 1 and 2 in both the x, y, z direction and the other placed between site 1 and 2 in the xz direction, and 4 and 5 in the y direction. The lattice is of size 16×16 . The figure shows the first and last 16 sites in the case of additional oxygen without a superconducting phase.*

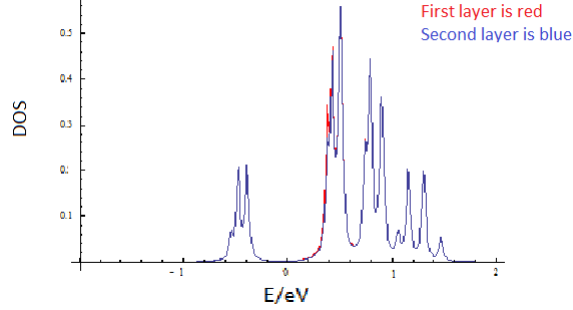


Figure 5.20: *DOS for a two layer system. The first layer (red) is a striped system with Coulomb term $U = 4t$ and doping $x = 0.125$. The second layer (blue) is a homogeneous system with Coulomb term $U = 0$, and doping $x = 0.125$. The calculations are for a system of 16×16 and with the next nearest neighbor term $t' = -0.2t$ and $t_{\perp} = -0.1t$. The two-layer system stabilizes to two homogeneous layers but with the different densities.*

5.2.1 Mirroring

An interesting question is whether the layers mirror each other, and if so, for which parameter value? The important parameters in mirroring calculations are the hopping interaction parameter in between layers t_{\perp} and the Coulomb term U . We will test the mirroring of the two layered system for different parameters.

In the case of $U_1 = 4t$ and a striped density corresponding to the first layer, and $U_2 = 0$ and a homogeneous density corresponding to the second layer and a hopping between the layers $t_{\perp} = 0.1t$ we see that the stripes are destroyed and the two layered system becomes homogeneous (see fig 5.20). The same happens for $U_1 = 5t$, $U_1 = 6t$ and $U_1 = 7t$. For $U_1 = 8t$ the two layered system does not want to stabilize, where for the same layers but uncoupled they stabilize easily. DOS is shown for the case $U_1 = 5t$ in 5.21, but not for the case $U_1 = 6t$ and $U_1 = 7t$ as the illustrations are almost identical. The magnitude of the densities in this case are as in the homogeneous case with the same doping, however the DOS shows a superconducting gap at $E = 0\text{eV}$.

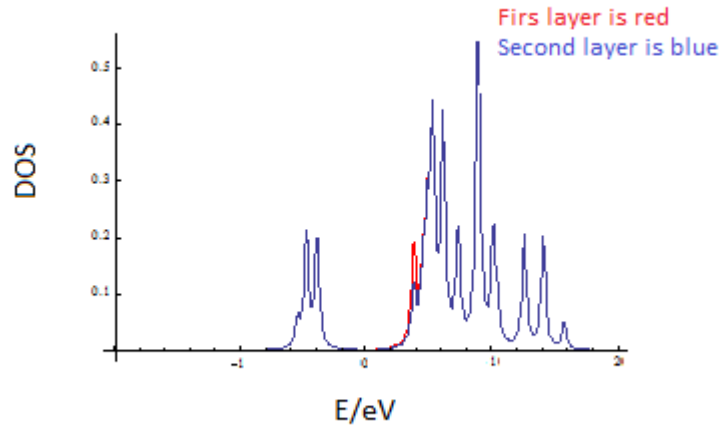


Figure 5.21: *DOS for a two layer system. The first layer (red) is a striped system with Coulomb term $U = 5t$ and doping $x = 0.125$. The second layer (blue) is a homogeneous system with Coulomb term $U = 0$, and doping $x = 0.125$. The calculations are for a system of 16×16 and with the next nearest neighbor term $t' = -0.2t$ and $t_{\perp} = -0.1t$. The two-layer system stabilizes to two homogeneous layers but with the different densities.*

It is not a good sign that we are not able to find parameters for which it is possible to couple a metallic system with a striped system and keep the stripes. However it does not mean that it is not possible with at mean field potential to pin the stripes in one layer. We will examine this later in this chapter.

5.2.2 Modulation of stripes in the z -direction

We have just established from the calculations above, that a metallic system coupled to a striped system kills the stripes and provides two metallic layers. We want then to investigate the effect of two coupled striped systems. Will they be identical copies of each other, or can they lie anti-parallel?

In fig. 5.22 we see stable stripes in a two layer system. In addition to be antiparallel from row to row, we also see the the spins are antiparallel from one layer to the other. The z -axis does not destroy the stripes but ensure that the planes are mirrored. The density plot of the two-layered system is as in the case of the one layered system fig. 5.3. In the two layered case we see an identical DOS for the two layers (see fig. 5.23), which also is very similar to the one layer case (see fig. 5.4). We see that a coupled two-layer system does not change much from a one-layer system, however the most interesting aspect of this calculation is that the layers can "figure out" how to lie antiparallel. This is illustrated in cartoon plot fig. 5.22.

5.2.3 Stripes with intermediate oxygen

We will now expand the two-layer system to include the oxygen potential. We want to examine whether the potential can help keep the modulations in z -direction. To do so, we look at the case of two layers with a mean-field potential from the intermediate oxygen that affects the layers differently (see fig. 5.24). In this particular case, where the parameters for the potential are given by $\kappa = 0.4t$ and $\alpha = 0.1t$, we see mirroring of the layers. The two-layer system maintains the order of the stripes but the magnetude is the same for the two layers. In figure 5.24, we see how the potential of the intermediate oxygen affects the two layers. The stripes (illustrated in cartoon plot) in a coupled and uncoupled system are shown in the figures 5.25 and 5.26. All

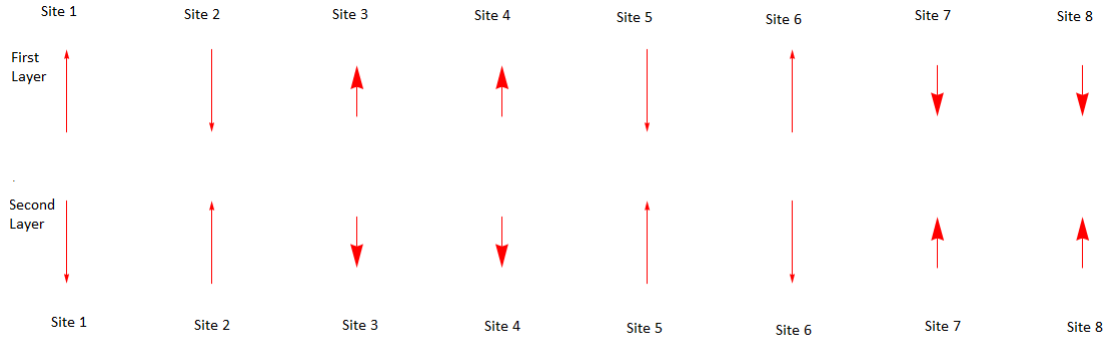


Figure 5.22: *The stripe order for a two layered system with doping at $x = 0.125$ and the Coulomb term at $U = 4t$. The length and size of the stripes should be understood relative to each other. Computed for a 16×16 system.*

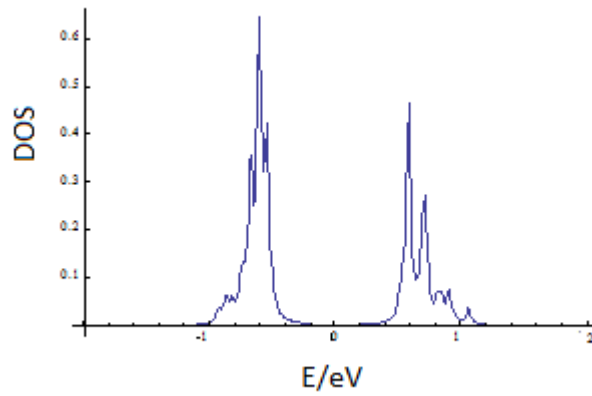


Figure 5.23: *The DOS for a striped two layered system with doping at $x = 0.125$ and the Coulomb term at $U = 4t$. The first layer is red the second layer is blue. Computed for a 16×16 system.*

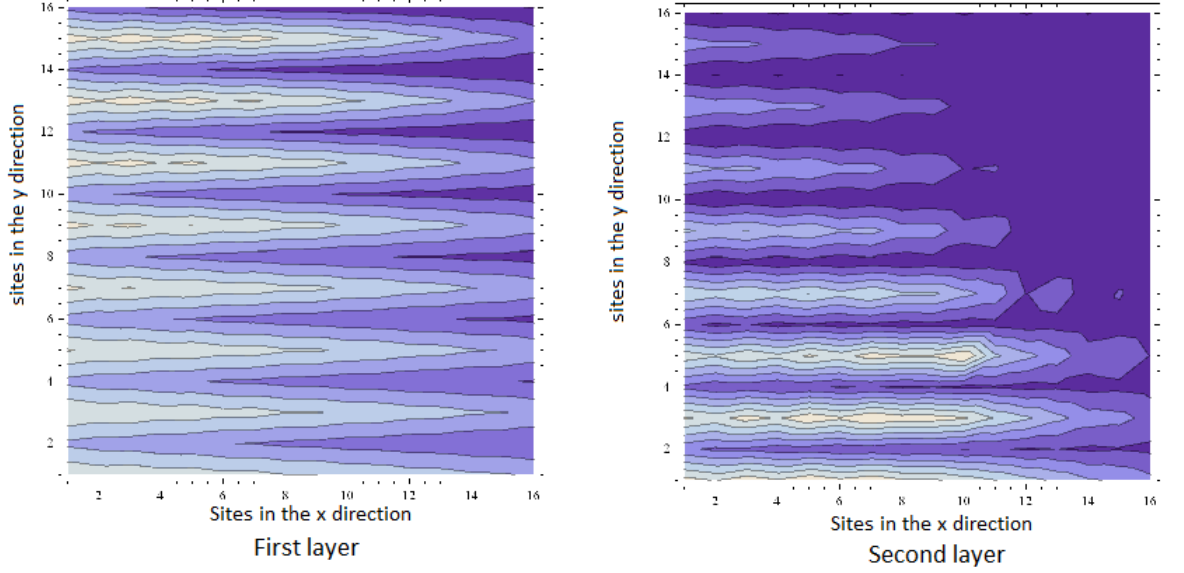


Figure 5.24: *Contour plot of the effect of the mean field potential from intermediate oxygen placed with a periodicity of 4 in the y direction. Left correspond to the first layer and right side corresponds to the second layer. The lattices are of size 16×16 . Dark purple/blue corresponds to a value of 0.01 and white correspond to a value of size 0.18*

calculations in the section is for Coulomb term $U = 5t$, and doping $x = 0.125$ and with the next nearest neighbor term $t' = -0.2t$ and $t_{\perp} = -0.1t$.

We see a big difference from the coupled to the uncoupled system. As soon as we link the layers they mirror each other. Unfortunately, this shows that this model is unlikely to find modulations in the z -direction. We have, however, not tried all possible combinations for the positions of the oxygen or possibilities for the parameters in the potential $W_{R_o}(r)$, so we can not completely exclude the possibility that we can pin stripes in one layer while having another metallic layer. The specific difference in magnitude is given in table 5.1. The pattern of the spin orientation is the same through the sites, but the size of n_i^s and m_i^s changes slightly.

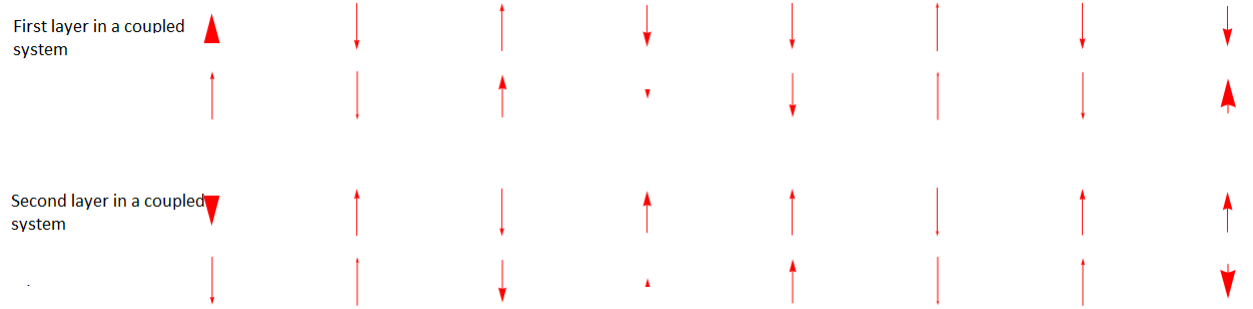


Figure 5.25: *The stripe order for a two layered coupled system with doping at $x = 0.125$, the Coulomb term at $U = 4$ and a mean field potential from intermediate oxygen placed with a periodicity of 4 in the y direction. The first 16 sites from above corresponds to the first layer and the next 16 sites correspond to the second layer. The length and size of the stripes should be understood relative to each other. Computed for a 16×16 system.*

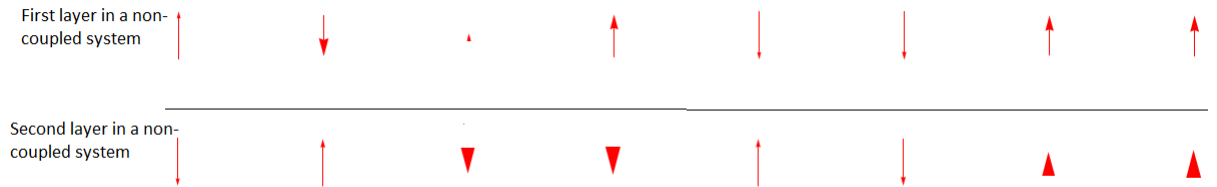


Figure 5.26: *The stripe order for a two non-coupled layers with doping at $x = 0.125$, the Coulomb term at $U = 4$ and a mean field potential from intermediate oxygen placed with a periodicity of 4 in the y direction. The first 8 sites from above corresponds to the first layer and the next 8 sites correspond to the second layer. The length and size of the stripes should be understood relative to each other. Computed for a 16×16 system.*

m_i^s	m_1^s	m_2^s	m_3^s	m_4^s	m_5^s	m_6^s	m_7^s	m_8^s
1 Layer uncoupled	0.740695	-0.632073	0.0740311	0.660488	-0.744446	-0.750406	0.617793	0.631926
2 Layer uncoupled	0.741557	-0.731048	0.350227	0.386431	-0.730592	0.726415	-0.323257	-0.391287
1 Coupled Layers	0.418608	-0.723449	0.73582	-0.646789	-0.714538	0.753969	-0.71353	-0.623592
2 Coupled Layers	-0.418608	0.723449	-0.73582	0.646789	0.714538	-0.753969	0.71353	0.623592
n_i^s	n_1^s	n_2^s	n_3^s	n_4^s	n_5^s	n_6^s	n_7^s	n_8^s
1 Layer uncoupled	0.0543421	0.134936	0.3277	0.112516	0.0555386	0.0615876	0.116686	0.122794
2 Layer uncoupled	0.0555736	0.0663345	0.266109	0.25209	0.0636732	0.0677532	0.273435	0.250091
1 Coupled Layers	0.289769	0.0753441	0.061667	0.115397	0.0769686	0.0407922	0.0816337	0.136162
2 Coupled Layers	0.289769	0.0753441	0.061667	0.115397	0.0769686	0.0407922	0.0816337	0.136162

Table 5.1: The table shows the magnitude of n_i^s and m_i^s for a striped system of, respectively, two coupled layers and two uncoupled layers. In the calculations the Colomn termnet is $U = 5$ and the hopping terms are $t = -1, t' = 0.2$ and $t_\perp = 0.05$.

5.3 3D model

In this section, we will look at a three-dimensional system where the interaction between electrons are strong in the xy - plane weak in the z -direction. We will examine the case where the chemical potential μ can be different from layer to layer and examine how the stripes behave in a multi-layered system. Finally, we will examine the case with a mean-field potential from the intermediate oxygen. The multi-layer system is constructed as described in Chapter 4.

5.3.1 Different μ

In this subsection, we will examine a multi-layer system with different chemical potential μ from layer to layer. This is done by letting each layer (which is coupled to each other) be solved self-consistently under the premise that the overall average density per layer should be $(1 - x)$. Under these assumptions, μ can stabilize for each layer without necessarily having the same value. This could have been interesting in regard to deMello [15].

However, the results from this experiment are quite tedious. If we guess on the same μ in a simple system where the layers do not vary we simply stabilize a μ with the same value for every layer. In case of a more complex system (different layers or too many layers) we see a different μ assigned to each layer, but the system does not want to stabilize.

5.3.2 Stripes

When we include the z -axis in the calculations the stripes are less visible. The stripes of the multiple layer system are in an anti-ferromagnetic order, and has no period of 8 as in the single layer system. The multi-layer system is more difficult to stabilize than the single layer system. Only with a coulomb term $U = 5t$ could the system stabilize. For comparison, the stripes in a single layer system stabilizes at $U = 3.2t$.

In the following table 5.2 n_i^s and m_i^s are noted for respectively one layer, two layers and five layers. The table shows the magnitude of n_i^s and m_i^s for

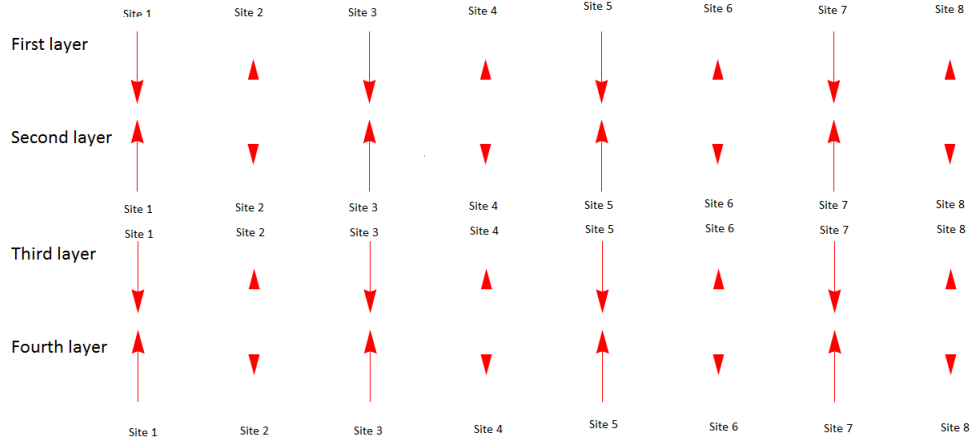


Figure 5.27: *The stripe order for a multiple-layered system with doping at $x = 0.125$ and the Coulomb term at $U = 5t$ and hopping between layers are $t_{\perp} = 0.05t$. The length and size of the stripes should be understood relative to each other. Computed for a 8×8 system.*

a striped system where the Coulomb term is $U = 5$ and the hopping terms are $t' = 0.2t$ and $t_{\perp} = 0.05t$.

5.3.3 The excess oxygen

It does not appear that we can stabilize stripes in a three dimensional system with intermediate oxygen. By putting a mean-field potential that is different from layer to layer, it seems that solving the system self-consistently results in a homogeneous configuration. I have not tried all permitted combinations for the position of the intermediate oxygen.

m_i^s	m_1^s	m_2^s	m_3^s	m_4^s	m_5^s	m_6^s	m_7^s	m_8^s
1 Layer	-0.728808	0.728808	-0.500198	-0.500198	0.728808	-0.728808	0.500198	0.500198
2 Layer	0.619625	-0.742705	-0.565581	0.625905	-0.758493	0.755011	-0.786861	-0.646204
5 Layer	0.00139805	-0.000355837	0.00139805	-0.000355837	0.00139805	-0.0003558378	0.00139805	-0.0003558378
n_i^s	n_1^s	n_2^s	n_3^s	n_4^s	n_5^s	n_6^s	n_7^s	n_8^s
1 Layer	0.0526494	0.0526494	0.197348	0.197348	0.0526494	0.0526494	0.0526494	0.197348
2 Layer	-0.0865827	-0.0347572	-0.158739	-0.0842631	-0.014188	-0.00706835	-0.000803118	-0.113858
5 Layer	-0.184727	-0.101004	-0.140527	-0.140527	-0.101004	-0.184727	-0.0898967	-0.0898967

Table 5.2: The table shows the magnitude of n_i^s and m_i^s for a striped system of, respectively, one layer two layers and five layers. In the calculations the Colomn termet is $U = 5t$ and the hopping terms are $t' = 0.2t$ and $t_{\perp} = 0.05t$.

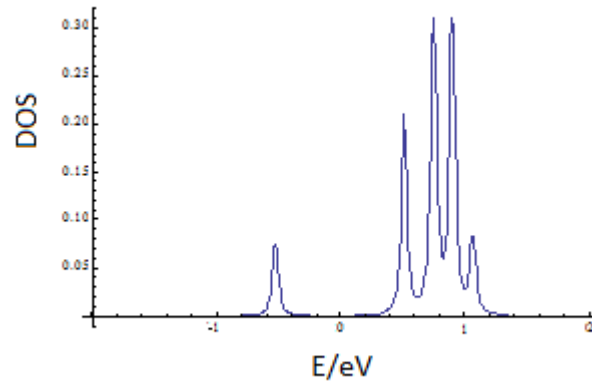


Figure 5.28: *DOS for the first layer of a striped multiple layered system with doping at $x = 0.125$ and the Coulomb term at $U = 5t$. All DOS for the different layers are identical. Computed for a 8×8 system.*

CHAPTER 6

Conclusion

In general, in the model I find that the homogeneous order usually wins. This means that if there is a dominant homogeneous element such as Δ or n_i , the system will stabilize homogeneously. Furthermore we also experience that the system is very sensitive in z -direction, which means that if there are modulations both in the plane and along the z axis they are of low magnitude compared with a 2D computations. For a two layered system with different Hamiltonian we experience mirroring. Take, for example, a coupled system with one homogeneous layer with a Coulomb term at $U_1 = 0$ and another striped layer with $U_2 = 4t$ coupled with intermediate hopping term $t_{\perp} = 0.05 - 0.1$. In this case, among many others, we see that the two layers become homogeneous. The stripes are thus destroyed if we couple it to a homogeneous system whereas both layers with no intermediate hopping term stabilizes rapidly. The homogeneous layer stabilizes to a homogeneous system with an electron density that adapts the doping and the striped layers stabilize with period 8. The same homogeneous behavior happens for $U = 5$, $U = 6$ and $U = 7$. For $U = 8$ the system do not stabilized within a reasonable amount of iterations. This of course can cause problems for a system of intermediate oxygen that has modulations in z -axis. The intermediate oxygen is presumably in every other unit cell which in this model means on every fourth layer.

For a two layered striped system we see 8 period stripes that settles antiparallel in the layers. As expected, the layers have the same DOS. This model appears to work well with similar layers through the z -axis, but however the stripes are more difficult to see the more layers there are.

For a one layered system without a superconducting phase with intermediate oxygen the system do not stabilise within a reasonable number of iteration. This has not been tested for all possible values of κ and α and the position of the oxygen R_o . However the intermediate oxygen supports the stripes in the calculation for various positions and amounts. We did not succeed

in stabilization of a mixed plane with both striped and metallic areas by using the potential from excess oxygen. We do not want to exclude the possibility of this under different assumptions. For a two layered system with intermediate oxygen we see that the potential from the oxygen support the stripes, however the layers become mirror images of each other as we do in the other cases.

In the case of a multi layered system with intermediate oxygen the system becomes homogeneous or simply do not want to stabilize. There are many things that can go wrong in this calculation. First, researchers do not agree on the location of the oxygen. Even if one of the groups were correct location, there are still too many symmetry allowed positions. Second, the amount of oxygen is not something researchers can agree on either. Thirdly, we have not incorporated the tight-binding between the added intermediate oxygen and Cu atoms. The parameters that control the mean field potential are guessed. How they are to be normalized to the system is not fully known. Fifthly see the system does not seem to cope with major changes in the different layers. To me knowledge there is no experimental evidence of the universality of the excess oxygen in LCO+O and LSCO+O. The doping with oxygen is not controlled in the same way as Sr doping since it is done with electrolyze. We have no way of knowing if the amount of oxygen is specific to given sample, with probability is the case. The question is then how much does it differ from sample to sample? The same problem occurs regarding the position of the oxygen. Assuming that different samples prepared the same way shows the same permitted positions in the compound, do we really know if they will place themselves in the exact same positions. It would be relevant to know if the variation in the samples will result in different results in the theoretical results.

I do not think that the method used in this thesis can be used to evaluate whether or not the guessed oxygen position are correct since there are too many unknown parameters. So even if the guessed position were to be right ones, the other parameters as the amount or the potential could be the reason for non-stable or homogeneous solution.

I suggest a brute force approach like reverse Monte Carlo for finding a local stable minimum and use that solution for regulating the potential. With less unknowns the method in this theses could perhaps be used to stabilize stripes.

Regarding the case of $T_c = T_N$, which is a consequence of the intermediate

oxygen, the method used in the theses do not seem to be able to reproduce the same result. We cannot calculate the ordering temperature dependence directly but we can look at the quantities Δ and M and see if they order similarly. However considering the models tendency to mirror along the z axis the physics in 3 dimensional case might not be that interesting. Perhaps some interesting result can appear from studying the 2 dimensional case this is unfortunately a future project.

APPENDIX A

Appendix

A.1 Mathematica code

Examples of the mathematica code.

A.1.1 Multiple layers

```

Nx = 16;

Ny = 16;
t = -1.0;
tt = 0.2;
tperp = 0.05;
x = 0.0;
U1 = 0.0;
U2 = U1;

U3 = U1;

U4 = U1;

U5 = 4;

mu = 1.0;
mu1 = mu;
mu2 = mu;

mu3 = mu;

mu4 = mu;

mu5 = mu;

kT = 0.01;

null = Flatten[Table[0.0, {Nx * Ny}]];

fermi[ $\omega$ _] := 1.0 / (1.0 + Exp[( $\omega$ ) / kT]);

eta = 0.10;

wsteps = 512;

dwDOS = 0.05;

dw = 5.0 / wsteps;

spectral[x_] := eta / Pi / (x^2 + eta^2);

(*the spectral funktion, the Im part of the Greens'
s function.For the homogeneous part of Hamilton *)

(*delta=0.5;*)

nup1 = Flatten[Table[0.5, {iy, 1, Ny}, {ix, 1, Nx}]]; (*Flatten[
Table[0.5-0.05*Cos[0.750*Pi*ix+0.375*Pi]*(-1)^(iy), {iy,1,Ny},{ix,1,Nx}]]];*)

nup2 = Flatten[Table[0.5, {iy, 1, Ny}, {ix, 1, Nx}]]; (*Flatten[
Table[0.5-0.05*Cos[0.750*Pi*ix+0.375*Pi]*(-1)^(iy), {iy,1,Ny},{ix,1,Nx}]]];*)

nup3 = Flatten[Table[0.5, {iy, 1, Ny}, {ix, 1, Nx}]]; (*Flatten[
Table[0.5-0.05*Cos[0.750*Pi*ix+0.375*Pi]*(-1)^(iy), {iy,1,Ny},{ix,1,Nx}]]];*)

nup4 = Flatten[Table[0.5, {iy, 1, Ny}, {ix, 1, Nx}]]; (*Flatten[
Table[0.5-0.05*Cos[0.750*Pi*ix+0.375*Pi]*(-1)^(iy), {iy,1,Ny},{ix,1,Nx}]]];*)

nup5 = Flatten[Table[0.5 - 0.05 * Cos[0.750 * Pi * ix + 0.375 * Pi] * (-1)^(iy),
{iy, 1, Ny}, {ix, 1, Nx}]]];

```



```

ndown1 = Flatten[Table[0.5, {iy, 1, Ny}, {ix, 1, Nx}]]; (*Flatten[
  Table[0.5+0.05*Cos[0.750*Pi*ix+0.375*Pi]*(-1)^(iy), {iy,1,Ny},{ix,1,Nx}]]];*)
ndown2 = Flatten[Table[0.5, {iy, 1, Ny}, {ix, 1, Nx}]]; (*Flatten[
  Table[0.5+0.05*Cos[0.750*Pi*ix+0.375*Pi]*(-1)^(iy), {iy,1,Ny},{ix,1,Nx}]]];*)
ndown3 = Flatten[Table[0.5, {iy, 1, Ny}, {ix, 1, Nx}]]; (*Flatten[
  Table[0.5+0.05*Cos[0.750*Pi*ix+0.375*Pi]*(-1)^(iy), {iy,1,Ny},{ix,1,Nx}]]];*)
ndown4 = Flatten[Table[0.5, {iy, 1, Ny}, {ix, 1, Nx}]]; (*Flatten[
  Table[0.5+0.05*Cos[0.750*Pi*ix+0.375*Pi]*(-1)^(iy), {iy,1,Ny},{ix,1,Nx}]]];*)
ndown5 = Flatten[Table[0.5+0.05*Cos[0.750*Pi*ix+0.375*Pi]*(-1)^(iy),
  {iy, 1, Ny}, {ix, 1, Nx}]]];

(*fermi[ω_]:=1.0/(1.0+Exp[(ω)/kT]);*)

NNNeighbors[i_] := Module[{ix, iy, n1, n2, n3, n4, n1x, n2x, n3y, n4y},
  If[Mod[i, Nx] == 0, ix = Nx, ix = Mod[i, Nx]]; iy = (i - ix) / Nx + 1;
  If[ix + 1 > Nx, n1x = 1, n1x = ix + 1]; n1 = {n1x, iy};
  If[ix - 1 < 1, n2x = Nx, n2x = ix - 1]; n2 = {n2x, iy};
  If[iy + 1 > Ny, n3y = 1, n3y = iy + 1]; n3 = {ix, n3y};
  If[iy - 1 < 1, n4y = Ny, n4y = iy - 1]; n4 = {ix, n4y};
  {n1x + (iy - 1) * Nx, n2x + (iy - 1) * Nx, ix + (n3y - 1) * Nx, ix + (n4y - 1) * Nx}];

NNNeighbors[i_] :=
Module[{ix, iy, n1, n2, n3, n4, n1x, n1y, n2x, n2y, n3x, n3y, n4x, n4y},
  If[Mod[i, Nx] == 0, ix = Nx, ix = Mod[i, Nx]]; iy = (i - ix) / Nx + 1;
  If[ix + 1 > Nx, n1x = 1, n1x = ix + 1]; If[iy + 1 > Ny, n1y = 1, n1y = iy + 1];
  n1 = {n1x, n1y}; If[ix - 1 < 1, n2x = Nx, n2x = ix - 1];
  If[iy - 1 < 1, n2y = Ny, n2y = iy - 1]; n2 = {n2x, n2y};
  If[ix + 1 > Nx, n3x = 1, n3x = ix + 1]; If[iy - 1 < 1, n3y = Ny, n3y = iy - 1];
  n3 = {n3x, n3y}; If[ix - 1 < 1, n4x = Nx, n4x = ix - 1];
  If[iy + 1 > Ny, n4y = 1, n4y = iy + 1]; n4 = {n4x, n4y};
  {n1x + (n1y - 1) * Nx, n2x + (n2y - 1) * Nx, n3x + (n3y - 1) * Nx, n4x + (n4y - 1) * Nx}];

zero = Table[0.0, {i, 1, Nx * Ny}, {j, 1, Nx * Ny}];

Hup1 = Module[{tab, i, j, ix, iy},
  tab = Table[If[i == j, -mu + U1 * ndown1[[i]], If[MemberQ[NNNeighbors[i], j],
    t, If[MemberQ[NNNeighbors[i], j], 0.0, 0.0]]],
    {i, 1, Nx * Ny}, {j, 1, Nx * Ny}]; tab];

Hdown1 = Module[{tab, i, j, ix, iy},
  tab = Table[If[i == j, -mu + U1 * nup1[[i]], If[MemberQ[NNNeighbors[i], j],
    t, If[MemberQ[NNNeighbors[i], j], 0.0, 0.0]]],
    {i, 1, Nx * Ny}, {j, 1, Nx * Ny}]; tab];

(*Hkup1= ArrayFlatten[{{Hup1,zero},{zero,Hdown1}}];*)
(*Hkdown1= ArrayFlatten[{{Hdown1,zero},{zero,-Hup1}}];*)

Hup2 = Module[{tab, i, j, ix, iy},
  tab = Table[If[i == j, -mu + U2 * ndown2[[i]], If[MemberQ[NNNeighbors[i], j],
    t, If[MemberQ[NNNeighbors[i], j], 0.1, 0.0]]],
    {i, 1, Nx * Ny}, {j, 1, Nx * Ny}]; tab];

```

```

Hdown2 = Module[{tab, i, j, ix, iy},
  tab = Table[If[i == j, -mu + U2 * nup2[[i]], If[MemberQ[NNeighbors[i], j],
    t, If[MemberQ[NNNeighbors[i], j], 0.1, 0.0]]],
    {i, 1, Nx * Ny}, {j, 1, Nx * Ny}]; tab];

Hup3 = Module[{tab, i, j, ix, iy},
  tab = Table[If[i == j, -mu + U3 * ndown3[[i]], If[MemberQ[NNeighbors[i], j],
    t, If[MemberQ[NNNeighbors[i], j], 0.2, 0.0]]],
    {i, 1, Nx * Ny}, {j, 1, Nx * Ny}]; tab];

Hdown3 = Module[{tab, i, j, ix, iy},
  tab = Table[If[i == j, -mu + U3 * nup3[[i]], If[MemberQ[NNeighbors[i], j],
    t, If[MemberQ[NNNeighbors[i], j], 0.2, 0.0]]],
    {i, 1, Nx * Ny}, {j, 1, Nx * Ny}]; tab];

Hup4 = Module[{tab, i, j, ix, iy},
  tab = Table[If[i == j, -mu + U4 * ndown4[[i]], If[MemberQ[NNeighbors[i], j],
    t, If[MemberQ[NNNeighbors[i], j], 0.3, 0.0]]],
    {i, 1, Nx * Ny}, {j, 1, Nx * Ny}]; tab];

Hdown4 = Module[{tab, i, j, ix, iy},
  tab = Table[If[i == j, -mu + U4 * nup4[[i]], If[MemberQ[NNeighbors[i], j],
    t, If[MemberQ[NNNeighbors[i], j], 0.3, 0.0]]],
    {i, 1, Nx * Ny}, {j, 1, Nx * Ny}]; tab];

Hup5 = Module[{tab, i, j, ix, iy}, tab = Table[If[i == j, -mu + U5 * ndown5[[i]],
  If[MemberQ[NNeighbors[i], j], t, If[MemberQ[NNNeighbors[i], j], tt, 0.0]]],
  {i, 1, Nx * Ny}, {j, 1, Nx * Ny}]; tab];

Hdown5 = Module[{tab, i, j, ix, iy}, tab = Table[If[i == j, -mu + U5 * nup5[[i]],
  If[MemberQ[NNeighbors[i], j], t, If[MemberQ[NNNeighbors[i], j], tt, 0.0]]],
  {i, 1, Nx * Ny}, {j, 1, Nx * Ny}]; tab];

couplingup = Module[{tab, i, j},
  tab = Table[If[i == j, tperp, If[MemberQ[NNeighbors[i], j], 0.0, If[MemberQ[
    NNNeighbors[i], j], 0.0, 0.0]]], {i, 1, Nx * Ny}, {j, 1, Nx * Ny}]; tab];

couplingdown = Module[{tab, i, j},
  tab = Table[If[i == j, -tperp, If[MemberQ[NNeighbors[i], j], 0.0, If[MemberQ[
    NNNeighbors[i], j], 0.0, 0.0]]], {i, 1, Nx * Ny}, {j, 1, Nx * Ny}]; tab];

Hup = ArrayFlatten[{{Hup1, couplingup, zero, zero, zero},
  {couplingup, Hup2, couplingup, zero, zero}, {zero, couplingup, Hup3,
  couplingup, zero}, {zero, zero, couplingup, Hup4, couplingup},
  {zero, zero, zero, couplingup, Hup5}}]; (*bytter om på 1 og 2 UPPP*)

Hdown = ArrayFlatten[{{Hdown1, couplingup, zero, zero, zero},
  {couplingup, Hdown2, couplingup, zero, zero},
  {zero, couplingup, Hdown3, couplingup, zero}, {zero, zero, couplingup,
  Hdown4, couplingup}, {zero, zero, zero, couplingup, Hdown5}}];

{valueup, vectorup} = Eigensystem[Hup];

{valuedown, vectordown} = Eigensystem[Hdown];

vectorup1 = Table[vectorup[[n, i]], {n, 1, 5 * Nx * Ny}, {i, 1, Nx * Ny}];

vectorup2 = Table[vectorup[[n, i]], {n, 1, 5 * Nx * Ny}, {i, 1 + Nx * Ny, 2 * Nx * Ny}];

```

```

vectorup3 = Table[vectorup[[n, i]], {n, 1, 5 * Nx * Ny}, {i, 1 + 2 * Nx * Ny, 3 * Nx * Ny}];
vectorup4 = Table[vectorup[[n, i]], {n, 1, 5 * Nx * Ny}, {i, 1 + 3 * Nx * Ny, 4 * Nx * Ny}];
vectorup5 = Table[vectorup[[n, i]], {n, 1, 5 * Nx * Ny}, {i, 1 + 4 * Nx * Ny, 5 * Nx * Ny}];
vectordown1 = Table[vectordown[[n, i]], {n, 1, 5 * Nx * Ny}, {i, 1, Nx * Ny}];
vectordown2 =
  Table[vectordown[[n, i]], {n, 1, 5 * Nx * Ny}, {i, 1 + Nx * Ny, 2 * Nx * Ny}];
vectordown3 =
  Table[vectordown[[n, i]], {n, 1, 5 * Nx * Ny}, {i, 1 + 2 * Nx * Ny, 3 * Nx * Ny}];
vectordown4 =
  Table[vectordown[[n, i]], {n, 1, 5 * Nx * Ny}, {i, 1 + 3 * Nx * Ny, 4 * Nx * Ny}];
vectordown5 =
  Table[vectordown[[n, i]], {n, 1, 5 * Nx * Ny}, {i, 1 + 4 * Nx * Ny, 5 * Nx * Ny}];
EgsysUp1 = {Eup1, EVup1} = Eigensystem[Hup1];
Egsysdown1 = {Edown1, EVdown1} = Eigensystem[Hdown1];

```

```

For[n = 100, n < 1, n++,
  densupcalc = Table[
    Total[Table[(fermi[Eup1[[n]]) * Abs[EVup1[[n, i]]]^2,
      {n, 1, Nx * Ny}]], {i, 1, Nx * Ny}];
  densdowncalc = Table[Total[Table[
    fermi[Edown1[[n]]] * Abs[EVdown1[[n, i]]]^2,
    {n, 1, Nx * Ny}]], {i, 1, Nx * Ny}];
  densup1 = densupcalc;
  densdown1 = densdowncalc;
  dens1 = (Total[densup1] + Total[densdown1]) / (Nx * Ny);
  munew = mu + 0.1 * (1.0 - 0.125 - dens1);
  nup1 = 0.5 * nup1 + 0.5 * densup1;
  ndown1 = 0.5 * ndown1 + 0.5 * densdown1;
  mag1 = 0.5 * (nup1 - ndown1);
  Hup1 = Module[{tab, i, j, ix, iy},
    tab = Table[If[i == j, -munew + U1 * ndown1[[i]],
      If[MemberQ[NNeighbors[i], j], t,
        If[MemberQ[NNNeighbors[i], j], 0.0, 0.0]]],
      {i, 1, Nx * Ny}, {j, 1, Nx * Ny}]; tab];
  Hdown1 = Module[{tab, i, j, ix, iy}, tab = Table[If[i == j,
    -munew + U1 * nup1[[i]], If[MemberQ[NNeighbors[i], j],
      t, If[MemberQ[NNNeighbors[i], j], 0.0, 0.0]]],
    {i, 1, Nx * Ny}, {j, 1, Nx * Ny}]; tab];
  EgsysUp1 = {Eup1, EVup1} = Eigensystem[Hup1];
  Egsysdown1 = {Edown1, EVdown1} = Eigensystem[Hdown1];
  mu = munew;
  (* Print[densdown1];
  Print[densup1];
  Print[mu]; *)

```

]

```

DOS1 := Module[{n, i, w, en, dos, spectralup, spectraldown,
  normalizationup, normalizationdown, absEVup, absEVdown},
  dos = Table[0.0, {en, 1, wsteps}]; w = Table[0.0, {en, 1, wsteps}];
  For[n = 1, n < Nx * Ny + 1, n++, For[en = 1, en < wsteps + 1, en++,
    normalizationup = (en - 1 - wsteps / 2) * dwdos - Eup1[[n]];
    normalizationdown = (en - 1 - wsteps / 2) * dwdos - Edown1[[n]];
    w[[en]] = (en - 1 - wsteps / 2) * dwdos; i = 1;
    If[Abs[normalizationup] < 20.0 * eta ||
      Abs[normalizationdown] < 20.0 * eta, absEVup =
      Abs[EVup1[[n, i]]]^2; absEVdown = Abs[EVdown1[[n, i]]]^2;
      spectralup = spectral[normalizationup];
      spectraldown = spectral[normalizationdown]; dos[[en]] =
      dos[[en]] + absEVup * spectralup + absEVdown * spectraldown,
      dos[[en]] = dos[[en]]]; Chop[dos]]
ListLinePlot[DOS1, PlotRange -> All]

EgsysUp2 = {Eup2, EVup2} = Eigensystem[Hup2];
Egsysdown2 = {Edown2, EVdown2} = Eigensystem[Hdown2];

```

```

For[n = 1, n < 1, n++,
  densupcalc = Table[
    Total[Table[(fermi[Eup2[[n]]) * Abs[EVup2[[n, i]]]^2,
      {n, 1, Nx * Ny}]], {i, 1, Nx * Ny}];
  densdowncalc = Table[Total[Table[
    fermi[Edown2[[n]] * Abs[EVdown2[[n, i]]]^2,
    {n, 1, Nx * Ny}]], {i, 1, Nx * Ny}];
  densup2 = densupcalc;
  densdown2 = densdowncalc;
  dens2 = (Total[densup2] + Total[densdown2]) / (Nx * Ny);
  munew = mu + 0.1 * (1.0 - 0.0 - dens2);
  nup2 = 0.5 * nup2 + 0.5 * densup2;
  ndown2 = 0.5 * ndown2 + 0.5 * densdown2;
  mag2 = 0.5 * (nup2 - ndown2);
  Hup2 = Module[{tab, i, j, ix, iy},
    tab = Table[If[i == j, -munew + U2 * ndown2[[i]],
      If[MemberQ[NNeighbors[i], j], t,
        If[MemberQ[NNNeighbors[i], j], 0.1, 0.0]]],
      {i, 1, Nx * Ny}, {j, 1, Nx * Ny}]; tab];
  Hdown2 = Module[{tab, i, j, ix, iy}, tab = Table[If[i == j,
    -munew + U2 * nup2[[i]], If[MemberQ[NNeighbors[i], j],
      t, If[MemberQ[NNNeighbors[i], j], 0.1, 0.0]]],
    {i, 1, Nx * Ny}, {j, 1, Nx * Ny}]; tab];
  EgsysUp2 = {Eup2, EVup2} = Eigensystem[Hup2];
  Egsysdown2 = {Edown2, EVdown2} = Eigensystem[Hdown2];
  mu = munew;
  (* Print[densdown2];
  Print[densup2];
  Print[mu]; *)

```

]

```

DOS2 := Module[{n, i, w, en, dos, spectralup, spectraldown,
  normalizationup, normalizationdown, absEVup, absEVdown},
  dos = Table[0.0, {en, 1, wsteps}]; w = Table[0.0, {en, 1, wsteps}];
  For[n = 1, n < Nx * Ny + 1, n++, For[en = 1, en < wsteps + 1, en++,
    normalizationup = (en - 1 - wsteps / 2) * dwdos - Eup2[[n]];
    normalizationdown = (en - 1 - wsteps / 2) * dwdos - Edown2[[n]];
    w[[en]] = (en - 1 - wsteps / 2) * dwdos; i = 1;
    If[Abs[normalizationup] < 20.0 * eta ||
      Abs[normalizationdown] < 20.0 * eta, absEVup =
      Abs[EVup2[[n, i]]]^2; absEVdown = Abs[EVdown2[[n, i]]]^2;
      spectralup = spectral[normalizationup];
      spectraldown = spectral[normalizationdown]; dos[[en]] =
      dos[[en]] + absEVup * spectralup + absEVdown * spectraldown,
      dos[[en]] = dos[[en]]]; Chop[dos]]
ListLinePlot[DOS2, PlotRange -> All]

EgsysUp3 = {Eup3, EVup3} = Eigensystem[Hup3];
Egsysdown3 = {Edown3, EVdown3} = Eigensystem[Hdown3];

```

```

For[n = 100, n < 1, n++,
  densupcalc = Table[
    Total[Table[(fermi[Eup3[[n]]) * Abs[EVup3[[n, i]]]^2,
      {n, 1, Nx * Ny}]], {i, 1, Nx * Ny}];
  densdowncalc = Table[Total[Table[
    fermi[Edown3[[n]]] * Abs[EVdown3[[n, i]]]^2,
    {n, 1, Nx * Ny}]], {i, 1, Nx * Ny}];
  densup3 = densupcalc;
  densdown3 = densdowncalc;
  dens3 = (Total[densup3] + Total[densdown3]) / (Nx * Ny);
  munew = mu + 0.1 * (1.0 - 0.0 - dens3);
  nup3 = 0.5 * nup3 + 0.5 * densup3;
  ndown3 = 0.5 * ndown3 + 0.5 * densdown3;
  mag3 = 0.5 * (nup3 - ndown3);
  Hup3 = Module[{tab, i, j, ix, iy},
    tab = Table[If[i == j, -munew + U3 * ndown3[[i]],
      If[MemberQ[NNeighbors[i], j], t,
        If[MemberQ[NNNeighbors[i], j], 0.2, 0.0]]],
      {i, 1, Nx * Ny}, {j, 1, Nx * Ny}]; tab];
  Hdown3 = Module[{tab, i, j, ix, iy}, tab = Table[If[i == j,
    -munew + U3 * nup3[[i]], If[MemberQ[NNeighbors[i], j],
      t, If[MemberQ[NNNeighbors[i], j], 0.2, 0.0]]],
    {i, 1, Nx * Ny}, {j, 1, Nx * Ny}]; tab];
  EgsysUp3 = {Eup3, EVup3} = Eigensystem[Hup3];
  Egsysdown3 = {Edown3, EVdown3} = Eigensystem[Hdown3];
  mu = munew;
  (* Print[densdown3];
  Print[densup3];
  Print[mu]; *)

```

]


```

DOS3 := Module[{n, i, w, en, dos, spectralup, spectraldown,
  normalizationup, normalizationdown, absEVup, absEVdown},
  dos = Table[0.0, {en, 1, wsteps}]; w = Table[0.0, {en, 1, wsteps}];
  For[n = 1, n < Nx * Ny + 1, n++, For[en = 1, en < wsteps + 1, en++,
    normalizationup = (en - 1 - wsteps / 2) * dwdos - Eup3[[n]];
    normalizationdown = (en - 1 - wsteps / 2) * dwdos - Edown3[[n]];
    w[[en]] = (en - 1 - wsteps / 2) * dwdos; i = 1;
    If[Abs[normalizationup] < 20.0 * eta ||
      Abs[normalizationdown] < 20.0 * eta, absEVup =
      Abs[EVup3[[n, i]]]^2; absEVdown = Abs[EVdown3[[n, i]]]^2;
      spectralup = spectral[normalizationup];
      spectraldown = spectral[normalizationdown]; dos[[en]] =
      dos[[en]] + absEVup * spectralup + absEVdown * spectraldown,
      dos[[en]] = dos[[en]]]; Chop[dos]]
ListLinePlot[DOS3, PlotRange -> All]

EgsysUp4 = {Eup4, EVup4} = Eigensystem[Hup4];
Egsysdown4 = {Edown4, EVdown4} = Eigensystem[Hdown4];

```

```

For[n = 1, n < 100, n++,
  densupcalc = Table[
    Total[Table[(fermi[Eup4[[n]]) * Abs[EVup4[[n, i]]]^2,
      {n, 1, Nx * Ny}]], {i, 1, Nx * Ny}];
  densdowncalc = Table[Total[Table[
    fermi[Edown4[[n]]] * Abs[EVdown4[[n, i]]]^2,
    {n, 1, Nx * Ny}]], {i, 1, Nx * Ny}];
  densup4 = densupcalc;
  densdown4 = densdowncalc;
  dens4 = (Total[densup4] + Total[densdown4]) / (Nx * Ny);
  munew = mu + 0.1 * (1.0 - 0.0 - dens4);
  nup4 = 0.5 * nup4 + 0.5 * densup4;
  ndown4 = 0.5 * ndown4 + 0.5 * densdown4;
  mag4 = 0.5 * (nup4 - ndown4);
  Hup4 = Module[{tab, i, j, ix, iy},
    tab = Table[If[i == j, -munew + U4 * ndown4[[i]],
      If[MemberQ[NNeighbors[i], j], t,
        If[MemberQ[NNNeighbors[i], j], 0.3, 0.0]]],
      {i, 1, Nx * Ny}, {j, 1, Nx * Ny}]; tab];
  Hdown4 = Module[{tab, i, j, ix, iy}, tab = Table[If[i == j,
    -munew + U4 * nup4[[i]], If[MemberQ[NNeighbors[i], j],
      t, If[MemberQ[NNNeighbors[i], j], 0.3, 0.0]]],
    {i, 1, Nx * Ny}, {j, 1, Nx * Ny}]; tab];
  EgsysUp4 = {Eup4, EVup4} = Eigensystem[Hup4];
  Egsysdown4 = {Edown4, EVdown4} = Eigensystem[Hdown4];
  mu = munew;
  (* Print[densdown4];
  Print[densup4];
  Print[mu]; *)

```

]

```

DOS4 := Module[{n, i, w, en, dos, spectralup, spectraldown,
  normalizationup, normalizationdown, absEVup, absEVdown},
  dos = Table[0.0, {en, 1, wsteps}]; w = Table[0.0, {en, 1, wsteps}];
  For[n = 1, n < Nx * Ny + 1, n++, For[en = 1, en < wsteps + 1, en++,
    normalizationup = (en - 1 - wsteps / 2) * dwdos - Eup4[[n]];
    normalizationdown = (en - 1 - wsteps / 2) * dwdos - Edown4[[n]];
    w[[en]] = (en - 1 - wsteps / 2) * dwdos; i = 1;
    If[Abs[normalizationup] < 20.0 * eta ||
      Abs[normalizationdown] < 20.0 * eta, absEVup =
      Abs[EVup4[[n, i]]]^2; absEVdown = Abs[EVdown4[[n, i]]]^2;
      spectralup = spectral[normalizationup];
      spectraldown = spectral[normalizationdown]; dos[[en]] =
      dos[[en]] + absEVup * spectralup + absEVdown * spectraldown,
      dos[[en]] = dos[[en]]]; Chop[dos]]
ListLinePlot[DOS4, PlotRange → All]

Show[ListLinePlot[DOS4, PlotRange → All, PlotStyle → {Red}],
  ListLinePlot[DOS3, PlotRange → All, PlotStyle → {Yellow}],
  ListLinePlot[DOS2, PlotRange → All, PlotStyle → {Black}],
  ListLinePlot[DOS1, PlotRange → All]]

EgssysUp5 = {Eup5, EVup5} = Eigensystem[Hup5];
Egssysdown5 = {Edown5, EVdown5} = Eigensystem[Hdown5];

For[n = 1, n < 100, n++,
  densupcalc = Table[
    Total[Table[(fermi[Eup5[[n]]]) * Abs[EVup5[[n, i]]]^2, {n, 1, Nx * Ny}]],
    {i, 1, Nx * Ny}];
  densdowncalc = Table[Total[Table[(fermi[Edown5[[n]]]) * Abs[EVdown5[[n, i]]]^2,
    {n, 1, Nx * Ny}]], {i, 1, Nx * Ny}];
  densup5 = densupcalc;
  densdown5 = densdowncalc;
  dens5 = (Total[densup5] + Total[densdown5]) / (Nx * Ny);
  munew = mu + 0.1 * (1.0 - 0.125 - dens5);
  nup5 = 0.5 * nup5 + 0.5 * densup5;
  ndown5 = 0.5 * ndown5 + 0.5 * densdown5;
  mag5 = 0.5 * (nup5 - ndown5);
  Hup5 =
    Module[{tab, i, j, ix, iy}, tab = Table[If[i == j, -munew + U5 * ndown5[[i]], If[
      MemberQ[NNNeighbors[i], j], t, If[MemberQ[NNNeighbors[i], j], tt, 0.0]]],
      {i, 1, Nx * Ny}, {j, 1, Nx * Ny}]; tab];
  Hdown5 = Module[{tab, i, j, ix, iy}, tab =
    Table[If[i == j, -munew + U5 * nup5[[i]], If[MemberQ[NNNeighbors[i], j],
      t, If[MemberQ[NNNeighbors[i], j], tt, 0.0]]],
      {i, 1, Nx * Ny}, {j, 1, Nx * Ny}]; tab];
  EgssysUp5 = {Eup5, EVup5} = Eigensystem[Hup5];
  Egssysdown5 = {Edown5, EVdown5} = Eigensystem[Hdown5];
  mu = munew;
  (*Print[densdown5];
  Print[densup5];
  Print[mu];*)
]

```

densdown5

```

(*For[n=1,n<300, n++,
(*densupcalc=
  Table[Total[Table[(fermi[valueup[[n]])*Abs[vectorup5[[n,i]]]^2,
    {n,1,5*Nx*Ny}]],{i,1,Nx*Ny}];
densdowncalc= Table[Total[Table[fermi[valuedown[[n]])*
  Abs[vectordown5[[n,i]]]^2,{n,1,5*Nx*Ny}]],{i,1,Nx*Ny}];
densup5=densupcalc;
densdown5=densdowncalc;
dens5=(Total[densup5]+Total[densdown5])/(Nx*Ny);
munew5=mu5+0.5*(1.0-x-dens5);
nup5=0.5*nup5+0.5*densup5;
ndown5=0.5*ndown5+0.5*densdown5;
Hup5=Module[{tab,i,j,ix,iy},
  tab=Table[If[i==j,-munew5+U5*ndown5[[i]],If[MemberQ[NNeighbors[i],j],t,If[
    MemberQ[NNNeighbors[i],j],tt,0.0]]],{i,1,Nx*Ny},{j,1,Nx*Ny}];tab];
Hdown5=Module[{tab,i,j,ix,iy},tab=Table[If[i==j,-munew5+U5*nup5[[i]],
  If[MemberQ[NNeighbors[i],j],t,If[MemberQ[NNNeighbors[i],j],tt,0.0]]],
  {i,1,Nx*Ny},{j,1,Nx*Ny}];tab];*)
(*-----*)
densupcalc1=Table[Total[Table[fermi[valueup[[n]])*Abs[vectorup1[[n,i]]]^2,
  {n,1,5*Nx*Ny}]],{i,1,Nx*Ny}];
densdowncalc1=Table[Total[Table[(fermi[valuedown[[n]])*
  Abs[vectordown1[[n,i]]]^2,{n,1,5*Nx*Ny}]],{i,1,Nx*Ny}];
densup1=densupcalc1;
densdown1=densdowncalc1;
dens1=(Total[densup1]+Total[densdown1])/(Nx*Ny);
munew1=mu1+0.5*(1.0-x-dens1);
nup1=0.5*nup1+0.5*densup1;
ndown1=0.5*ndown1+0.5*densup1;
Hup1=Module[{tab,i,j},
  tab=Table[If[i==j,-munew1+U1*ndown1[[i]],If[MemberQ[NNeighbors[i],j],t,If[
    MemberQ[NNNeighbors[i],j],tt,0.0]]],{i,1,Nx*Ny},{j,1,Nx*Ny}];tab];
Hdown1=Module[{tab,i,j},tab=Table[If[i==j,-munew1+U1*nup1[[i]],
  If[MemberQ[NNeighbors[i],j],t,If[MemberQ[NNNeighbors[i],j],tt,0.0]]],
  {i,1,Nx*Ny},{j,1,Nx*Ny}];tab];*)
(*-----*)
densupcalc2=Table[Total[Table[fermi[valueup[[n]])*Abs[vectorup2[[n,i]]]^2,
  {n,1,5*Nx*Ny}]],{i,1,Nx*Ny}];
densdowncalc2=Table[Total[Table[(fermi[valuedown[[n]])*
  Abs[vectordown2[[n,i]]]^2,{n,1,5*Nx*Ny}]],{i,1,Nx*Ny}];
densup2=densupcalc2;
densdown2=densdowncalc2;
dens2=(Total[densup2]+Total[densdown2])/(Nx*Ny);
munew2=mu2+0.5*(1.0-x-dens2);
nup2=0.5*nup2+0.5*densup2;
ndown2=0.5*ndown2+0.5*densup2;
Hup2=Module[{tab,i,j},
  tab=Table[If[i==j,-munew2+U2*ndown2[[i]],If[MemberQ[NNeighbors[i],j],t,If[

```

```

      MemberQ[NNNeighbors[i],j],tt,0.0]]],{i,1,Nx*Ny},{j,1,Nx*Ny}];tab];
Hdown2=Module[{tab,i,j},tab=Table[If[i==j,-munew2+U2*nup2[[i]],
      If[MemberQ[NNeighbors[i],j],t,If[MemberQ[NNNeighbors[i],j],tt,0.0]]],
      {i,1,Nx*Ny},{j,1,Nx*Ny}];tab];
(*-----
                                     -----*)
densupcalc3=Table[Total[Table[fermi[valueup[[n]]]*Abs[vectorup3[[n,i]]]^2,
      {n,1,5*Nx*Ny}]],{i,1,Nx*Ny}];
densdowncalc3=Table[Total[Table[(fermi[valuedown[[n]])*
      Abs[vectordown3[[n,i]]]^2,{n,1,5*Nx*Ny}]],{i,1,Nx*Ny}];
densup3=densupcalc3;
densdown3=densdowncalc3;
dens3=(Total[densup3]+Total[densdown3])/(Nx*Ny);
munew3=mu3+0.5*(1.0-x-dens3);
nup3=0.5*nup3+0.5*densup3;
ndown3=0.5*ndown3+0.5*densdown3;
Hup3=Module[{tab,i,j},
      tab=Table[If[i==j,-munew3+U3*ndown3[[i]],If[MemberQ[NNeighbors[i],j],t,If[
      MemberQ[NNNeighbors[i],j],tt,0.0]]],{i,1,Nx*Ny},{j,1,Nx*Ny}];tab];
Hdown3=Module[{tab,i,j},tab=Table[If[i==j,-munew3+U3*nup3[[i]],
      If[MemberQ[NNeighbors[i],j],t,If[MemberQ[NNNeighbors[i],j],tt,0.0]]],
      {i,1,Nx*Ny},{j,1,Nx*Ny}];tab];
(*-----
                                     -----*)
densupcalc4=Table[
      Total[Table[fermi[valueup[[n]]]*Abs[vectorup4[[n,i]]]^2,{n,1,5*Nx*Ny}]],
      {i,1,Nx*Ny}];
densdowncalc4=Table[Total[Table[(fermi[valuedown[[n]])*
      Abs[vectordown4[[n,i]]]^2,{n,1,5*Nx*Ny}]],{i,1,Nx*Ny}];
densup4=densupcalc4;
densdown4=densdowncalc4;
dens4=(Total[densup4]+Total[densdown4])/(Nx*Ny);
munew4=mu4+0.5*(1.0-x-dens4);
nup4=0.5*nup4+0.5*densup4;
ndown4=0.5*ndown4+0.5*densdown4;
Hup4=Module[{tab,i,j},
      tab=Table[If[i==j,-munew4+U4*ndown4[[i]],If[MemberQ[NNeighbors[i],j],t,If[
      MemberQ[NNNeighbors[i],j],tt,0.0]]],{i,1,Nx*Ny},{j,1,Nx*Ny}];tab];
Hdown4=Module[{tab,i,j},tab=Table[If[i==j,-munew4+U4*nup4[[i]],
      If[MemberQ[NNeighbors[i],j],t,If[MemberQ[NNNeighbors[i],j],tt,0.0]]],
      {i,1,Nx*Ny},{j,1,Nx*Ny}];tab];
(*-----
                                     -----*)
densupcalc5=Table[
      Total[Table[fermi[valueup[[n]]]*Abs[vectorup5[[n,i]]]^2,{n,1,5*Nx*Ny}]],
      {i,1,Nx*Ny}];
densdowncalc5=Table[Total[Table[(fermi[valuedown[[n]])*
      Abs[vectordown5[[n,i]]]^2,{n,1,5*Nx*Ny}]],{i,1,Nx*Ny}];
densup5=densupcalc5;
densdown5=densdowncalc5;
dens5=(Total[densup5]+Total[densdown5])/(Nx*Ny);

```

```

munew5=mu5+0.5*(1.0-x-dens5);
nup5=0.5*nup5+0.5*densup5;
ndown5=0.5*ndown5+0.5*densup5;
Hup5=Module[{tab,i,j},
  tab=Table[If[i==j,-munew5+U5*ndown5[[i]],If[MemberQ[NNeighbors[i],j],t,If[
    MemberQ[NNNeighbors[i],j],tt,0.0]]],{i,1,Nx*Ny},{j,1,Nx*Ny}];tab];
Hdown5=Module[{tab,i,j},tab=Table[If[i==j,-munew5+U5*nup5[[i]],
  If[MemberQ[NNeighbors[i],j],t,If[MemberQ[NNNeighbors[i],j],tt,0.0]]],
  {i,1,Nx*Ny},{j,1,Nx*Ny}];tab];

(*densupcalc5=Table[
  Total[Table[fermi[valueup[[n]]]*Abs[vectorup5[[n,i]]]^2,{n,1,5*Nx*Ny}]],
  {i,1,Nx*Ny}];
densdowncalc5=Table[Total[Table[(fermi[valuedown[[n]])*
  Abs[vectordown5[[n,i]]]^2,{n,1,5*Nx*Ny}]],{i,1,Nx*Ny}];
densup5=densupcalc5;
densdown5=densdowncalc5;
dens5=(Total[densup5]+Total[densdown5])/(Nx*Ny);
munew5=mu5+0.5*(1.0-x-dens5);
nup5=0.5*nup5+0.5*densup5;
ndown5=0.1*ndown5+0.5*densup5;
Hup5=Module[{tab,i,j},
  tab=Table[If[i==j,-munew5+U5*ndown5[[i]],If[MemberQ[NNeighbors[i],j],t,If[
    MemberQ[NNNeighbors[i],j],tt,0.0]]],{i,1,Nx*Ny},{j,1,Nx*Ny}];tab];
Hdown5=Module[{tab,i,j},tab=Table[If[i==j,-munew5+U5*nup5[[i]],
  If[MemberQ[NNeighbors[i],j],t,If[MemberQ[NNNeighbors[i],j],tt,0.0]]],
  {i,1,Nx*Ny},{j,1,Nx*Ny}];tab];*)

(*-----*)
Hup=ArrayFlatten[{{Hup1,couplingup,zero,zero,zero},{couplingup,Hup2,
  couplingup,zero,zero},{zero,couplingup,Hup3,couplingup,zero},{zero,
  zero,couplingup,Hup4,couplingup},{zero,zero,zero,couplingup,Hup5}}];
Hdown=ArrayFlatten[{{Hdown1,couplingup,zero,zero,zero},
  {couplingup,Hdown2,couplingup,zero,zero},
  {zero,couplingup,Hdown3,couplingup,zero},{zero,zero,couplingup,
  Hdown4,couplingup},{zero,zero,zero,couplingup,Hdown5}}];
{valueup,vectorup}=Eigensystem[Hup];
{valuedown,vectordown}=Eigensystem[Hdown];
vectorup1=Table[vectorup[[n,i]],{n,1,5*Nx*Ny},{i,1,Nx*Ny}];
vectorup2=Table[vectorup[[n,i]],{n,1,5*Nx*Ny},{i,1+Nx*Ny,2*Nx*Ny}];
vectorup3=Table[vectorup[[n,i]],{n,1,5*Nx*Ny},{i,1+2*Nx*Ny,3*Nx*Ny}];
vectorup4=Table[vectorup[[n,i]],{n,1,5*Nx*Ny},{i,1+3*Nx*Ny,4*Nx*Ny}];
vectorup5=Table[vectorup[[n,i]],{n,1,5*Nx*Ny},{i,1+4*Nx*Ny,5*Nx*Ny}];
vectordown1=Table[vectordown[[n,i]],{n,1,5*Nx*Ny},{i,1,Nx*Ny}];
vectordown2=Table[vectordown[[n,i]],{n,1,5*Nx*Ny},{i,1+Nx*Ny,2*Nx*Ny}];
vectordown3=Table[vectordown[[n,i]],{n,1,5*Nx*Ny},{i,1+2*Nx*Ny,3*Nx*Ny}];
vectordown4=Table[vectordown[[n,i]],{n,1,5*Nx*Ny},{i,1+3*Nx*Ny,4*Nx*Ny}];
vectordown5=Table[vectordown[[n,i]],{n,1,5*Nx*Ny},{i,1+4*Nx*Ny,5*Nx*Ny}];

mul1=munew1;
mu2=munew2;
mu3=munew3;

```

```

mu4=munew4;
mu5=munew5;

(*-----*)
Print[mu1];
Print[mu2];
Print[mu3];
Print[mu4];
Print[mu5];
(*Print[densup1];
Print[densdown1];
Print[densup2];
Print[densdown2];
Print[densup3];
Print[densdown3];
Print[densup4];
Print[densdown4];
Print[densup5];
Print[densdown5];*)
]*)

```

```

densupcalc1 = Table[Total[Table[fermi[valueup[[n]]] * Abs[vectorup1[[n, i]]]^2,
  {n, 1, 5 * Nx * Ny}]], {i, 1, Nx * Ny}];
densdowncalc1 = Table[Total[Table[(fermi[valuedown[[n]]]) *
  Abs[vectordown1[[n, i]]]^2, {n, 1, 5 * Nx * Ny}]], {i, 1, Nx * Ny}];
densup1 = densupcalc1;
densdown1 = densdowncalc1;
dens1 = (Total[densup1] + Total[densdown1]) / (Nx * Ny);
densupcalc2 = Table[Total[Table[fermi[valueup[[n]]] * Abs[vectorup2[[n, i]]]^2,
  {n, 1, 5 * Nx * Ny}]], {i, 1, Nx * Ny}];
densdowncalc2 = Table[Total[Table[(fermi[valuedown[[n]]]) *
  Abs[vectordown2[[n, i]]]^2, {n, 1, 5 * Nx * Ny}]], {i, 1, Nx * Ny}];
densup2 = densupcalc2;
densdown2 = densdowncalc2;
dens2 = (Total[densup2] + Total[densdown2]) / (Nx * Ny);
densupcalc3 = Table[Total[Table[fermi[valueup[[n]]] * Abs[vectorup3[[n, i]]]^2,
  {n, 1, 5 * Nx * Ny}]], {i, 1, Nx * Ny}];
densdowncalc3 = Table[Total[Table[(fermi[valuedown[[n]]]) *
  Abs[vectordown3[[n, i]]]^2, {n, 1, 5 * Nx * Ny}]], {i, 1, Nx * Ny}];
densup3 = densupcalc3;
densdown3 = densdowncalc3;
dens3 = (Total[densup3] + Total[densdown3]) / (Nx * Ny);
densupcalc4 = Table[Total[Table[fermi[valueup[[n]]] * Abs[vectorup4[[n, i]]]^2,
  {n, 1, 5 * Nx * Ny}]], {i, 1, Nx * Ny}];
densdowncalc4 = Table[Total[Table[(fermi[valuedown[[n]]]) *
  Abs[vectordown4[[n, i]]]^2, {n, 1, 5 * Nx * Ny}]], {i, 1, Nx * Ny}];
densup4 = densupcalc4;
densdown4 = densdowncalc4;
dens4 = (Total[densup4] + Total[densdown4]) / (Nx * Ny);
densupcalc5 = Table[Total[Table[fermi[valueup[[n]]] * Abs[vectorup5[[n, i]]]^2,
  {n, 1, 5 * Nx * Ny}]], {i, 1, Nx * Ny}];
densdowncalc5 = Table[Total[Table[(fermi[valuedown[[n]]]) *
  Abs[vectordown5[[n, i]]]^2, {n, 1, 5 * Nx * Ny}]], {i, 1, Nx * Ny}];
densup5 = densupcalc5;
densdown5 = densdowncalc5;
dens5 = (Total[densup5] + Total[densdown5]) / (Nx * Ny);
(*-----*)
dens = (dens1 + dens2 + dens3 + dens4 + dens5) / 5;
munew = mu + 0.5 * (1.0 - x - dens);

```

```

For[n = 1, n < 1, n++,
  densupcalc1 =
    Table[Total[Table[fermi[valueup[[n]]] * Abs[vectorup1[[n, i]]]^2,
      {n, 1, 5 * Nx * Ny}]], {i, 1, Nx * Ny}];
  densdowncalc1 = Table[Total[Table[(fermi[valuedown[[n]]]) *
    Abs[vectordown1[[n, i]]]^2, {n, 1, 5 * Nx * Ny}]], {i, 1, Nx * Ny}];
  densup1 = densupcalc1;
  densdown1 = densdowncalc1;
  dens1 = (Total[densup1] + Total[densdown1]) / (Nx * Ny);
  densupcalc2 =
    Table[Total[Table[fermi[valueup[[n]]] * Abs[vectorup2[[n, i]]]^2,
      {n, 1, 5 * Nx * Ny}]], {i, 1, Nx * Ny}];
  densdowncalc2 = Table[Total[Table[(fermi[valuedown[[n]]]) *

```



```

      Abs[vectordown2[[n, i]]]^2, {n, 1, 5 * Nx * Ny}], {i, 1, Nx * Ny}];
densup2 = densupcalc2;
densdown2 = densdowncalc2;
dens2 = (Total[densup2] + Total[densdown2]) / (Nx * Ny);
densupcalc3 =
  Table[Total[Table[fermi[valueup[[n]]] * Abs[vectorup3[[n, i]]]^2,
    {n, 1, 5 * Nx * Ny}], {i, 1, Nx * Ny}];
densdowncalc3 = Table[Total[Table[(fermi[valuedown[[n]]]) *
  Abs[vectordown3[[n, i]]]^2, {n, 1, 5 * Nx * Ny}], {i, 1, Nx * Ny}];
densup3 = densupcalc3;
densdown3 = densdowncalc3;
dens3 = (Total[densup3] + Total[densdown3]) / (Nx * Ny);
densupcalc4 =
  Table[Total[Table[fermi[valueup[[n]]] * Abs[vectorup4[[n, i]]]^2,
    {n, 1, 5 * Nx * Ny}], {i, 1, Nx * Ny}];
densdowncalc4 = Table[Total[Table[(fermi[valuedown[[n]]]) *
  Abs[vectordown4[[n, i]]]^2, {n, 1, 5 * Nx * Ny}], {i, 1, Nx * Ny}];
densup4 = densupcalc4;
densdown4 = densdowncalc4;
dens4 = (Total[densup4] + Total[densdown4]) / (Nx * Ny);
densupcalc5 =
  Table[Total[Table[fermi[valueup[[n]]] * Abs[vectorup5[[n, i]]]^2,
    {n, 1, 5 * Nx * Ny}], {i, 1, Nx * Ny}];
densdowncalc5 = Table[Total[Table[(fermi[valuedown[[n]]]) *
  Abs[vectordown5[[n, i]]]^2, {n, 1, 5 * Nx * Ny}], {i, 1, Nx * Ny}];
densup5 = densupcalc5;
densdown5 = densdowncalc5;
dens5 = (Total[densup5] + Total[densdown5]) / (Nx * Ny);
(*-----*)

dens = (dens1 + dens2 + dens3 + dens4 + dens5) / 5;
munew = mu + 0.2 * (1.0 - x - dens);
(*-----*)

nup1 = 0.6 * nup1 + 0.4 * densup1;
ndown1 = 0.6 * ndown1 + 0.4 * densup1;
Hup1 = Module[{tab, i, j},
  tab = Table[If[i == j, -munew + U1 * ndown1[[i]], If[MemberQ[NNeighbors[i], j],
    t, If[MemberQ[NNNeighbors[i], j], tt, 0.0]]],
    {i, 1, Nx * Ny}, {j, 1, Nx * Ny}]; tab];
Hdown1 = Module[{tab, i, j}, tab = Table[If[i == j, -munew + U1 * nup1[[i]], If[
  MemberQ[NNeighbors[i], j], t, If[MemberQ[NNNeighbors[i], j], tt, 0.0]]],
    {i, 1, Nx * Ny}, {j, 1, Nx * Ny}]; tab];

(*-----*)

(*munew2=mu1+0.5*(1.0-x-dens2);*)
nup2 = 0.6 * nup2 + 0.4 * densup2;
ndown2 = 0.6 * ndown2 + 0.4 * densup2;
Hup2 = Module[{tab, i, j},
  tab = Table[If[i == j, -munew + U2 * ndown2[[i]], If[MemberQ[NNeighbors[i], j],

```

```

      t, If[MemberQ[NNNeighbors[i], j], tt, 0.0]]],
      {i, 1, Nx * Ny}, {j, 1, Nx * Ny}]; tab];
Hdown2 = Module[{tab, i, j}, tab = Table[If[i == j, -munew + U2 * nup2[[i]], If[
      MemberQ[NNeighbors[i], j], t, If[MemberQ[NNNeighbors[i], j], tt, 0.0]]],
      {i, 1, Nx * Ny}, {j, 1, Nx * Ny}]; tab];
(*-----*)

(*munew3=mul+0.5*(1.0-x-dens3);*)
nup3 = 0.6 * nup3 + 0.4 * densup3;
ndown3 = 0.6 * ndown3 + 0.4 * densup3;
Hup3 = Module[{tab, i, j},
      tab = Table[If[i == j, -munew + U3 * ndown3[[i]], If[MemberQ[NNeighbors[i], j],
      t, If[MemberQ[NNNeighbors[i], j], tt, 0.0]]],
      {i, 1, Nx * Ny}, {j, 1, Nx * Ny}]; tab];
Hdown3 = Module[{tab, i, j}, tab = Table[If[i == j, -munew + U3 * nup3[[i]], If[
      MemberQ[NNeighbors[i], j], t, If[MemberQ[NNNeighbors[i], j], tt, 0.0]]],
      {i, 1, Nx * Ny}, {j, 1, Nx * Ny}]; tab];
(*-----*)

(*munew4=mul+0.5*(1.0-x-dens4);*)
nup4 = 0.6 * nup4 + 0.4 * densup4;
ndown4 = 0.6 * ndown4 + 0.4 * densup4;
Hup4 = Module[{tab, i, j},
      tab = Table[If[i == j, -munew + U4 * ndown4[[i]], If[MemberQ[NNeighbors[i], j],
      t, If[MemberQ[NNNeighbors[i], j], tt, 0.0]]],
      {i, 1, Nx * Ny}, {j, 1, Nx * Ny}]; tab];
Hdown4 = Module[{tab, i, j}, tab = Table[If[i == j, -munew + U4 * nup4[[i]], If[
      MemberQ[NNeighbors[i], j], t, If[MemberQ[NNNeighbors[i], j], tt, 0.0]]],
      {i, 1, Nx * Ny}, {j, 1, Nx * Ny}]; tab];
(*-----*)

(*munew5=mul+0.5*(1.0-x-dens5);*)
nup5 = 0.6 * nup5 + 0.4 * densup5;
ndown5 = 0.6 * ndown5 + 0.4 * densup5;
Hup5 = Module[{tab, i, j},
      tab = Table[If[i == j, -munew + U5 * ndown5[[i]], If[MemberQ[NNeighbors[i], j],
      t, If[MemberQ[NNNeighbors[i], j], tt, 0.0]]],
      {i, 1, Nx * Ny}, {j, 1, Nx * Ny}]; tab];
Hdown5 = Module[{tab, i, j}, tab = Table[If[i == j, -munew + U5 * nup5[[i]], If[
      MemberQ[NNeighbors[i], j], t, If[MemberQ[NNNeighbors[i], j], tt, 0.0]]],
      {i, 1, Nx * Ny}, {j, 1, Nx * Ny}]; tab];
(*-----*)

Hup = ArrayFlatten[{{Hup1, couplingup, zero, zero, zero}, {couplingup,
      Hup2, couplingup, zero, zero}, {zero, couplingup, Hup3, couplingup, zero},
      {zero, zero, couplingup, Hup4, couplingup},
      {zero, zero, zero, couplingup, Hup5}}];

```

```

Hdown = ArrayFlatten[{{Hdown1, couplingup, zero, zero, zero},
  {couplingup, Hdown2, couplingup, zero, zero},
  {zero, couplingup, Hdown3, couplingup, zero}, {zero, zero, couplingup,
    Hdown4, couplingup}, {zero, zero, zero, couplingup, Hdown5}}];
{valueup, vectorup} = Eigensystem[Hup];
{valuedown, vectordown} = Eigensystem[Hdown];
vectorup1 = Table[vectorup[[n, i]], {n, 1, 5 * Nx * Ny}, {i, 1, Nx * Ny}];
vectorup2 =
  Table[vectorup[[n, i]], {n, 1, 5 * Nx * Ny}, {i, 1 + Nx * Ny, 2 * Nx * Ny}];
vectorup3 = Table[vectorup[[n, i]], {n, 1, 5 * Nx * Ny},
  {i, 1 + 2 * Nx * Ny, 3 * Nx * Ny}];
vectorup4 = Table[vectorup[[n, i]], {n, 1, 5 * Nx * Ny},
  {i, 1 + 3 * Nx * Ny, 4 * Nx * Ny}];
vectorup5 = Table[vectorup[[n, i]], {n, 1, 5 * Nx * Ny},
  {i, 1 + 4 * Nx * Ny, 5 * Nx * Ny}];
vectordown1 = Table[vectordown[[n, i]], {n, 1, 5 * Nx * Ny}, {i, 1, Nx * Ny}];
vectordown2 =
  Table[vectordown[[n, i]], {n, 1, 5 * Nx * Ny}, {i, 1 + Nx * Ny, 2 * Nx * Ny}];
vectordown3 = Table[vectordown[[n, i]],
  {n, 1, 5 * Nx * Ny}, {i, 1 + 2 * Nx * Ny, 3 * Nx * Ny}];
vectordown4 = Table[vectordown[[n, i]], {n, 1, 5 * Nx * Ny},
  {i, 1 + 3 * Nx * Ny, 4 * Nx * Ny}];
vectordown5 = Table[vectordown[[n, i]], {n, 1, 5 * Nx * Ny},
  {i, 1 + 4 * Nx * Ny, 5 * Nx * Ny}];

mu = munew;
(*mu2=munew2;
mu3=munew3;
mu4=munew4;
mu5=munew5;*)

(*-----*)
Print[mu];
(*Print[mu2];
Print[mu3];
Print[mu4];
Print[mu5];*)
(*Print[densup1];
Print[densdown1];
Print[densup2];
Print[densdown2];
Print[densup3];
Print[densdown3];
Print[densup4];
Print[densdown4];
Print[densup5];
Print[densdown5];*)
]

```

```

DOS1 := Module[{n, i, w, en, dos, spectralup, spectraldown,
  normalizationup, normalizationdown, absEVup, absEVdown},
  dos = Table[0.0, {en, 1, wsteps}];
  w = Table[0.0, {en, 1, wsteps}];
  For[n = 1, n < Nx * Ny + 1, n++, For[en = 1, en < wsteps + 1, en++,
    normalizationup = (en - 1 - wsteps / 2) * dwdos - valueup[[n]];
    normalizationdown = (en - 1 - wsteps / 2) * dwdos -
      valuedown[[n]]; w[[en]] = (en - 1 - wsteps / 2) * dwdos;
    i = 1; If[Abs[normalizationup] < 20.0 * eta ||
      Abs[normalizationdown] < 20.0 * eta,
      absEVup = Abs[vectorup1[[n, i]]]^2;
      absEVdown = Abs[vectordown2[[n, i]]]^2;
      spectralup = spectral[normalizationup];
      spectraldown = spectral[normalizationdown]; dos[[en]] =
        dos[[en]] + absEVup * spectralup + absEVdown * spectraldown,
      dos[[en]] = dos[[en]]]; Chop[dos]]; (**)
ListLinePlot[DOS1, PlotRange → All]

```

A.1.2 Potential

Model of super oxygenated LSCO

Initial settings for the ststem

The size of the lattice :

```
Nx = 16;
```

```
Ny = 16;
```

The size of the lattice in 3D:

```
Nz = 0;
```

The periodicity of the oxygen in given in x, y, z coordinates

In the x-direction

```
xperiodicity = 10;
```

In the y-direction

```
yperiodicity = 4;
```

In the z-direction

```
zperiodicity = 0;
```

The position of the oxygen between the lattice

```
xpos = 1.5;
```

```
ypos = 1.5;
```

```
zpos = 1.5;
```

Other settings for the oxygen induced potential

```
a = 1(*5.38*);(*Convert to term in tt???)
```

```
b = a;
```

```
c = a(*2.48*a*);
```

```
No = 1;
```

```
Statinpoint = 1;
```

```
Alpha = 0.7;
```

```

Kapa = 0.4;

Ro = {Xo, Yo, Zo} = {Table[xpos * a + xperiodicity * i, {i, Statinpoint, No}],
  Table[ypos * a + yperiodicity * i, {i, Statinpoint, No}],
  Table[zpos * a + zperiodicity * i, {i, Statinpoint, No}]}
(*Position of oxygen the length of the lattice is set to a*)
{{11.5}, {5.5}, {1.5}}

POx[x_, y_, z_, Xo_, Yo_, Zo_] := alpha * Exp[
  -kapa * ((x - Xo) + (y - Yo) + (z - Zo)) / Sqrt[(x - Xo)^2 + (y - Yo)^2 + (z - Zo)^2]];

(*PotVal=Flatten[Table[Chop[Total[Table[POx[xval, yval, zval, XoVal, YoVal, ZoVal],
  {XoVal, Ro[[1]]}, {YoVal, Ro[[2]]}, {ZoVal, Ro[[3]]}], 3]],
  {xval, 1, Nx*Ny}, {yval, 1, Nx*Ny}, {zval, 1, Nx*Ny}]]]; *)

PotVal = Flatten[Table[Chop[
  Total[Table[Alpha * Exp[-Kapa * ((xval - XoVal) + (yval - YoVal) + (zval - ZoVal)) /
    Sqrt[(xval - XoVal)^2 + (yval - YoVal)^2 + (zval - ZoVal)^2]],
  {XoVal, Ro[[1]]}, {YoVal, Ro[[2]]}, {ZoVal, Ro[[3]]}], 3]],
  {xval, 1, Nx}, {yval, 1, Ny}, {zval, 0, Nz}]]]
{1.2413, 1.21948, 1.19192, 1.15885, 1.12098, 1.07954, 1.03604, 0.992069, 0.949077,
  0.908194, 0.870174, 0.835417, 0.804036, 0.775944, 0.750928, 0.728714, 1.2551,
  1.23371, 1.2053, 1.16998, 1.12859, 1.08267, 1.03429, 0.985575, 0.938422,
  0.894208, 0.85376, 0.817412, 0.785146, 0.756717, 0.731768, 0.709902, 1.2702,
  1.24994, 1.22109, 1.18341, 1.13781, 1.08637, 1.03192, 0.977433, 0.925405,
  0.877514, 0.834599, 0.796836, 0.763974, 0.735543, 0.710993, 0.689775, 1.28639,
  1.26841, 1.23984, 1.19984, 1.14923, 1.0908, 1.02863, 0.966994, 0.909262,
  0.857411, 0.812153, 0.773331, 0.740327, 0.712351, 0.688615, 0.668404, 1.30303,
  1.28911, 1.26224, 1.22029, 1.16367, 1.09613, 1.02387, 0.953272, 0.888932,
  0.833025, 0.785832, 0.746578, 0.714088, 0.687162, 0.664738, 0.645932,
  1.31874, 1.3115, 1.28888, 1.24619, 1.1824, 1.10258, 1.01667, 0.934713,
  0.862955, 0.80333, 0.75508, 0.716382, 0.685296, 0.660143, 0.639586, 0.6226,
  1.33068, 1.33369, 1.31973, 1.27934, 1.20736, 1.11023, 1.00515, 0.908851,
  0.829413, 0.767276, 0.719544, 0.682816, 0.654236, 0.631657, 0.613533, 0.598756,
  1.33369, 1.35081, 1.35244, 1.32129, 1.2413, 1.11852, 0.985506, 0.871843,
  0.786104, 0.724157, 0.679382, 0.64641, 0.621535, 0.602308, 0.587108, 0.57485,
  1.31973, 1.35244, 1.37755, 1.36933, 1.28639, 1.12368, 0.949635, 0.818364,
  0.731419, 0.674371, 0.635679, 0.608324, 0.588218, 0.572934, 0.560984,
  0.551415, 1.27934, 1.32129, 1.36933, 1.39954, 1.33068, 1.10756, 0.881849,
  0.744029, 0.666615, 0.620469, 0.590779, 0.570392, 0.555651, 0.54455, 0.535914,
  0.529019, 1.20736, 1.2413, 1.28639, 1.33068, 1.27934, 1.00515, 0.767276,
  0.654236, 0.598756, 0.567604, 0.548092, 0.534859, 0.525345, 0.518198,
  0.512641, 0.508203, 1.11023, 1.11852, 1.12368, 1.10756, 1.00515, 0.789725,
  0.638623, 0.571488, 0.539532, 0.521944, 0.511091, 0.503815, 0.498633, 0.494769,
  0.491785, 0.489415, 1.00515, 0.985506, 0.949635, 0.881849, 0.767276, 0.638623,
  0.555651, 0.515988, 0.497207, 0.487489, 0.481968, 0.478578, 0.476363,
  0.474843, 0.473757, 0.472956, 0.908851, 0.871843, 0.818364, 0.744029,
  0.654236, 0.571488, 0.515988, 0.486167, 0.471505, 0.464415, 0.461004,
  0.459419, 0.45877, 0.458612, 0.458716, 0.458956, 0.829413, 0.786104, 0.731419,
  0.666615, 0.598756, 0.539532, 0.497207, 0.471505, 0.457472, 0.450349,
  0.447027, 0.445746, 0.445549, 0.445922, 0.446586, 0.447385, 0.767276,
  0.724157, 0.674371, 0.620469, 0.567604, 0.521944, 0.487489, 0.464415,
  0.450349, 0.442415, 0.43832, 0.436522, 0.436066, 0.436378, 0.437116, 0.438079}

```

```

Dimensions[PotVal]
{256}

{64}
{64}

wsteps = 400; (*to be verified*)
dwdos = 0.05; (*to be verified*)
dw = 5.0 / wsteps; (*to be verified*)

tt = -1.0;
(*nearest neighbor interaction8-1.0-for AF put to zero*)
ttl原因 = 00;

NotSC = 0.0; (*to make nulmatrice,to be replaced by superconductivity*)
NOTSC = Table[NotSC, {i, 1, Nx * Ny}, {j, 1, Nx * Ny}];
(*to make nulmatrice,to be replaced by superconductivity*)

U = 4.0;
alpha = 0.5;

mu = 1.0; (*the chemical potential,
the exact value is to be verified-stating guess *)

nt = 0.2; (*to do with nest nearest neighbor-to be verified*)

kT = 0.01; (*the boltzmann konstan k and the temperatur T,
the exat value is to be verified*)

ndownguess = 0.5;
nupguess = 0.5;

(*nup=Table[
  densup[If[Mod[i,Nx]==0,ix=Nx,ix=Mod[i,Nx]],(i-ix)/Nx+1},{i,1,Nx*Ny}];*)
nup = Flatten[Table[0.5 - 0.05 * Cos[0.750 * Pi * ix + 0.375 * Pi] * (-1)^(iy),
  {iy, 1, Ny}, {ix, 1, Nx}]];

Dimensions[nup]
{256}

(*ndown=Table[
  densdown[If[Mod[i,Nx]==0,ix=Nx,ix=Mod[i,Nx]],(i-ix)/Nx+1},{i,1,Nx*Ny}];*)
ndown = Flatten[Table[0.5 + 0.05 * Cos[0.750 * Pi * ix + 0.375 * Pi] * (-1)^(iy),
  {iy, 1, Ny}, {ix, 1, Nx}]];

null = Flatten[Table[0.0, {Nx * Ny}]];

Dimensions[null]
{256}

```



```

eta = 0.1;

V = 1;

deltadens = 0.10;

delta = deltdens; (*Maximum value of the SC gab-
    not valid value only for testing*)

spectral[x_] := eta / Pi / (x^2 + eta^2);
(*the spectral funktion, the Im part of the Greens'
    s function. For the homogeneous part of Hamilton *)

(*deltak[kx_,ky_] := 2.0*delta*(Cos[kx]-Cos[ky])*
(*d-wave symetry in 2d*)

fermi[omega_] := 1.0 / (1.0 + Exp[(omega) / kT]);
(*The Fermi-Dirac probability distribution function,
    used to find the probability that a fermion
    occupies a specific quantum state in a system at
    thermal equilibrium. mu included in Hamiltonian*)

NNeighbors[i_] :=
Module[{ix, iy, n1, n2, n3, n4, n1x, n2x, n3y, n4y},
    If[Mod[i, Nx] == 0, ix = Nx, ix = Mod[i, Nx]];
    iy = (i - ix) / Nx + 1; If[ix + 1 > Nx, n1x = 1, n1x = ix + 1];
    n1 = {n1x, iy}; If[ix - 1 < 1, n2x = Nx, n2x = ix - 1];
    n2 = {n2x, iy}; If[iy + 1 > Ny, n3y = 1, n3y = iy + 1];
    n3 = {ix, n3y}; If[iy - 1 < 1, n4y = Ny, n4y = iy - 1];
    n4 = {ix, n4y}; {n1x + (iy - 1) * Nx, n2x + (iy - 1) * Nx,
        ix + (n3y - 1) * Nx, ix + (n4y - 1) * Nx}];
(*Define the periodic boundary conditions for
    the nearest neighbor for
    the homogenius Hamiltonian*)

```

```

NNNeighbors[i_] := Module[
  {ix, iy, n1, n2, n3, n4, n1x, n1y, n2x, n2y, n3x, n3y, n4x, n4y},
  If[Mod[i, Nx] == 0, ix = Nx, ix = Mod[i, Nx]];
  iy = (i - ix) / Nx + 1; If[ix + 1 > Nx, n1x = 1, n1x = ix + 1];
  If[iy + 1 > Ny, n1y = 1, n1y = iy + 1];
  n1 = {n1x, n1y}; If[ix - 1 < 1, n2x = Nx, n2x = ix - 1];
  If[iy - 1 < 1, n2y = Ny, n2y = iy - 1];
  n2 = {n2x, n2y}; If[ix + 1 > Nx, n3x = 1, n3x = ix + 1];
  If[iy - 1 < 1, n3y = Ny, n3y = iy - 1];
  n3 = {n3x, n3y}; If[ix - 1 < 1, n4x = Nx, n4x = ix - 1];
  If[iy + 1 > Ny, n4y = 1, n4y = iy + 1]; n4 = {n4x, n4y};
  {n1x + (n1y - 1) * Nx, n2x + (n2y - 1) * Nx,
   n3x + (n3y - 1) * Nx, n4x + (n4y - 1) * Nx}];
(*Define the periodic boundary conditions for
the nearest neighbor
in the Hamiltonian*)

SCxNNNeighbors[i_] := Module[{ix, iy, n1, n2, n3, n4, n1x, n2x, n3y, n4y},
  If[Mod[i, Nx] == 0, ix = Nx, ix = Mod[i, Nx]]; iy = (i - ix) / Nx + 1;
  If[ix + 1 > Nx, n1x = 1, n1x = ix + 1]; n1 = {n1x, iy};
  If[ix - 1 < 1, n2x = Nx, n2x = ix - 1]; {n1x + (iy - 1) * Nx, n2x + (iy - 1) * Nx}]; (**)

SCyNNNeighbors[i_] := Module[{ix, iy, n1, n2, n3, n4, n1x, n2x, n3y, n4y},
  If[Mod[i, Nx] == 0, ix = Nx, ix = Mod[i, Nx]]; iy = (i - ix) / Nx + 1;
  n2 = {n2x, iy}; If[iy + 1 > Ny, n3y = 1, n3y = iy + 1];
  n3 = {ix, n3y}; If[iy - 1 < 1, n4y = Ny, n4y = iy - 1];
  n4 = {ix, n4y}; {ix + (n3y - 1) * Nx, ix + (n4y - 1) * Nx}]; (**)

Hup = Module[{tab, i, j, ix, iy},
  tab = Table[If[i == j, -mu + U * ndown[[i]] + PotVal[[i]],
    If[MemberQ[NNNeighbors[i], j], tt,
      If[MemberQ[NNNeighbors[i], j], nt, 0.0]]],
    {i, 1, Nx * Ny}, {j, 1, Nx * Ny}]; tab];
(*Hamiltonian for spin up with
periodic
boundary
conditions
and
interaction
with nearest
and next nearest
neighbor*)

```

```

Hdown = Module[{tab, i, j, ix, iy},
  tab = Table[If[i == j, -mu + U * nup[[i]] + PotVal[[i]], If[
    MemberQ[NNNeighbors[i], j], tt, If[MemberQ[NNNeighbors[i], j], nt, 0.0]]],
    {i, 1, Nx * Ny}, {j, 1, Nx * Ny}]; tab];

(*SC=
  Module[{tab, i, j}, tab = Table[If[MemberQ[SCxNNNeighbors[i], j], delta, If[MemberQ[
    SCyNNNeighbors[i], j], -delta, 0.0]], {i, 1, Nx * Ny}, {j, 1, Nx * Ny}]]; *)

(*SCC=Conjugate[SC];*)

(*Homo= ArrayFlatten[{{Hup, NOTSC}, {NOTSC, Hdown}}];*)

(*Eigenvalues[Homo]*)

(*Hscup= ArrayFlatten[{{Hup, SC}, {SC, -Hdown}}];*)

(*Hscdown=ArrayFlatten[{{Hdown, -SC}, {-SC, -Hup}}];*)

{Eup, EVup} = Eigensystem[Hup];
{Edown, EVdown} = Eigensystem[Hdown];

```

```

For[n = 1, n < 250, n++,
  densupcalc =
    Table[Total[Table[(fermi[Eup[[n]])] * Abs[EVup[[n, i]]]^2,
      {n, 1, Nx * Ny}]], {i, 1, Nx * Ny}];
  densdowncalc = Table[Total[Table[
    fermi[Edown[[n]]] * Abs[EVdown[[n, i]]]^2,
    {n, 1, Nx * Ny}]], {i, 1, Nx * Ny}];
  densup = densupcalc;
  densdown = densdowncalc;
  dens = (Total[densup] + Total[densdown]) / (Nx * Ny);
  munew = mu + 0.1 * (1.0 - 0.125 - dens);
  nup = 0.5 * nup + 0.5 * densup;
  ndown = 0.5 * ndown + 0.5 * densdown;
  mag = 0.5 * (nup - ndown);
  Hup = Module[{tab, i, j},
    tab = Table[If[i == j, -munew + U * ndown[[i]] + PotVal[[i]],

```

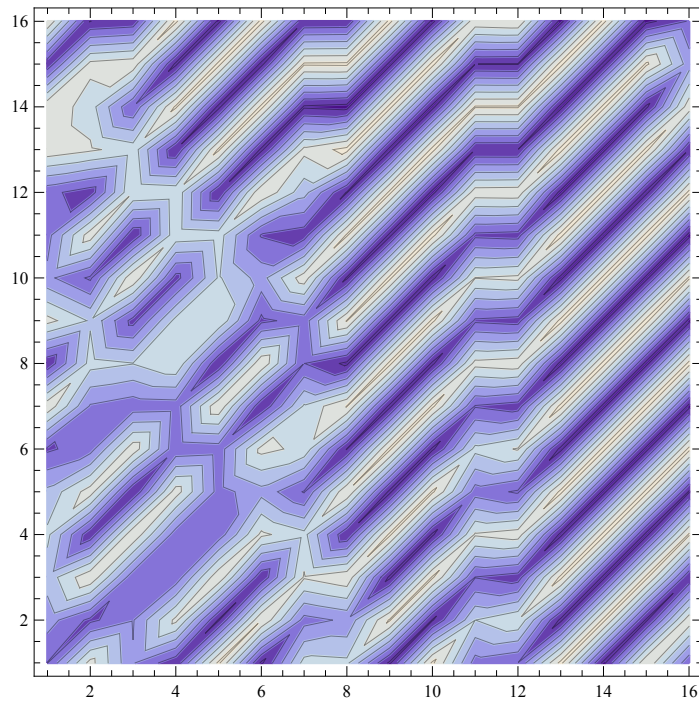
```

      If[MemberQ[NNeighbors[i], j], tt,
        If[MemberQ[NNNeighbors[i], j], nt, 0.0]]],
    {i, 1, Nx * Ny}, {j, 1, Nx * Ny}]; tab];
Hdown = Module[{tab, i, j}, tab =
  Table[If[i == j, -munew + U * nup[[i]] + PotVal[[i]],
    If[MemberQ[NNeighbors[i], j], tt,
      If[MemberQ[NNNeighbors[i], j], nt, 0.0]]],
    {i, 1, Nx * Ny}, {j, 1, Nx * Ny}]; tab];
EgsysUp = {Eup, EVup} = Eigensystem[Hup];
Egsysdown = {Edown, EVdown} = Eigensystem[Hdown];
mu = munew;
Print[densdown];
Print[densup];
Print[mu];

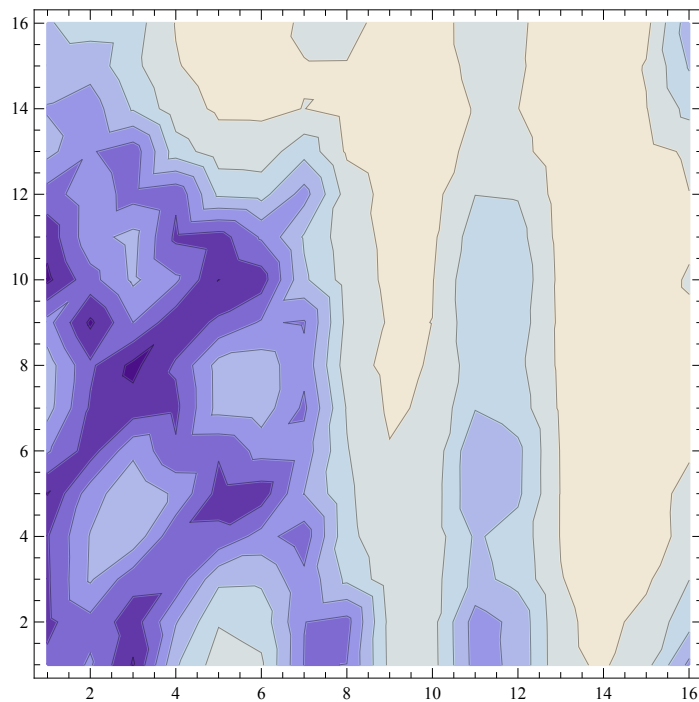
]

```

```
ListContourPlot[magoxplot1]
```



ListContourPlot[densoxplot1]



```
(*densxpos=
Flatten[Table[Total[Table[Abs[EVBscup[[n,Xpositive[j]]]],{n,1,Nx*Ny}]],
{j,Nx*Ny+1,Nx*Ny*2}]]*
Table[Total[Table[Abs[EVBscup[[n,i]]]^2,{n,1,Nx*Ny}]],{i,1,Nx*Ny}]*
Chop[Table[fermi[EVBscup[[n]]],{n,1,Nx*Ny}]]+
Table[Total[Table[Abs[EVBscdown[[n,Xpositive[j]]]],{n,1,Nx*Ny*2}]],
{j,Nx*Ny+1,Nx*Ny*2}]]*Flatten[
Table[Total[Table[Abs[EVBscdown[[n,i]]],{n,1,Nx*Ny}]],{i,1,Nx*Ny}]]*
Chop[Table[fermi[EVBscdown[[n]]],{n,1,Nx*Ny}]]*)
```

```

(*densypos=
Flatten[Table[Total[Table[Abs[EVScup[[n,Ypositive[j]]]],{n,1,Nx*Ny}]],
  {j,Nx*Ny+1,Nx*Ny*2}]]*
  Table[Total[Table[Abs[EVScup[[n,i]]],{n,1,Nx*Ny}]],{i,1,Nx*Ny}] *
  Chop[Table[fermi[EVScup[[n]]],{n,1,Nx*Ny}]]+
Table[Total[Table[Abs[EVSdown[[n,i]]],{n,1,Nx*Ny}]],{i,1,Nx*Ny}] *
  Flatten[Table[Total[Table[Abs[EVSdown[[n,Ypositive[j]]]],{n,1,Nx*Ny}]],
    {j,Nx*Ny+1,Nx*Ny*2}]]*Chop[Table[fermi[EVSdown[[n]]],{n,1,Nx*Ny}]]*)

(*densxneg=
Flatten[Table[Total[Table[Abs[EVScup[[m,Xnegative[j]]]],{m,Nx*Ny+1,
  Nx*Ny*2}]],{j,Nx*Ny+1,Nx*Ny*2}]]*
  Table[Total[Table[Abs[EVScup[[n,i]]]^2,{n,1,Nx*Ny}]],{i,1,Nx*Ny}] *
  Chop[Table[fermi[EVScup[[n]]],{n,1,Nx*Ny}]]+Table[
    Total[Table[Abs[EVSdown[[m,i]]]^2,{m,Nx*Ny+1,Nx*Ny*2}]],{i,1,Nx*Ny}] *
  Flatten[Table[Total[Table[Abs[EVSdown[[n,Xnegative[j]]]],{n,1,Nx*Ny}]],
    {j,Nx*Ny+1,Nx*Ny*2}]]*
  Chop[Table[fermi[EVSdown[[m]]],{m,Nx*Ny+1,2*Nx*Ny}]];*)

(*densyneg=
Flatten[Table[Total[Table[Abs[EVScup[[n,Ynegative[j]]]],{n,1,Nx*Ny}]],
  {j,Nx*Ny+1,Nx*Ny*2}]]*
  Table[Total[Table[Abs[EVScup[[n,i]]],{n,1,Nx*Ny}]],{i,1,Nx*Ny}] *
  Chop[Table[fermi[EVScup[[n]]],{n,1,Nx*Ny}]]+
Table[Total[Table[Abs[EVSdown[[n,i]]],{n,1,Nx*Ny}]],{i,1,Nx*Ny}] *
  Flatten[Table[Total[Table[Abs[EVSdown[[n,Ynegative[j]]]],{n,1,Nx*Ny}]],
    {j,Nx*Ny+1,Nx*Ny*2}]]*Chop[Table[fermi[EVSdown[[n]]],{n,1,Nx*Ny}]]*)

(*For[n=1,n<200, n++,

deltadensx=0.5*V*(densxpos+densypos);
deltadensy=0.5*V*(-densxneg-densyneg);
densupcalc=Table[Total[
  Table[(fermi[Eup[[n]])]*Abs[EUp[[n,i]]]^2,{n,1,Nx*Ny}]],{i,1,Nx*Ny}] ;
densdowncalc= Table[Total[Table[fermi[Edown[[n]]]*Abs[EDown[[n,i]]]^2,
  {n,1,Nx*Ny}]],{i,1,Nx*Ny}];
densup=densupcalc;
densdown=densdowncalc;
dens=(Total[densup]+Total[densdown])/(Nx*Ny);
munew=mu+0.1*(1.0-deltaelectron-dens);
nup=0.5*nup+0.5*densup;
ndown=0.5*ndown+0.5*densdown;
mag=0.5*(nup-ndown);
Hup=Module[{tab,i,j},
  tab=Table[If[i==j,-munew+U*ndown[[i]],If[MemberQ[NNeighbors[i],j],tt,If[
    MemberQ[NNNeighbors[i],j],nt,0.0]]],{i,1,Nx*Ny},{j,1,Nx*Ny}];tab];
Hdown=Module[{tab,i,j},tab=Table[If[i==j,-munew+U*nup[[i]],
  If[MemberQ[NNeighbors[i],j],tt,If[MemberQ[NNNeighbors[i],j],nt,0.0]]],
  {i,1,Nx*Ny},{j,1,Nx*Ny}];tab];
{Eup,EVup}=Eigensystem[Hup];
{Edown,EVdown}=Eigensystem[Hdown];
SC=Module[{tab,i,j},
  tab=Table[If[MemberQ[SCxNNNeighbors[i],j],deltadensx,If[MemberQ[
    SCyNNNeighbors[i],j],deltadensy,0.0]],{i,1,Nx*Ny},{j,1,Nx*Ny}]]];

```

```

SCC=Conjugate[SC];

Hscup= ArrayFlatten[{Hup,SC},{SCC,-Hdown}];

EigensystemHscup={EHscup,EVHscup}=Eigensystem[Hscup];
Hscdown= ArrayFlatten[{Hdown,-SC},{-SCC,-Hup}];

EigensystemHscdown={EHscdown,EVHscdown}=Eigensystem[Hscdown];
densxpos=
  Flatten[Table[Total[Table[Abs[EVHscup[[m,Xpositive[j]]]],{m,Nx*Ny+1,
    Nx*Ny*2}]],{j,Nx*Ny+1,Nx*Ny*2}]]*
  Table[Total[Table[Abs[EVHscup[[n,i]]]^2,{n,1,Nx*Ny}]],{i,1,Nx*Ny}] *
  Chop[Table[fermi[EHscup[[n]]],{n,1,Nx*Ny}]]+
  Table[Total[Table[Abs[EVHscdown[[m,i]]]^2,{m,Nx*Ny+1,Nx*Ny*2}]],
    {i,1,Nx*Ny}] *Flatten[
    Table[Total[Table[Abs[EVHscdown[[n,Xpositive[j]]]],{n,1,Nx*Ny}]],
      {j,Nx*Ny+1,Nx*Ny*2}]]*
  Chop[Table[fermi[EHscdown[[m]]],{m,Nx*Ny+1,2*Nx*Ny}]];
densypos=Flatten[Table[Total[Table[Abs[EVHscup[[m,Ypositive[j]]]],
  {m,Nx*Ny+1,Nx*Ny*2}]],{j,Nx*Ny+1,Nx*Ny*2}]]*
  Table[Total[Table[Abs[EVHscup[[n,i]]]^2,{n,1,Nx*Ny}]],{i,1,Nx*Ny}] *
  Chop[Table[fermi[EHscup[[n]]],{n,1,Nx*Ny}]]+
  Table[Total[Table[Abs[EVHscdown[[m,i]]]^2,{m,Nx*Ny+1,Nx*Ny*2}]],
    {i,1,Nx*Ny}] *Flatten[
    Table[Total[Table[Abs[EVHscdown[[n,Ypositive[j]]]],{n,1,Nx*Ny}]],
      {j,Nx*Ny+1,Nx*Ny*2}]]*
  Chop[Table[fermi[EHscdown[[m]]],{m,Nx*Ny+1,2*Nx*Ny}]];
densxneg=Flatten[Table[Total[Table[Abs[EVHscup[[m,Xnegative[j]]]],
  {m,Nx*Ny+1,Nx*Ny*2}]],{j,Nx*Ny+1,Nx*Ny*2}]]*
  Table[Total[Table[Abs[EVHscup[[n,i]]]^2,{n,1,Nx*Ny}]],{i,1,Nx*Ny}] *
  Chop[Table[fermi[EHscup[[n]]],{n,1,Nx*Ny}]]+
  Table[Total[Table[Abs[EVHscdown[[m,i]]]^2,{m,Nx*Ny+1,Nx*Ny*2}]],
    {i,1,Nx*Ny}] *Flatten[
    Table[Total[Table[Abs[EVHscdown[[n,Xnegative[j]]]],{n,1,Nx*Ny}]],
      {j,Nx*Ny+1,Nx*Ny*2}]]*
  Chop[Table[fermi[EHscdown[[m]]],{m,Nx*Ny+1,2*Nx*Ny}]];
densyneg=Flatten[Table[Total[Table[Abs[EVHscup[[m,Ynegative[j]]]],
  {m,Nx*Ny+1,Nx*Ny*2}]],{j,Nx*Ny+1,Nx*Ny*2}]]*
  Table[Total[Table[Abs[EVHscup[[n,i]]]^2,{n,1,Nx*Ny}]],{i,1,Nx*Ny}] *
  Chop[Table[fermi[EHscup[[n]]],{n,1,Nx*Ny}]]+
  Table[Total[Table[Abs[EVHscdown[[m,i]]]^2,{m,Nx*Ny+1,Nx*Ny*2}]],
    {i,1,Nx*Ny}] *Flatten[
    Table[Total[Table[Abs[EVHscdown[[n,Ynegative[j]]]],{n,1,Nx*Ny}]],
      {j,Nx*Ny+1,Nx*Ny*2}]]*
  Chop[Table[fermi[EHscdown[[m]]],{m,Nx*Ny+1,2*Nx*Ny}]];

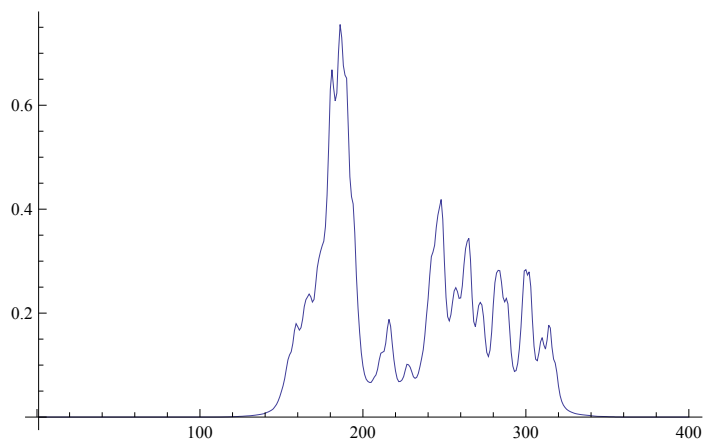
munew=mu;
Print[mu];
Print[deltadensx];
Print[deltadensy];
Print[nup];
Print[ndown];
]*)

```

(*DOS without superconductivity*)

```
DOS := Module[{n, i, w, en, dos, spectralup, spectraldown,
  normalizationup, normalizationdown, absEVup, absEVdown},
  dos = Table[0.0, {en, 1, wsteps}];
  w = Table[0.0, {en, 1, wsteps}];
  For[n = 1, n < Nx * Ny + 1, n++, For[en = 1, en < wsteps + 1, en++,
    normalizationup = (en - 1 - wsteps / 2) * dwdos - Eup[[n]];
    normalizationdown = (en - 1 - wsteps / 2) * dwdos - Edown[[n]];
    w[[en]] = (en - 1 - wsteps / 2) * dwdos; i = 1;
    If[Abs[normalizationup] < 20.0 * eta ||
      Abs[normalizationdown] < 20.0 * eta, absEVup =
      Abs[EVup[[n, i]]]^2; absEVdown = Abs[EVdown[[n, i]]]^2;
      spectralup = spectral[normalizationup];
      spectraldown = spectral[normalizationdown]; dos[[en]] =
      dos[[en]] + absEVup * spectralup + absEVdown * spectraldown,
      dos[[en]] = dos[[en]]]; Chop[dos]] (**)
```

```
ListLinePlot[DOS, PlotRange → All]
```



```
PotVal
```

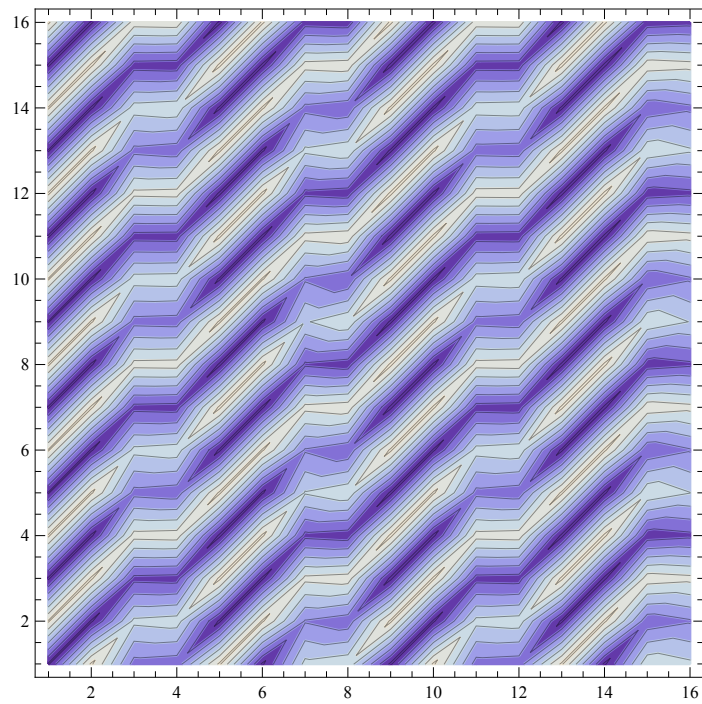
```
Dimensions[plottest]
```

```
{16, 16}
```

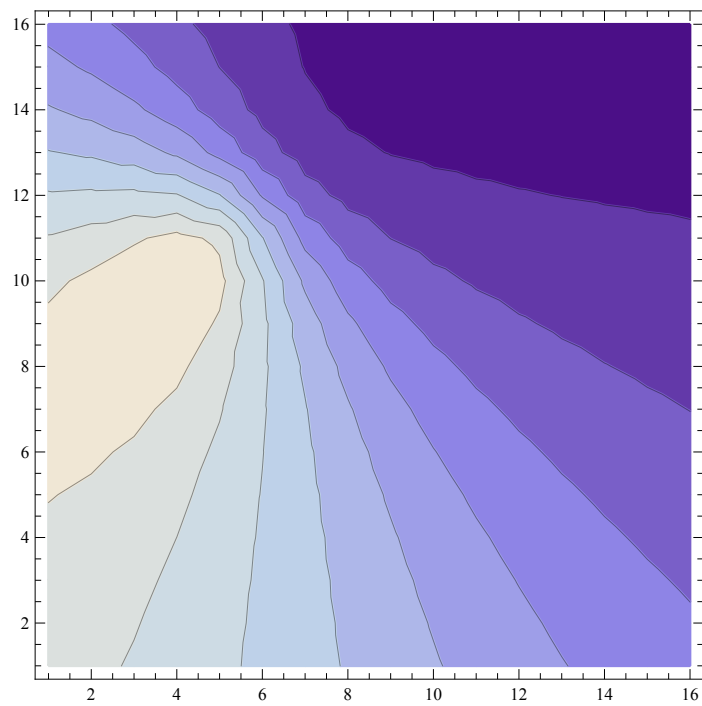
```
ListContourPlot[plottest]
```

```
densup
```


`ListContourPlot[magoxplot]`



`ListContourPlot[potplot]`



Bibliography

- [1] I. M. Gat T. Ito M. I. Larkin Y. J. Uemura G. M. Luke K. M. Kojima Y. S. Lee M. A. Kastner R. J. Birgeneau A. T. Savici, Y. Fudamoto and K. Yamada. Muon spin relaxation studies of incommensurate magnetism and superconductivity in stage-4 $\text{La}_2\text{CuO}_{4.11}$ and $\text{La}_{1.88}\text{Sr}_{0.12}\text{CuO}_4$. *Phys. Rev. B*, 2002.
- [2] P. W. Anderson. *Superconductivity in High- T_c Cuprates*. Princeton Series in Physics, 1997.
- [3] J. F. Annett. *Superconductivity, Superfluids, and Condensates*. Oxford Master Series in Condensed Matter Physics, 2004.
- [4] N.B Christensen G. Aeppli D. F. Mcmorrow H.M. Ronnow P. Vorderwisch P. Smeibidl N. Mangkorntong T. Sasagawa M. Nohara B. Lake, K. Lefmann and H. Takagi. Three-dimensionality of field-induced magnetism in a high-temperature superconductor. *Nature*, 4, 2005.
- [5] M.A. Kastner R.J. Christianson R.J. Birgeneu K. Yamda Y. Endoh B. O. Wells, Y. S. Lee and G. Shirane. Incommensurate spin fluctuations in high-transition temperature superconductores. *Science*, 277(5329)(1067-1071), 1997.
- [6] Henrik Bruus and Karsten Flensberg. *Many-Body Quantum Theory in Condensed Matter Physics*. Oxford University Press, 2004.
- [7] Sthephen Bundell. *Magnetism in condensed matter*. Oxford University Press, 2001.
- [8] A. Gupta C. C Tsuei, J. R. Kirtley and M. B. Ketchen. *Rev. of Mod. Phys*, 72,969, 2000.
- [9] M. Rupp J. Z. Sun A. Gupta C. C Tsuei, J. R. Kirtley and M. B. Ketchen. *Science*, 272,393, 1996.

- [10] M. A. Alario-Franco U. Amador N. H. Andersen C. Rial, E. Morán. Room temperature chemically oxidized $\text{La}_2\text{CuO}_{4+y}$: Phase separation induced by thermal treatment. *Physica C*, 1997.
- [11] W. C. Lee D. M. Ginsberg D. A. Wolleermann, D. J. van Harlingen and A. J. Leggett. *Phys.Rev.Lett*, 71,2134, 1993.
- [12] R. Hackl D. Einzel. *J. Raman Spectroscopy*, 27,307, 1996.
- [13] R. Das Sharma A. Bock D. Fay D. Manske, C. T. Rieck. *Phy.Rev.*, B 56(R2940), 1997.
- [14] P. G de Gennes. *Superconductivity of Metals and Alloys*. Benjamin, New York, 1966.
- [15] E. V. L. de Mello. Description and connection between the oxygen order evolution and the superconducting transition in $\text{La}_2\text{CuO}_{4+y}$. 2012.
- [16] A.M. Kini U. Geiser A. Umezawa G.W Gabtree E.H Appelman, L. R Morss and K. D. Carlson. Oxygen content of superconducting perovskites, $\text{La}_{2-x}\text{Sr}_x\text{CuO}_y$ and $\text{YBa}_2\text{Cu}_3\text{O}_y$. *Inorganic Chemistry*, 26(20):3237-3239, 1997.
- [17] Ch. Niedermayer et al. Common phase diagram for antiferromagnetism in $\text{La}_{2-x}\text{Sr}_x\text{CuO}_4$ and $\text{Y}_{1-x}\text{Ca}_x\text{Ba}_2\text{Cu}_3\text{O}_6$ as seen by muon spin rotation. *Phys. Rev. Lett.*, 80(3843-3846), 1998.
- [18] Y. S. Lee et al.. Neutron scattering study of spin-density wave order in the superconducting state of excess-oxygen-doped $\text{La}_2\text{CuO}_{4+y}$. *Phys. Rev. B*, 1999.
- [19] X. Z. Shen et al. *Phys.Rev.Lett*, 70,1553, 1993.
- [20] M. Schmid A.P. Kampf F. Loder, S. Graser and T. Kopp. Modeling of superconducting stripe phases in high- t_c cuprates. *New Journal of Physics*, 13, 201.
- [21] S.W. Cheong F.C. Chou, D.C. Johnston and J. D Jorgensen A.J. Schultz P.C Canfield, P.G Radaelli. Preparation, magnetization and electrical resistivity of electrochemically oxidized $\text{La}_2\text{CuO}_{y+\delta}$. *Physica C: Superconductivity*, 216:66-76, 1992.
- [22] Department of Engineering Physics GITAM.

- [23] J. I. Budnick W. A. Hines C. Niedermayer L. Udby C. Bernhard A. Moodenbaugh H. E. Mohottala, B. O. Wees and F. C. Chou. Phase separation in superoxygenated $\text{La}_{2-x}\text{Sr}_x\text{CuO}_{4+y}$. *Nature Materials*, 5:377-282, 2006.
- [24] J. R. Schrieffer J. Berden, L. N. Cooper. Microscopic theory of superconductivity). *Phys. Rev*, 106(162), 1957.
- [25] J. R. Schrieffer J. Berden, L. N. Cooper. Theory of superconductivity. *Phy.Rev.*, 108(1175), 1957.
- [26] A. Wattiaux J-P. Doumerc J. Etourneau M. Pouchard J.B. Goode-nough J. C. Grenier, N. Lagueyte and J.S Zhou. Transport and mag-netic properties of the superconducting $\text{La}_{2-x}\text{CuO}_{4+\delta}$ phases ($0 < \delta < 0.09$) prepared by electrochemical oxidation. *Physica C: superconduc-tivity*, 202:209-218., 1992.
- [27] R. Gilardi N. B. Christensen H. M RÅ,nnow D. F. McMorro M. Ay J. Sthn O. Sobolev A. Hiess S. Pailhes C. Baines N. Momono M. Oda M. Ido J. Chang, Ch. Niedermayer and J. Mesot. Tuning competing orders in $\text{La}_{2-x}\text{Sr}_x\text{CuO}_4$ cuprate superconductors by the application of an external magnetic field. *Physical Review*, B 78(104525), 2008.
- [28] K. A. M J. G. Bednorz.
- [29] J.D. Axe Y. Nakamura J.M. Tranquada, B.J. Sternlleb and Uchida. Evidence for stripe correlations of spins and holes in copper oxide su-perconductors. *Nature*, 375, 1995.
- [30] J.Z. Sun C.C. Chi Yu-Jahness A. Gupta M. Rupp J.R. Kirtley, C.C Tsuei and M. B. Ketchen. *Nature*, 373,225, 1995.
- [31] F.C. Chou N. B. Christensen-S.B Emery K. Lefmann J.W. Lynn H.E. Mohottala Ch. Niedermayer L. Udby, N.H. Andersen and O.B. Wells. Manetic ordering in ellectronically phase-separated $\text{La}_{2-x}\text{Sr}_x\text{CuO}_{4+y}$ neu-tron diffraction experiments. *Physical Review*, B 80, 2009.
- [32] N. B. Christensen M. Boehm-Ch. Niedermayer H. E. Mohottala T. B. S. Jensen R. Toft-Petersen F. C. Chou N. H. Andersen K. Lefmann B. O. Wells L. Udby, J. Larsen. Direct proof of unique magnetic and superconducting phases in superoxygenated high-tc cuprates. *Phys. Rev. Lett.*, 111, 227001 (2013), 2014.
- [33] M. Cardona M. C. Krantz.

- [34] K. A. Muller and J. G. Bednorz. Perovskite-type oxides, the new approach to high- t_c superconductivity. 1987.
- [35] H. K. Onnes. Investigations into the properties of substances at low temperatures, which have led, amongst other things, to the preparation of liquid helium, 1913.
- [36] A. J. Schultz-B. A. Hunter J. L. Waner F. C. Chou P. G. Redaelli, J. D. Jorgensen and D. C. Johnston. Structure of the superconducting $\text{La}_2\text{CuO}_{4+\delta}$ phases ($\delta \approx 0.08, 0.12$) prepared by electrochemical oxidation. *Physical. Rev. B*, 8(1):499-510, 1993.
- [37] P. Philips. Review: Mottness collapse and t-linear resistivity in cuprate superconductors. *Philosophical Transactions of Royal Society, A*: 369:1574 -1598, 2011.
- [38] T. Roy and T.E Mitchell. On the space group of $\text{La}_2\text{CuO}_{4-\delta}$. *Material-letters*, 6(10), 1988.
- [39] Ajay Kumar Saxena. *High-Temperature Superconductors*. Springer Series in Material Science.
- [40] J. Solyom. *Fundamentals of the Physics of solids*. Springer.
- [41] Superconductors.org, 2014.
- [42] D. Einzel T. P. Devereaux. *Phy.Rev.*, B5116336, 1995.
- [43] U. Tricoli and B.M. Andersen. Pinning of stripes by local structural distortions in cuprate high- t_c superconductors. 2012.
- [44] F. Fujiwara T. Kondo K. Asayama M. Horvatic Y. Berthier P. Butaud P. Segransan C. Berthier-H. Katayana-Yoshida Y. Okabe Y. Kitaoka, K. Ishida and T. Takahashi. *Strong Correlations and Superconductivity*. Springer series in Solid-State Sciences 89, 1989.
- [45] Z.Y. Yang A. Hamed S.T. Ting Z.G. Li, H.H. Feng and P. H. Hor. Carrier controlled doping efficiency in $\text{La}_2\text{CuO}_{4+\delta}$. *Phys. Rev. Lett.*, 77(27), 1996.
- [46] F. C. Zhang and R. M. Rice. *Phys. Rev.*, B 37(3759), 1988.